Synthesis, phase transfer, and deposition of polyoxyethylene alkyl amine surfactant-functionalized gold nanoparticles

A DISSERTATION

Submitted to the Department of Innovation Systems Engineering
and the Graduate School of Engineering of Utsunomiya University
in partial fulfillment of the requirements for the degree of
Doctor of Philosophy

MD ABDULLAH AL NAHID

MARCH 2022

ACKNOWLEDGEMENTS

All praise is due to Allah, Creator of the universe, who has enabled me to do this wonderful work at Utsunomiya University.

My most sincere thanks go to my supervisor, Professor Ken-ichi Iimura, for his guidance and support throughout my entire doctoral research. He always tried to see my potential and encourage me to succeed. His valuable insights and constructive suggestions led me to achieve my goals for PhD.

I also want to thank my dissertation committee members, Dr. Ken-ichi Iimura, Dr. Masahide Sato, Dr. Keitaro Tezuka, Dr. Norihiro Kato and Dr. Takeshi Furusawa for their time, valuable advice and suggestions. Their advice and comments have led to the better quality of this dissertation.

I am also grateful to Prof. Dr. Md. Mufazzal Hossain for his recommendation to me for higher studies.He is the mentor who inspires me a lot in achieving academic success

I would like to express my gratitude and best wishes to the students of the Soft Materials Laboratory for their cooperation and their support during my research. In addition, I prefer to address thankfully Kazutoshi Hasegawa san and Makoto Roppongi san for their assistance in learning the operation of the analytical instrument.

I wish to thank my beloved wife Fahmida Afroz for all the love, support, and encouragement she has shown to me. Her continuous sacrifices mad my Ph. D journey comfortably possible Special thanks to my son Muhammad Shadman Sadiq whose smiling face inspires my everyday work.

In my honor and dedication, I show my gratitude to my parents through whom Allah blessed me with existence and guided me to achieve a wonderful deed.

I am very grateful to the Japanese government for providing me financial support for the am highly Manbukagakusho scholarship (Ministry of Education, Culture, Sports, Science and Technology) that I received throughout my Ph.D. study. I would also like to thank the Creative Department for Innovations, Utsunomiya University for partially supporting my researches.

Preface

Gold nanoparticles (AuNPs) are undergoing a revolution in terms of its multidisciplinary applications in both environmental, medical and molecular sensing due to the unique properties, including quantum effect or fluorescence quenching. The extent of these properties depends strongly on the size, morphology, and nanoparticle stabilization, and is therefore related with the synthesis conditions of the nanoparticles. However, nanoparticles can be synthesized using both hydrophilic and hydrophobic solvents but the preparation of the desired particles in organic solvents require more complicated and meticulous steps due to the law solubility of gold salts in organic phase and the complexity in controlling the size and shape of AuNPs. On the contrary, synthesis in aqueous phase is more prevalent because it is simple, rapid, and environmentally friendly. The synthesis of AuNPs in water is thus the most convenient and economical method considering its applications. Therefore, in this research gold nanoparticles were prepared through single step synthesis with the reduction of tetra chloroauric (III) acid using polyethoxylated alkyl amine that acts as a reducing agent as well as capping ligand. Afterwards, a convenient phase transfer approach was implied to make the AuNPs adaptable for various organic solvent in order to broaden its application area. Finally, thin film of polyoxyethylene alkyl amine (AMIET)-AuNPs was examined to envisage the prospect of the prepared gold nanoparticles.
Accordingly, a detailed investigation of AMIET-AuNPs including synthesis, characterization of morphology, phase transfer, surfactant removal, and thin film deposition was undertaken and is addressed in this dissertation sequentially as follows.

Chapter 1 introduces the concept of gold nanoparticles along the detailed description of it types, properties, surface chemistry, synthesis routes and applications. the aims and objectives of the thesis are also clearly highlighted at the end of this chapter.

Chapter 2 explores the synthesis of AMIET functionalized gold nanoparticles in aqueous media. The findings show that only specific ranges of concentrations of AMIET can produce gold nanoparticle with less residual organic and clear ruby red appearance. However, the synthesized gold nanoparticles were found to be spherical in shape confirmed by the TEM and UV-Vis spectra measurement. Moreover, it was observed that each AMIET-AuNPs contains particle of different

sizes. However, this polydisperse AMIET-AuNPs shows sufficient surface plasmon resonance, therefore may have potential application.

Chapter 3 describes the development of a feasible and reliable phase transfer method of AMIET-AuNPs to water immiscible organic solvents without the surface modification. It was noticed that the complete transfer can be achieved by using pH triggered phase transfer method while preserving the morphology. Hence, a comparative illustration between traditional and our developed method has also presented in this chapter.

Chapter 4 focuses on the development of the process for surfactant removal from nanoparticles after phase transfer without using laborious instruments and chemicals, which in turn enhances the dispersibility of AMIET-AuNPs in various organic solvents.

Chapter 5 investigates the immobilization of AMIET-AuNPs onto surface modified solid substrate. It was observed that HF passivated silicon surface and MPTMs functionalized silicon surface are suitable for the deposition of AuNPs from air-water interface. The detail information has been discussed in this section.

Chapter 6 summarizes the major findings of this dissertation and discusses the scope and recommendations for future work.

Table of Contents

Chapter I Introduction

1. Gold Nanoparticles

1.1 Nanoparticles

A nanometer is one-billionth of a meter; in practical terms it is one seven-thousandth of the width of a red blood cell or one eighty- thousandth of the width of a human hair. “Nanoscale” generally refers to the manipulation of materials of 100 nanometers or less on any dimension. "Nano" stems from the Greek *nanos,* i.e. dwarf. Consequently, a nanometer is a tiny fraction of a meter or, more precisely: one billionth of a meter. All particles with at least one outer dimension, i.e. length, width or height, between 1 and 100 nanometers are referred to as nano-objects in the jargon of the field. Nano-objects which are nanoscale in all three dimensions are nano-particles. The National Nanotechnology Initiative (NNI) defines nanotechnology at dimensions of roughly 1 to 100 nm (shaded scale region) in Fig-1.1 [1,2].

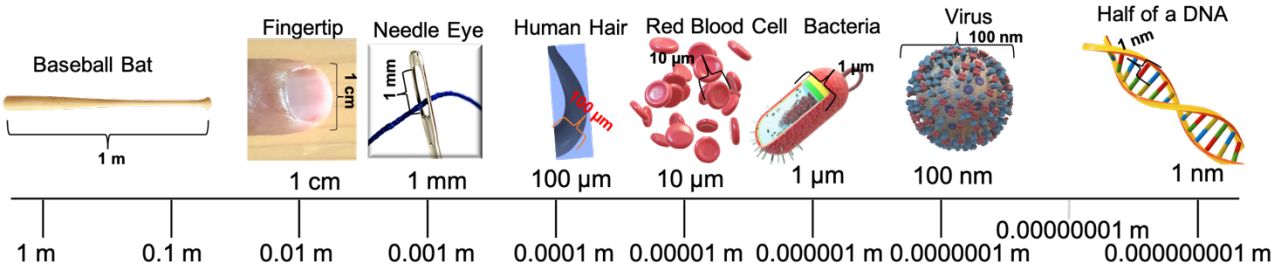

Fig-1.1 Comparing various entities' sizes in order to discern nanoscale measurements.

1.2 Historical overview of gold

The use of gold and silver particles in glass- blowing can be seen in the famous *Lycurgus Cup* exposed in the British Museum [3]. The most unusual feature of this cup however is its color. When viewed in reflected light, for example in daylight, it appears to be green, but when light is transmitted from the inside of the vessel through the glass, it appears to be red.

Humankind has linked the lustre of gold with the warm, life-giving light of the sun. In cultures, which deified the sun, gold represented its earthly form by the virtue of its bright yellow color [4,5]. To the primitive chemists, gold was considered as a metal of perfection. Because of its transmutation ability, gold was used as a universal medicine for longevity and immortality power.

In the early Middle Ages, gold was used mainly for its magico-religious powers, and its use in rational therapeutics did not come to fruition until Arnald of Villanova (1235-1311). Over 5000 years ago, the Egyptians ingested gold to purify their minds and bodies. Gold has been so valuable to man from the beginning that man has made every effort to find it in nature. Scientists have therefore tried to convert other metals into gold.

Gold was mainly used in medicine for its magico-religious powers and played almost no role in rational therapeutics until late Middle Age. Gold is a miracle of nature and it cleanses the substance of the heart and the fountain of life [6]. Nowadays the medicinal use of gold is almost entirely limited to the treatment of rheumatoid arthritis [7,8]. The work of Faraday has pointed towards specific optical properties of colloidal gold, long before the recognition of changing properties of matter at nanoscale [9,10].

1.2.1 The first uses of gold nanoparticles

The first use of gold nanoparticles is closely related with the history of the production of red glass started in Egypt and Mesopotamia back in 1400-1300 BCE with the beginning of glass making. Though the origin of the red color glass is debated, but some scientist stated it is due to metal copper nanoparticles. However, the production of the ruby gold ruby glass did not take place until the end of the seventeenth century [11,12]. First written documents about ruby glass was published by Antonio Neri in his famous book "L'Arte Vetraria" [13]. Johann Kunckel (1637-1703), the first important maker of gold ruby glass offered a detailed report about the manufacturing procedure of his gold ruby glass in posthumously published Laboratorium Chymicum in 1917 [14,15]. Nevertheless, it is still a mystery that how Kunckel managed to produce gold rubby glass on a rather large scale. However, in seventeenth century, alchemists were obsessed to unlock the secrets of nature by simulating natural processes in laboratory conditions as they believed that the color could be extracted, and it contains the spirit of the metal that could be used in alchemical transmutation. Therefore, new methods of coloring glass and mixing batches were invented [16].

1.3 Properties of gold nanoparticles

Gold is very stable and nontoxic, and is widely used in jewelry, dentistry because of its air-inertness and is not affected by most reagents. Even gold does not get corroded in the natural or industrial environment. Gold is also a good conductor of heat and electricity. Due to the fact that conduction electrons are free to move around the necleus, it is corrosion resistant which makes useful for electrical and electronic application. However, when the size of a material is reduced to nanoscale, it exhibits totally different properties including melting points, conductivity etc. from their bulk counterparts. A particular example of this is the well documented decrease in phase change temperature as the material dimensions decrease to nanoscale. More evidently, P. Schlexer, A. Andersen, B. Sebok et al showed that 2.7 nm gold nanoparticles melt around 400 ºC and 5 nm gold nanoparticles melt around 650 ºC whereas the melting point of metallic gold is 1064 ºC [17]. Molecular dynamic simulation for silver nanoparticles proves the change in melting temperature [18]. The reason behind this property change is the fact that matter at the nanoscale follows the laws of quantum mechanics rather than newtonian physics. Moreover, at the nanoscale the materials show new physical phenomena, collectively called quantum effects, which are size dependent and dramatically different for the properties of macroscale material [19]. For an example, about 20 nm gold colloid is no longer golden but appears ruby red in color.

1.3.1 Physical properties

The physical properties such as solubility and stability are dominated by the nature of nanoparticles surface including the ratio of surface are to volume, which is directly related with the shape and size of the nanomaterials. Size properties enhanced or hindered particle aggregation depending on the type of surface modification, enhanced photoemission, high electrical and heat conductivity, and improved surface catalytic activity [20]. Gold nanoparticles exhibit various sizes and shapes depending on the fabrication method [21,22], their shapes may be spherical, sub-octahedral, octahedral, decahedral, icosahedral multiple twined, multiple twined, irregular shape, tetrahedral, nanotriangles, nanoprisms, hexagonal platelets and nanorods [23]. Among the widely used morphological species of gold nanoparticles as shown in Fig-1.2, only four types of nanostructures are most extensively investigated. These are nanosphere, nanorods, nanoshells (silica balls covered with a polycrystal gold layer) and nanocubes [24]. However, in this thesis the discussion is about the prepared gold nanospheres. However, most of the nanospheres considered in the literature

possess an irregular spherical shape [25] and according to our observation it is better to call them quasi-spherical.

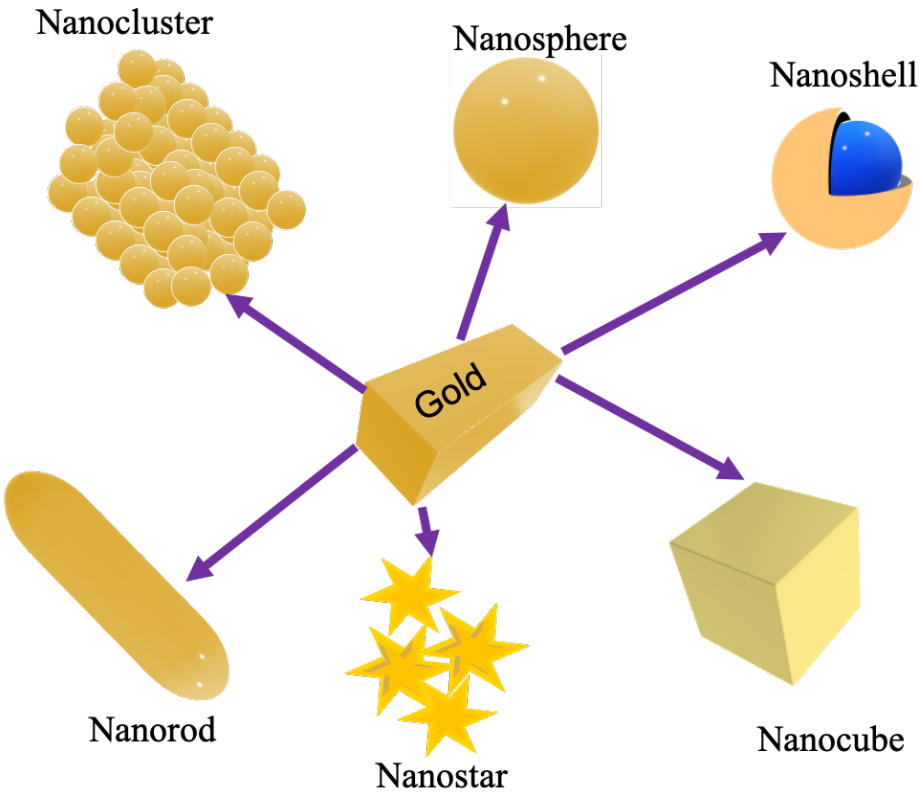

Fig- 1.2 Widely used shape of gold nanoparticles

M. sing et al. demonstrated that specific heat, melting entropy and enthalpy of nanomaterials (such as Au, Cu, Ag) affected by the particle size and shape [26]. The specific heat is observed to increase with the decrease in particle size, whereas the melting entropy and enthalpy decrease as the particle size decreases in their spherical, nanowire shapes. Z. Qin et al. showed the quantitively photothermal heat generation depends not only the shape of gold nanoparticles (i.e nanosphere and nanorods) but also depends on the polydispersity metric [27]. So the physicochemical properties such as size, shape, charge, surface chemistry and concentration impact gold nanoparticles stability in biological environments, mechanism and efficiency of uptake.

Surface chemistry of gold nanoparticles is of important importance to understand and plays an important role in various areas specially in biological application. The surface chemistry is strongly influenced by the local environment and the reactants of synthesis. Organic ligands often act as stabilizers, stabilizing agents or capping ligands and prevent aggregation, coalescence and unlimited growth, having a major role in the size and shape of the nanoparticles [28]. The particles stability is strongly influenced by the surface bound ligand that often remain adsorbed on the NP surface after the immobilization process and, therefore, influence both the immobilization efficiency and the catalyst performance, because of their binding affinity to the metallic surface [29]. The organic ligands is mostly inherent in the colloidal synthesis. But the advantage is that the surface can also be modified by other ligands that usually bind more strongly to the surface of nanoparticles referred as a post-synthesis ligand exchange process. This strategy is applied improve the colloidal stability or to study the new properties [30]. The frequently used ligands are thiol, amines, phophines, polymers, ammonium salts, alkynes or a mixture of different ligands. One of the drawbacks of this process is that the integrity of the particles may be disrupted.

1.3.2 Optical properties

When the bulk gold is reduced to the nanometer scale, the optical properties are dramatically modified properties and the resulting behaviors influence in many advanced application like cellular imaging, molecular diagnosis and targeted therapy [31]. The optical properties of spherical gold nanoparticles are highly dependent on the particles size. Smaller nanospheres gold absorb light near 520 nm, while larger spheres exhibit increased scattering and have peaks that broaden significantly and shift towards longer wavelengths [32]. Larger spheres scatter more light both because they have larger optical cross sections, and the ratio of scattering to total extinction increases with size. The optical properties also depends on the refractive index near the nanoparticle surface. The nanoparticle extinction spectrum shifts to longer wavelengths with the increase of the refractive index near the surface of the nanoparticles known as red-shifting. The optical properties of AuNPs also change when particle aggregate or coagulate and the conduction electrons near each particle surface become delocalized and are shared amongst neighboring particles. In this case, the surface plasmon resonance occurs at lower energies, causing the absorption and scattering peaks shift to longer wavelengths. The stability or aggregation state can be monitored by UV-Visible spectroscopy. For the destabilized nano-colloid, the original

extinction peak will decrease in intensity due to the depletion of stable nanoparticles, and often the peak will broaden or a secondary peak will form at longer wavelengths due to the formation of aggregates [33,34].

The fascination of gold nanoparticles is in their intense color because it can exhibit strong optical absorption and scattering with exceptional performance [35,36]. This is due to a coherent oscillation of the surface conduction electrons excited by electromagnetic radiation called surface plasmon resonance (SPR) [37,38]. The Lygurcus cup (400 AC) is probably the most famous example of the use of SP in the ancient times, exhibiting different coloration when observed upon illumination inside or outside of the cup. However, the complete explanation of the various color effects was not possible before Mie's publication. Gustav Mie's (1968-1957) gave a theoretical explanation of the beautiful coloration of metals in a colloidal state and was triggered by an experimental dissertation of his student Walter Steubing in a paper titled by "Beitrage zur Optik trüber Median, speziell kolloidaler Metallösungen" ("Contributions on the optics of turbid media, particularly colloidal metal solution") in 1908 [39].

1.3.2.1 Surface plasmon resonance

SPR is the manifestation of a resonance effect due to the interaction of conduction electrons of metal nanoparticles with incident photons. The interaction relies on the size and shape of the metal nanoparticles and on the nature and composition of the dispersion medium. Depending on the thickness of a molecular layer at the metal surface, the SPR phenomenon results in a significant reduction in intensity of the reflected light [40]. This is happened for the case of metallic NPs with a size that is significantly smaller than the wavelength of the excitation light [41]. The electromagnetic field of the incoming light wave induces polarization of the free electrons with respect to the much heavier ionic core of a spherical NP. As these positive charges are considered to confined inside, the NP negative charge (free electrons) will be accumulated in one side under the influence of external fields. Therefore, a displacement of the negative charges from the positive ones occurs when the metallic NP is placed in an electric field.

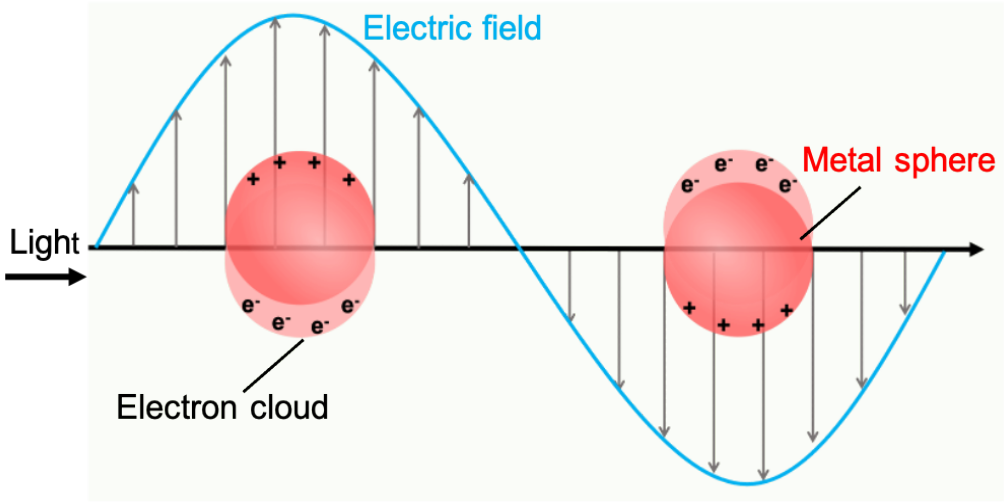

Fig-1.3 Oscillating dipoles induced by electromagnetic radiation at gold nanoparticles.

As a result, an electric dipole generates due to a net charge difference at the NP boundaries. Thus, in turn, gives rise to a linear force to return the electrons to the equilibrium position [42]. The larger the electron displacement, the larger the electric dipole and consequently the restoring force. The situation is similar to a linear oscillator with a restoring force proportional to the displacement from the equilibrium position.

Actually, the electron movement inside the NP suffers some dumping during the movement due to the scattering process with the ionic cores and the NP surface. Thus, the system is similar to linear oscillator with reducing the oscillation amplitude [43]. Therefore, when an alternating force is applied to a linear oscillator, the system oscillates with the same frequency than the external force but the amplitude and phase will depend on both the force and the intrinsic parameters of the oscillator. If the frequency of the external force is the same that the plasmonic frequency of the NP, it will be easy to make the electrons oscillate, but as we move far way from this frequency the movement of electrons will be more difficult, thus reduce the amplitude. As a result of this optical effect, a new type of resonance between the metal nanoparticles and the surrounding dielectric medium produces an enhanced electromagnetic field at the interface that can monitored by absorption spectroscopy as known as SPR as depicted in Fig-1.3. The resonance frequency of this SPR is strongly dependent on the size, shape, interparticle interactions, and dielectric properties of the surrounding environment [44]. Nevertheless, this collective oscillation is constrained by the

reduced dimensions of the NP in which the electrons are confined, leading to a significant absorption of the wavelengths around green. For this reason AuNPs appear with the complementary red color [45–48].

Surface plasmon offer the opportunity to amplify, concentrate and manipulate light at the nanoscale, overcoming the diffraction limit of traditional optics and increasing resolution and sensitivity of optical probes. Therefore SP opens a wide range of application fields, including biomedical, energy, environment protection, sensing and information technology applications [49]. Currently, there are many established applications of SP that increases rapidly with the development of fabrication and manipulation of nanomaterials [50]. The width, position, and number of SPRs are governed by the shape of the AuNPs. Small (≤50 nm) spherical AuNPs have only one SPR [51], whereas gold nanorods have two SPR modes, because of its antenna-like structures, the polarization pattern influence the light scattering by the combination of lightning rod effects [52] and the suppression of interband damping [53]. Moreover, for spherical AuNPs, the SPR is partially overlapped with the absorption originated by interband transitions, namely by single electron optical excitations from the occupied 5d band to the unoccupied levels of the 6s-6p band of the metal. The SPR intensity depends on the number of conduction electrons or excited atom that justify the incredibly high extinction cross-section, which is 10^5 times higher than that of organic chromophores for a 20 nm AuNP [54].

1.4 Gold species as a Lewis acid and its coordination with nitrogen

It has been shown that gold(I) and gold(III) centers activate alkenes and alkynes for nucleophilic addition [55,56]. Occasionally, reactivity differences between gold(I) and gold(III) have been observed and this is attributed to their different Lewis acidity levels [57,58]. Moreover, B. Reiner et al. explored the activity as Lewis acid catalyst by studying gold II and gold III complexes supported by phosphorous ylide ligands [59]. G. Lu et al. showed that gold surface could act as a Lewis acid coupling with Lewis bases (e.g. imine, nitrile) to generate effective frustrated Lewis pairs (FLPs) for activating H_2 and then achieving hydrogenation of small imine and nitrile [60]. The Ikuyo group has demonstrated that gold nanoclusters stabilized by poly (N-vinyl-2-pyrrolidone) (Au:PVP NCs) can act as Lewis acid catalysts to facilitate the hydroalkoxylation of inactivated alkenes in aqueous media under aerobic conditions [61]. An amine-based reducing agent has been demonstrated to be effective in preparation of nanoparticles [62–67]. However, due

to the high electronegativity of nitrogen atom and the presence of adjacent electron donating -CH_2- groups, the density of electron on nitrogen of AMIET is gained to a greater extent. Moreover, AMIET as a tertiary alkyl amine has a higher number of electron donating groups than primary alkyl amine surfactants such as oleylamine (OAm), octadecylamine (ODA) and hexadecylamine (HDA) [68]. Therefore, AMIET act as strong electron donor at elevated temperature [69] and can potentially reduce the Au^{3+} to Au^0 [70]. The coordination of Lewis acids to the nitrogen of complex species like AMIET leads to an acceleration of the rate of reductive elimination [71]. Thus, the highly Lewis acidic gold species coordinates to the nitrogen of tertiary amine [72]. The gold species have this coordination both in their higher oxidation state and zero states i.e the coordination may happen before and after reduction to AuNP. Moreover, the steric effect would increase the reductive elimination and thereby facilitate coordination. However, steric hindrance may be a factor for post-synthesis research, such as ligand exchange, new molecule incorporation, or additional surface modifications, which need further investigation.

1.5 Surface charge of gold nanoparticles and its origin

The charge of a particles' surface in a liquid three main sources: (1) the ionization or dissociation of surface groups; (2) the adsorption or binding of ions from the solution onto a previously uncharged surface; (3) when two dissimilar surfaces are very close, charges can hop across from one surface to the other [73].

The surface charge of gold nanoparticles depends on the synthetic strategies. For example, pulsed laser ablation in liquid (PLAL) produce highly stable colloid though it is free from any capping agents and surfactants. Therefore, the stability of nanoparticles synthesized by PLAL is not due to repulsive steric interactions rather it might be a electrostatic in nature. Even though the particles can be coagulated or unstable by changing the ionic strength of the solution, the origin of large negative zeta potential is not well reported [74]. However, several authors addressed the hydroxylation of Au-O compound in the solution, followed by a proton donation yields AuO^- and $AuCO_3^-$ that results the negative charge onto the naked particles [75–77]. In contrary, Lévy and co-workers investigated through XPS measurement's on free standing and deposited gold nanoparticles, and highlighted the absence of surface oxidation on gold nanoparticles prepared by laser ablation [78]. Therefore, there is still considerable uncertainty with regard to the origin of

those negative charges [79,80]. Nonetheless, recent study shows the presence of excess electrons formed within plasma phase and trapped on the nanoparticles may results the negative (zeta) ζ - potential [81–83]. M. Dell'Aglio and A. De Giacomo clearly demonstrate that nanoparticles produced by nano-second pulse laser ablation (ns-PLAL) are with negative charge in solution due to the absorbed electrons that enhances the stability of the colloidal solution [82].

It is known only that citrate anions coordinate to the metal surface by inner- sphere complexation of the carboxylate groups and there are trace amounts of $AuCl_4^-$, Cl^-, and OH^- on the metal surface [84]. In addition to coordinated citrates, IR analyses also indicate that there are dangling citrate species that are not in direct contact with the metal surface. D. B. Grys, B. De Nijs, A.R. Salmon et al. claimed influence of (chloride) chemical environment and the citrate coordination and the binding of the free COO^- and the hydroxyl group are responsible for the surface charge [85]. In other words, the enhancement of negatively charged carboxylate anions of citrate at higher pH results in the increase of citrate ions under alkaline conditions [86].

1.6 Gold nano-colloid

Colloidal dispersions differ from the solution, are homogeneous mixture of component particles with smallest dimension less than 1 nm. Colloids appear to be homogeneous, and the colloidal particles they contain are small enough (1-1000 nm) to exhibit Brownian motion, cannot be separated by filtration, and do not readily settle out under the influence of gravity. But these dispersions are inherently unstable and under certain circumstances, most colloidal dispersions can be broken and will flocculate or settle out. Most importantly, aqueous colloid is not usually redispersed in water after complete evaporation because nanoparticles are non-ionizable. Colloidal nanoparticles are intermediaries between suspension (particles size > 200 nm) and the real solutions (particles size <2 nm). Colloidal dispersions are distinguished from true solutions by their light-scattering properties. The nature of this scattering depends on the ratio of the particle size in the medium to

Fig-1.4 Light scattering by colloidal gold

the wavelength of the light. This phenomenon can easily be observed by shining a laser through a sample of the gold nano-particles as shown in Fig-1.4.

1.7 Synthesis routes of gold nanoparticles

There are physical, chemical, photochemical and biological methods of nanoparticle preparation [87]. Further, methods of preparation of colloidal nanoparticle solutions can be divided into dispersing and condensing. Dispersion methods are based on destruction of the crystal lattice of the material (laser ablation, cathode sputtering and electric arc dispersion), it belongs to the type "top-down". Condensation methods are based on the chemical reaction (reduction in solution, followed by the nanoparticle precipitation, formation and stabilization). Each method has its advantages and disadvantages. The modified Turkevich method results in monodisperse nanoparticles, the size of which varies depends on the reducing agent concentration and also the size of the ligand which it stabilizes [88]. By other methods, stabilization of the nanoparticles is accomplished by forming an organic monolayer on the growth surface, controlling the size and shape by the concentration of the reducing agent and the stabilizer. Also, the reducing agent may be a stabilizer [89]. Sodium citrate, alcohols, Na_2S, borohydrides [B_2H_6] and sodium borohydride [$NaBH_4$], including hydrogen gas [90] and sugars (fructose, glucose and sucrose) can be used for the reduction process [91,92]. White phosphorus and hydrazine can be used, however, these compounds are very toxic and solutions obtained by these methods cannot be used in biological applications. However, different synthetic route of gold nanoparticles can be summarized in Fig-1.5.

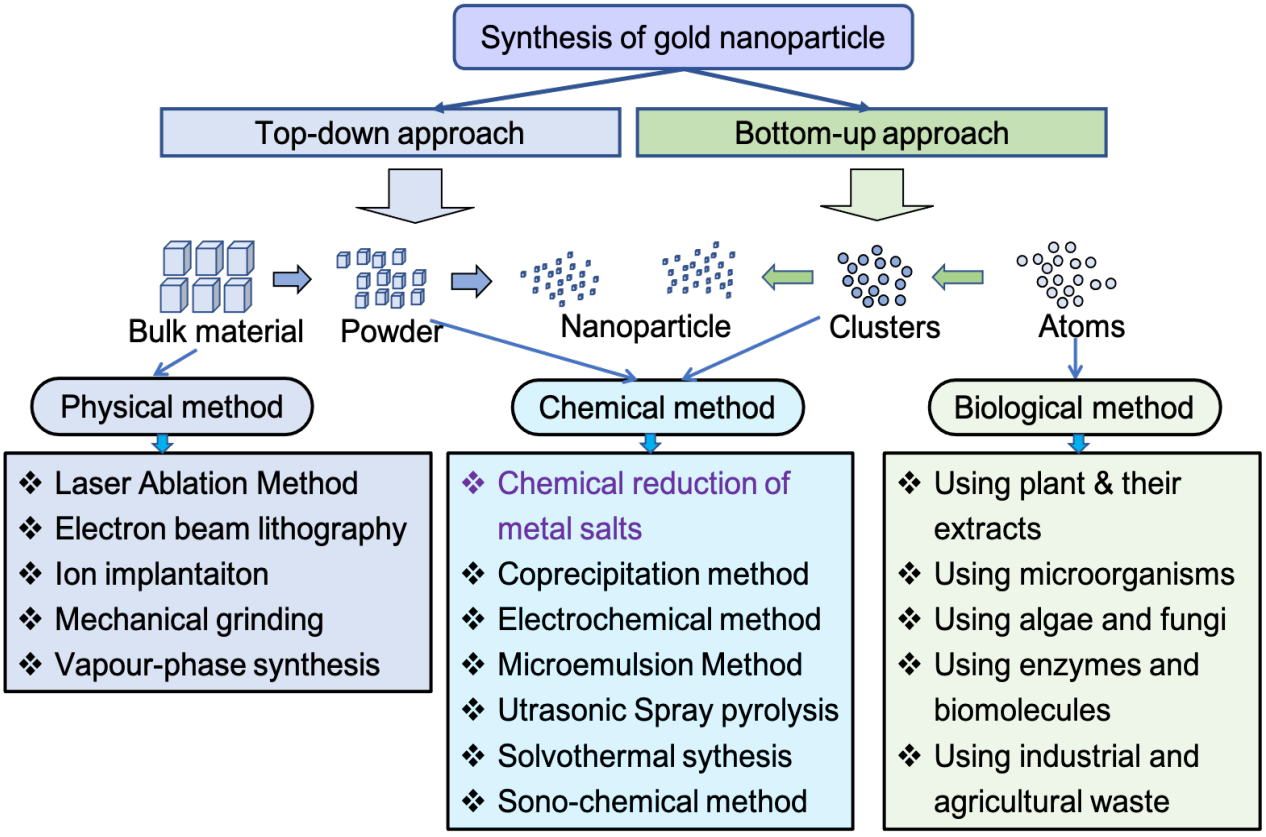

Fig-1.5 Schematic presentation of various synthetic route of gold nanoparticles

1.8 Applications of gold nanoparticles

Gold nanoparticle has ample application if various sections due it tunable surface plasmon properties. Its biomedical application is widely known and has a great contribution in medical sector. Nanoscale gold additives to or surface treatments of fabrics can provide lightweight ballistic energy deflection in personal body armor, or can help them resist wrinkling, staining, and bacterial growth. Moreover, Photothermal therapy (PTT) is referred to as photon mediated induction of the localized therapeutic temperature that can stimulate hyperthermic physiological responses. In simple terms, it melts the tumor in molten gold. This therapy uses metal nanoparticles (such as gold) that can exhibit SPR and efficiently convert light into heat. However, the application of gold nanoparticles can be illustrated by the presentation shown in Fig-1.6.

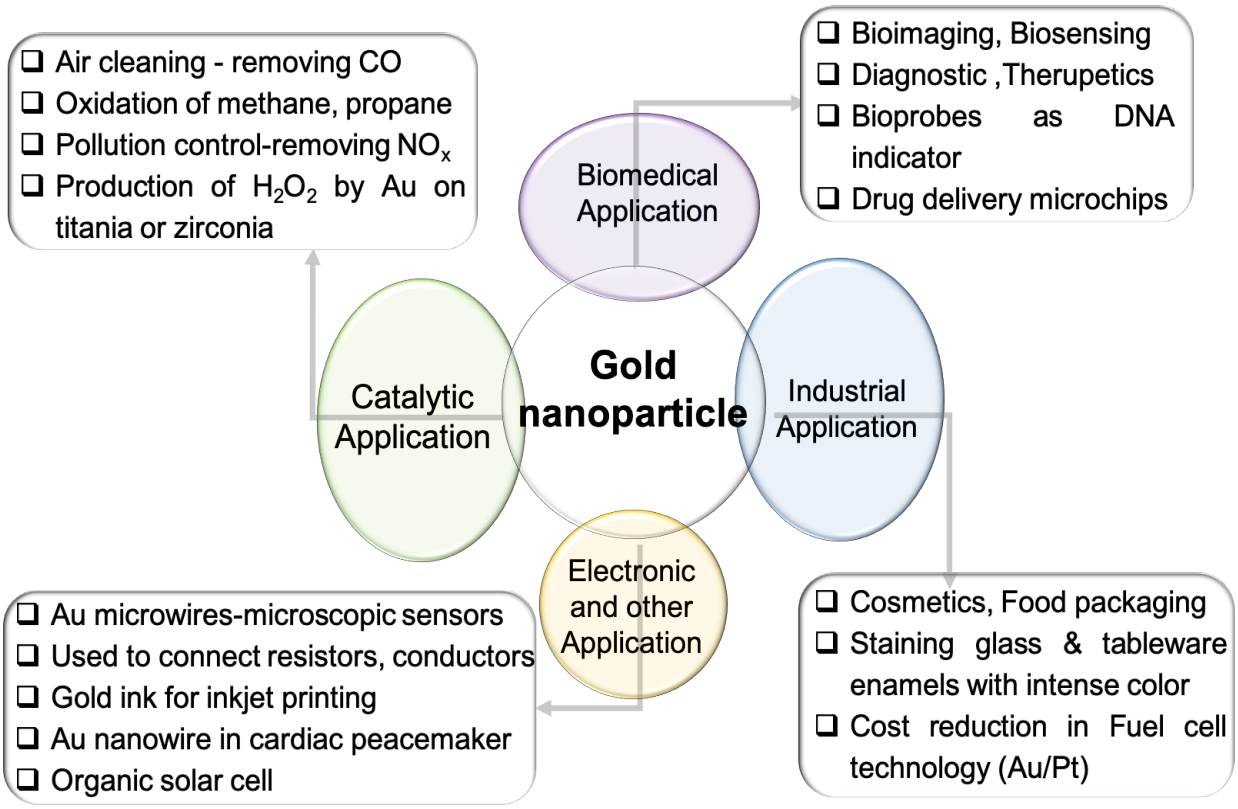

Fig-1.6 Illustration of currently used application area of gold nanoparticles

Catalytic application- AuNPs supported of metal oxide TiO_2 show very potent catalytic activity specially for oxidizing CO to CO_2 even at -70ºC. Moreover it is effective in various chemical processing and environmental remediation. It also help to manage emission by the oxidation of methane and propane. gold nanoparticles can promote the TiO_2 in the photocatalytic oxidation of water and removes contaminants such as thiocyanate ions, azo-dyes and 4- chlorophenol. Thereby, it can play an important role in pollution control and water purification.

Biomedical application- AuNPs are some of the most investigated nanotechnological tools for optical biosensing and bioimaging due to their easy fabrication, chemical stability, outstanding biocompatibility and versatile optical properties. AuNPs absorb incident photons and convert them to heat to destroy cancer cells. AuNPs easily conjugates with biomolecules and the LSPR shift caused by both scattering and absorption and tuned by size, shape, and interparticle distance can

be utilized to report the absence or presence of the target molecules thereby can detect, image or sense an specific target. improved in terms of their sensitivity, specificity, speed, contrast, resolution and penetration depth. That is why it is widely used in bioimaging and biosensing such as strong X-ray attenuation, MRI molecular imagaing. computed tomography (CT) [93], dark-field light scattering, optical coherence tomography (OCT), photothermal heterodyne imaging technique and Raman spectroscopy.

Industrial application- AuNPs have antioxidant, moisture-retaining, whitening and dermo-protective properties, moreover, AuNPs has antibacterial and antifungal properties. Therefore, it is used in anti-aging creams, face mask, toner mists, toothpaste due to its anti-sceptic and anti-inflammatory properties and long lasting effects and increased stability [94]. Lancome (L'Oreal), Dior and Olay (Procter and Gamble) has many cosmetic products using AuNPs [95,96]. Moreover, It can reduce microbial load in food stuff thus can be used in packaging. More interestingly, it is used as coloring agents in staining, glaze and enamels due to its intense and long lasting color. Now-a-days gold based electrocatalyst fuel cell are used instead of platinum in order to reduce the cost.

Electronic application- Gold based microsensors [97] can be used to look at water quality monitoring systems, to monitor chemical and biological reactions over large areas and to monitor algal blooms, chemical, and oil spill events. a way of tracking environmental and health hazards [98]. It can also be used to connect resistors, conductors, and other elements of an electronic chip colorimetric sensor with AuNPs can identify if foods are suitable for consumption [99]. New cardiac patch uses gold nanowires to enhance electrical signaling between cells, a promising step toward better treatment for heart-attack patients [100]. Finally, it is used as gold ink for inkjet printing [101,102] and as a conductor in electronic chips [103].

1.9 Used surfactants AMIET

AMIET is a trade name of non-ionic surfactant of polyoxyethylene alkyl amine given by Kao corporation, Japan. These surfactants are also referred as amine ethoxylates, polyethoxy alkyl amine, polyethoxylated alkyl amine, ethoxylated fatty amines. Each manufacturing company uses its own tradename such as Ethomeen by Akzo Nobel [104], AMIET by Kao Chemicals [105], Voronic®K by Evonik Nutrition & Care GmbH, Sulfonic®T by Huntsman and Viscofine by Kawaken Fine Chemicals Ltd and so forth. An ethoxylated alkylamine has at least one long alkyl chain and 2-50 EO groups (polyoxyethylene) covalently linked to a nitrogen atom [106].

Ethoxylated fatty amines are nonionic surfactants used as an emulsifier and in formulating emulsifier blends. Used as a wetting agents, dispersants, stabilizers, sanitizers and defoaming agents in various industries like textile, paper, drilling, chemical, paint, metal etc. They play an important role in the end applications include agrochemical emulsifiers, industrial cleaners, metal cleaners, textiles, paper de-inking, drilling products and detergents. They are also used as an intermediate for the synthesis of anionic surfactants [107]. Some popular forms of ethoxylated amines widely used in industrial processes include the tallow amine, coco amines, stearyl amines and oleyl amines.

Tallow is a hard fat consists chiefly of glyceryl esters of oleic, palmitic, and stearic acids (16-18 carbon chains). This substance is extracted from the fat deposits of animals, particularly the suet (fat around the kidneys of cattle and sheep). Tallow is used in soaps, leather dressings, candles, food, and lubricants [108].

In addition to tallow, there are other ethoxylated alkyl amines derived from plants, such as coco-amines, oleyamines, soyamines, etc. A major source of cocoamines or cocoalkylamines comes from coconut oil and is widely used in cosmetic formulation.

Usually, these are made by adding ethylene oxide to either primary or secondary fatty amines. In primary amines, both hydrogen atoms of the amine group react with ethylene oxide, resulting in the following structure as in Fig-1.7 [109].

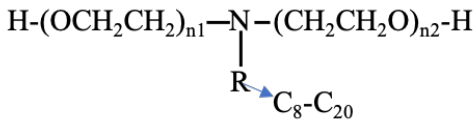

Fig-1.7 General structure of polyoxyethylene alkyl amine (AMIET)

To function as nonionics, R typically contains from 10 to 22 carbon while 5 to 20 moles ($n_1 + n_2$) of ethylene oxide is needed to give an appropriate HLB (hydrophilic-lipophilic balance).

These Surfactants acquire cationic properties when there are fewer EO units and a low pH <6. Nevertheless, at high EO levels and neutral pH, they behave like nonionics. A Low EO content impairs the solubility of surfactants in water, but they become soluble in acid solutions.Generally, amine ethoxylates are water soluble at high pH if the length of the alkyl chain of the compound is not long (usually a C12 chain suffices for reasonable solubility at sufficient EO content) [110].

Nonionic surfactants are usually prepared by reacting an alkylene oxide, typically ethylene oxide, with alcohol, alkylphenol, alkylamine, fatty acid or another appropriate compound containing at least one hydrogen atom. Nonionic surfactants contain a variety of species with different molecular weights, since the polyether chains contain varying numbers of oxyethylene units..

In the manufacturing process, primary amine is dehydrated under vacuum, padded with nitrogen, and ethylene oxide is added to produce diethanolamine. The addition of the second mole is more rapid than the first, but the diethanolamine is hardly ethoxylated over excess ethylene oxide The addition of the second mole is more rapid than the first but then, even in the presence of excess ethylene oxide, there is little or no ethoxylation of the diethanolamine [111]. The reaction takes place at a temperature of 120°C:

$$RNH_2 + CH_2CH_2O \rightarrow RNHCH_2CH_2OH$$

$$CH_2CH_2O + RNHCH_2CH_2OH \rightarrow RN(CH_2CH_2OH)_2$$

After the first step is complete, the further ethoxylation is catalyzed with either sodium or potassium hydroxide at 150 ºC temperature, depending on the degree of ethoxylation required. The

two main materials produced commercially are the diethanolamines, which are used in plastics as antistatic or antifog agents and the 15-mol ethoxylate, which is used as an adjuvant in herbicide formulations [111].

An important characteristic of Physico-chemical properties of surfactants relates to the balance between their hydrophilic and hydrophobic moieties i.e. HLB [112]. HLB value determines whether a surfactant will create an oil-in-water or oil-in-water emulsion. Emulsifier with lower HLB values of 3-6 are lipophilic and promote oil-in-water emulsification, while higher values of 10-18 are hydrophilic and promote oil-in-water emulsification [113]. It is known that surfactants can exist as monomers (numeric species) in very low concentrations in water. Under such conditions, the hydrophobic tail cannot form hydrogen bonds with surrounding water molecules, which disturbs the water structure, increasing the free energy of the system. At higher concentrations, when this effect is more pronounced, there can be a reduction in free energy because micelles can be formed where the hydrophobic tails are at the center and the hydrophilic heads are exposed to the bulk water [114].

A nonionic surfactant does not exhibit electrostatic interactions with the surface of the particle and the hydrophilic groups of the surfactant. During the aqueous phase of surfactants like Tween 20, the highly hydrated polyoxyethylene chain is extended into a coil which acts as an effective barrier against aggregation. The highly hydrated polyoxyethylene chain in Tween 20 is extended into the aqueous phase in the form of a coil that acts as an effective barrier against aggregation. As in AMIET320, 20 units of oxyethylene are sufficient for the formation of steric hindrance, whereas AMIET102, AMIET105 may not be able to provide a significant barrier for dispersing the Au particles due to their short chains of oxyethylene. The highly hydrated nature of polyoxyethylene chains will allow the polyoxyethylene chains to adhere to the particle surface and form a steric barrier [114]. It is noteworthy that polyoxyethylene is subject to oxidative attack and must be stabilized with an antioxidant. An effective method of stabilizing aqueous solutions is to add 2-5% of isopropyl alcohol to the aqueous solution [115].

Tallow alkyl amines and cocoalkyl-amine have a chain length distribution which resembles as in the following [116,117] table.

Table-1: Approximate alkyl chain length distribution of polyethoxylene alkyl amine surfactant

	Coco alkylamine [118]	Tallow alkyl amine [119]	The ' represents unsaturation degree 1, the " represents unsaturation degree 2, and so on.
C_6	0.5 %	-	
C_8	8 %	-	
C_{10}	7 %	-	
C_{12}	50 %	-	
C_{14}	18 %	0 % - 6 %	
C_{16}	8 %	20 % - 37%	
$C_{16'}$	-	3 % - 9%	
C_{18}	1.5 %	14 % - 21%	
$C_{18'}$	6 %	35 % - 46 %	
$C_{18''}$	1 %	4 % - 10 %	
$C_{18'''}$	-	0 % - 3 %	

The structure of five AMIETs used to synthesize AuNPs has been designated as AMIET 320, AMIET 302, AMIET 105, AMIET 105A, and AMIET 102 provided by Kao Chemical Corporation. Since no specific information regarding AMIET 105A is available, based on literature review, it is assumed that AMIET 105A is derived from plants other than coconuts. This could be soybean or olive.

AMIET labels started with 3 indicate tallow alkyl amine, whereas 1 indicates cocoalkyl amine. The last two digits represent the total amount of ethoxylene groups in AMIET. Based on Kao's material safety data sheet [105], AkzoNobel's catalog [104] and [120] present the structure as illustrated in Fig-1.8. Hydrophilic heads such as the ethoxylene $–(OCH_2CH_2)$ moiety are not dissociable into ions and contain hydrogen bonding ethoxylates $–(OCH_2CH_2)_nOH$. Therefore, nonionic surfactants have a good affinity for water due to their dipole-dipole interactions.

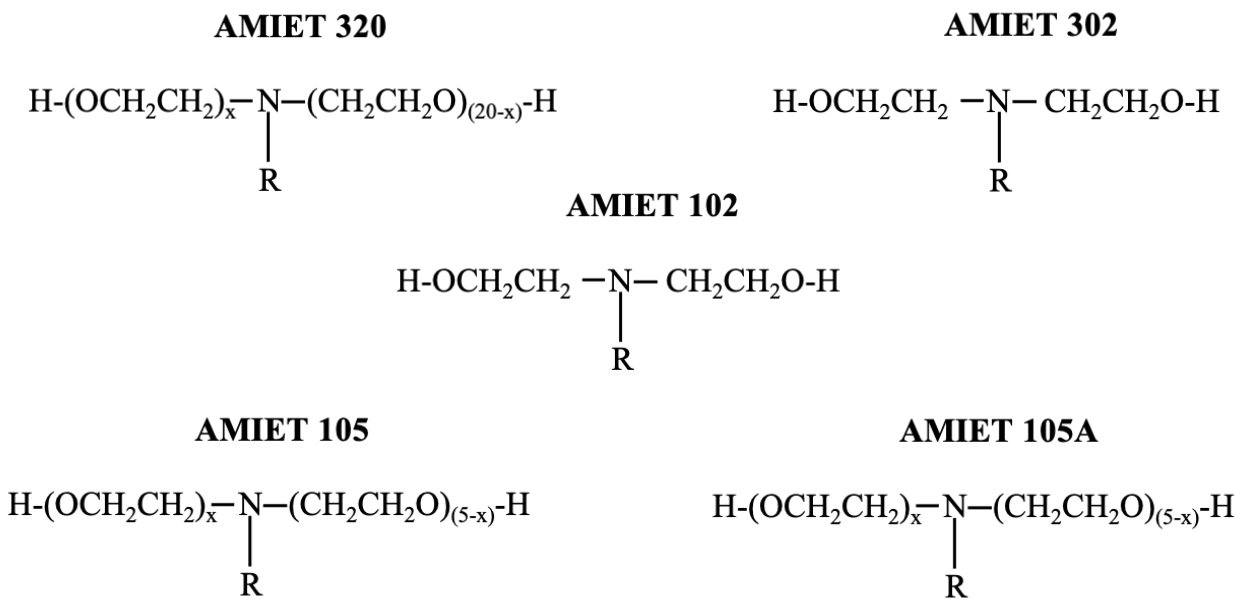

Fig-1.8 An overview of the AMIETs structure used in this thesis

The ratio of hydrophobic fatty amine radicals to hydrophilic polyglycol chains in the molecules determines their physical and chemical properties, especially their surface-activity. It is necessary to have at least 4-5 ethylene oxide groups to ensure good solubility in water with a lipophilic group such as a C13 alkyl. However, The ethoxylation degree can reach 20 and even 40 for some applications.

Furthermore, it is important to note that, Although the polyethylene-oxide (EO) chain is generally hydrophilic, each EO group is composed of two ($-CH_2$) units that are hydrophobic. It becomes evident when it is realized that the polypropylene-oxide chain, the counterpart with three carbon atoms, is globally hydrophobic. Thus, the hydrophilicity conferred by the oxygen atom is compensated by approximately 2.5 methylene groups. In this way, these surfactants can be dual in nature. Therefore, any change in formulation or temperature that alters the interaction between the poly EO chain and the water/oil physicochemical environment is likely to alter this surfactant's behavior [121].

1.10 A brief overview of the research

This research involved a one-step synthesis of gold nanoparticles by reducing tetra chloroauric (III) acid with polyethoxylated alkyl amine by hot injection method in aqueous media. However, TEM and UV-Vis spectra measurement revealed that the gold nanoparticles synthesized were spherical in shape. Following that, a convenient phase transfer approach was developed to make AuNPs adaptable to a variety of organic solvents, thereby expanding its application area, which was persistently problematic. Intriguingly, our developed phase transfer protocol eliminates limitations of traditional method and easily transfer AMIET-AuNPs to various organic solvents regardless of density without changing their original morphology. Furthermore, I have developed a procedure to remove surfactants from nanoparticles after phase transfer without the use of laborious instruments and chemicals, thereby improving their dispersibility in a variety of organic solvents. Finally, a thin film of AMIET- gold nanoparticles was assessed to observe the potential of the gold nanoparticles. Overall, this project involved an examination of AMIET-AuNPs in all its aspects, including synthesis, morphology, phase transfer, surfactant removal, and thin film deposition. Therefore, the research structure can be summarized as shown in Fig-1.9.

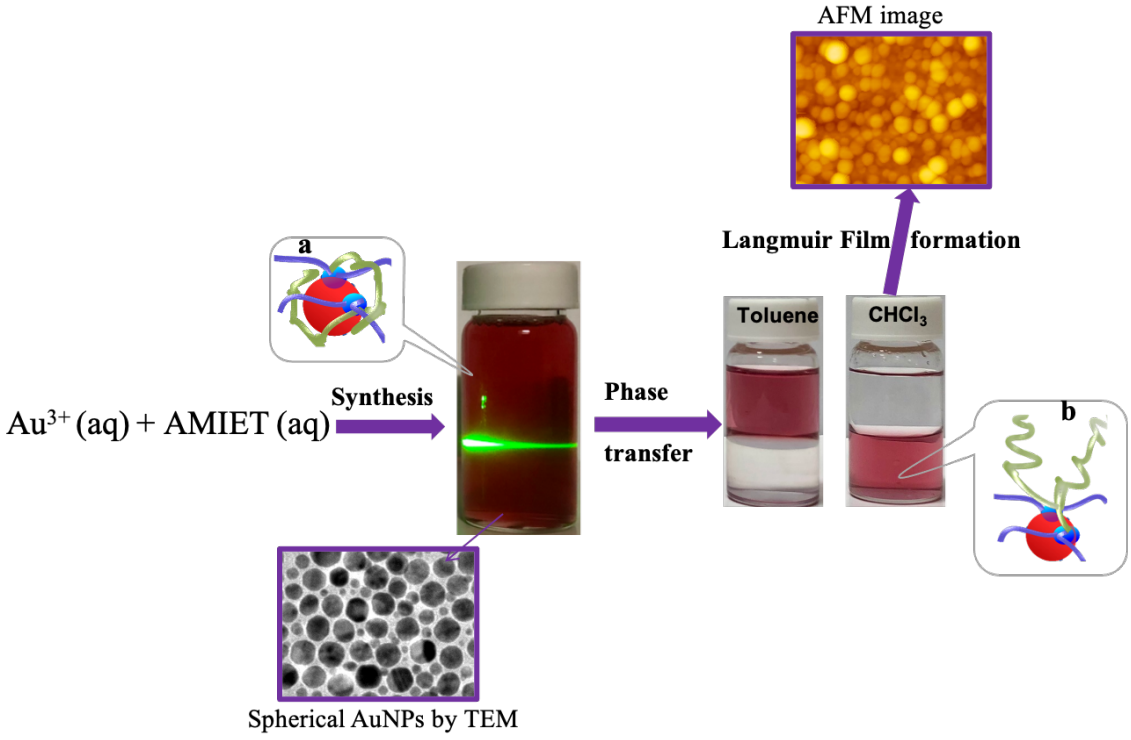

Fig-1.9 An illustration of the synthesis, phase transfer, and Langmuir film formation of AMIET-AuNPs; insets, a and b demonstrate the possible ligand arrangement based on the measurement of NMR spectra.

1.11 Objectives of this work

The primary scope of this thesis is to synthesis in-situ functionalized gold nanoparticle using AMIET, a nonionic surfactant widely is used in industry as antistatic agent, dispersant, emulsifier, detergent for textiles and for many other purposes. However, focusing on the following aims the research were progressed

i) To optimize the synthesis procedure including the ratio of reactant in order.
ii) To understand the reducing property of AMIET and its action on the reduction reaction
iii) To devise a facile phase transfer method of the aqueous AMIET-AuNPs to organic media
iv) To uncover the insight of role of the ligand in phase transfer or the effect of ligand arrangement in two immiscible solvents
v) To remove the indispensable organic residue originated from the synthesis procedure.
vi) To study the thin film formation of AMIET-AuNPs and characterize the AuNPs film.

1.12 References

[1] S.A. Mousa and D.J. Bharali, *Cancers (Basel).*, **3**, 2888–2903 (2011).

[2] A. López-Serrano, R.M. Olivas, J.S. Landaluze, and C. Cámara, *Anal. Methods*, **6**, 38–56 (2014).

[3] L.B. Hunt, *Gold Bull.*, **9**, 134–139 (1976).

[4] O. Dargaud, L. Stievano, and X. Faurel, *Gold Bull.*, **40**, 283–290 (2008).

[5] G.B. Kauffman, *Gold Bull.*, **18**, 31–44 (1985).

[6] Zbingniew Bela, *Brill*, **11**, 1–10 (2006).

[7] G.J. Higby, *Gold Bull.*, **15**, 130–140 (1982).

[8] W.F. Kean, F. Forestier, Y. Kassam, W.W. Buchanan, and P.J. Rooney, *Semin. Arthritis Rheum.*, **14**, 180–186 (1985).

[9] J.H. Brooke, *Br. J. Hist. Sci.*, **6**, 90–91 (1971).

[10] H. B. Hartley, *Oxford Clarendon Press*, **1**, 27–28 (1971).

[11] M. Verità and P. Santopadre, *J. Glass Stud.*, **52**, 11–24 (2010).

[12] S. Frank, *Glas. Technol*, **25**, 47–50 (1984).

[13] A. Neri, C. Merrett, and M. Cable, *By Christopher Merrett*, (1662).

[14] Yu. A. Guloyan, *Springer Sci. Bus. Media LLC Glas. Ceram.*, **68**, 293–296 (2012).

[15] W. Weyl, *Soc. Glas. Technol. Sheff.*, **1**, 24–27 (1951).

[16] D. von Kerssenbrock-Krosigk, *Glas. Technol. Eur. J. Glas. Sci. Technol. A*, **53**, 74–76 (2012).

[17] P. Schlexer, A.B. Andersen, B. Sebok, I. Chorkendorff, J. Schiøtz, and T.W. Hansen, *Part. Part. Syst. Charact.*, **36**, 1–7 (2019).

[18] H.A. Alarifi, M. Atis, A. Hu, M. Yavuz, and Y. Zhou, *J. Phys. Chem. C*, **117**, 12289–12298 (2013).

[19] J. Jeevanandam, A. Barhoum, Y.S. Chan, A. Dufresne, and M.K. Danquah, *Beilstein J. Nanotechnol.*, **9**, 1050–1074 (2018).

[20] M.A.K. Abdelhalim, M.M. Mady, and M.M. Ghannam, *J. Nanomedicine Nanotechnol.*, **3**, 1–5 (2012).

[21] R. Chen, J. Wu, H. Li, G. Cheng, Z. Lu, and C.M. Che, *Rare Met.*, **29**, 180–186 (2010).

[22] S. Bhaskaran, N. Sharma, P. Tiwari, S.R. Singh, and S. V. Sahi, *Sci. Rep.*, **9**, 1–9 (2019).

[23] D.B. Sanchez and F. Tracer, *Int. J. Mod. Phys. B*, **19**, 2604–2609 (2005).

[24] C.M. Cobley, J. Chen, E.C. Cho, L. V Wang, and Y. Xia, *Chem. Soc. Rev*, **40**, 44–56 (2011).

[25] V.A. Ogarev, V.M. Rudoi, and O. V. Dement'eva, *Inorg. Mater. Appl. Res.*, **9**, 134–140 (2018).

[26] M. Singh, S. Lara, S. Tlali, M. Singh, S. Lara, and S. Tlali, *Integr. Med. Res.*, **11**, 922–929 (2018).

[27] Z. Qin, Y. Wang, J. Randrianalisoa, V. Raeesi, W.C.W. Chan, W. Lipiński, and J.C. Bischof, *Sci. Rep.*, **6**, 29836 (2016).

[28] L.M. Rossi, J.L. Fiorio, M.A.S. Garcia, and C.P. Ferraz, *Dalt. Trans.*, **47**, 5889–5915 (2018).

[29] T.S. Rodrigues, A.G.M. Silva, and H.C.C. Pedro, *J. Mater. Chem. A*, **7**, 5857–5874 (2019).

[30] W.J. Sperling, R. A.; Parak, *Phil. Trans. R. Soc. A*, **368**, 1333–1383 (2010).

[31] X. Huang and M.A. El-Sayed, *J. Adv. Res.*, **1**, 13–28 (2010).

[32] P.K. Jain, W. Qian, and M.A. El-Sayed, *J. Phys. Chem. B*, **110**, 136–142 (2006).

[33] D.D. Li, X. Gu, V. Timchenko, Q.N. Chan, A.C.Y. Yuen, and G.H. Yeoh, *Langmuir*, **34**, 10340–10352 (2018).

[34] K.A. Fuller, *J. Opt. Soc. Am. A*, **12**, 881–892 (1995).

[35] J. Zhao, A.O. Pinchuk, J.M. McMahon, S. Li, L.K. Ausman, A.L. Atkinson, and G.C. Schatz, *Acc. Chem. Res.*, **41**, 1710–1720 (2008).

[36] M.B. Cortie and A.M. McDonagh, *Chem. Rev.*, **111**, 3713–3735 (2011).

[37] J. Tang, V. Thakore, and T. Ala-Nissila, *Sci. Rep.*, **7**, 1–20 (2017).

[38] X. Fan, W. Zheng, and D.J. Singh, *Light Sci. Appl.*, **3**, 179–193 (2014).

[39] D.T. Michael, I. M. ; Larry, *Am. Meteorol. Soc.*, **89**, 1853–1861 (2008).

[40] J. Jana, M. Ganguly, and T. Pal, *RSC Adv.*, **6**, 86174–86211 (2016).

[41] A.S. Rubio, *Springer*, **1**, 1–183 (2015).

[42] A. Liang, Q. Liu, G. Wen, and Z. Jiang, *TrAC - Trends Anal. Chem.*, **37**, 32–47 (2012).

[43] S.A. Maier, *Physics, Springer*, **677**, 21–50 (2004).

[44] K.A. Willets and R.P. Van Duyne, *Annu. Rev. Phys. Chem.*, **58**, 267–297 (2007).

[45] J. Conde, G. Doria, and P. Baptista, *J. Drug Deliv.*, **2012**, 1–12 (2012).

[46] P. Chandra, J. Singh, A. Singh, A. Srivastava, R.N. Goyal, and Y.B. Shim, *J. Nanoparticles*, **2013**, 1–12 (2013).

[47] K. Mahato, S. Nagpal, M. Ayesha, S. Ananya, S. Pawan, and K. Maurya, *3 Biotech*, **9**, 1–19 (2019).

[48] D. Wostek-Wojciechowska, J. Jeszka, P. Uznanski, C. Amiens, B. Chaudret, and P. Lecante, *Mater. Sci. Pol.*, **22**, 407–413 (2004).

[49] M.A. Garcia, *J. Phys. D. Appl. Phys.*, **44**, 283001 (2011).

[50] A.S. Bisht, K. Hoang-thi, I. Ledoux-rak, and H. Remita, *Inorganics*, **7**, 64–72 (2019).

[51] X. Tian, Y. Zhou, S. Thota, S. Zou, and J. Zhao, *J. Phys. Chem. C*, **118**, 13801–13808 (2014).

[52] P. Khan, G. Brennan, J. Lillis, S.A. Tofail, N. Liu, and C. Silien, *Symmetry (Basel).*, **12**, 1–57 (2020).

[53] C. Sönnichsen, T. Franzl, T. Wilk, G. von Plessen, J. Feldmann, O. Wilson, and P. Mulvaney, *Phys. Rev. Lett.*, **88**, 774021–774024 (2002).

[54] V. Amendola and M. Meneghetti, *J. Phys. Chem. C*, **113**, 4277–4285 (2009).

[55] R. Dorel and A.M. Echavarren, *Chem. Rev.*, **115**, 9028–9072 (2015).

[56] H.C. Shen, *Tetrahedron*, **64**, 3885–3903 (2008).

[57] N. Morita, A. Yasuda, M. Shibata, S. Ban, Y. Hashimoto, I. Okamoto, and O. Tamura, *Org. Lett.*, **17**, 2668–2671 (2015).

[58] C. Trujillo, G. Sánchez-Sanz, J. Elguero, and I. Alkorta, *Struct. Chem.*, **31**, 1909–1918 (2020).

[59] B.R. Reiner, M.W. Bezpalko, B.M. Foxman, and C.R. Wade, *Organometallics*, **35**, 2830–2835 (2016).

[60] G. Lu, P. Zhang, D. Sun, L. Wang, K. Zhou, Z.-X. Wang, and G.-C. Guo, *Chem. Sci.*, **5**, 1082–1090 (2014).

[61] I. Kamiya, H. Tsunoyama, T. Tsukuda, and H. Sakurai, *Chem. Lett.*, **36**, 13–14 (2007).

[62] A. Meffre, S. Lachaize, C. Gatel, M. Respaud, and B. Chaudret, *J. Mater. Chem.*, **21**, 13464–13469 (2011).

[63] B. Marchetti and Y. Joseph, *J. Nanoparticle Res.*, **13**, 3353–3362 (2011).

[64] M. Yamamoto, Y. Kashiwagi, and M. Nakamoto, *Zeitschrift Fur Naturforsch. - Sect. B J. Chem. Sci.*, **64**, 1305–1311 (2009).

[65] B.H. Wu, H.Y. Yang, H.Q. Huang, G.X. Chen, and N.F. Zheng, *Chinese Chem. Lett.*, **24**, 457–462 (2013).

[66] M. Devi, A. Dhir, and C.P. Pradeep, *Eur. J. Inorg. Chem.*, **48**, 4516–4522 (2020).

[67] T. Sainsbury, T. Ikuno, D. Okawa, D. Pacile, J.M.J. Fre, and A. Zettl, *J. Phys. Chem. C*,

111, 12992–12999 (2007).

[68] D. Wang and Y. Li, *Inorg. Chem.*, **50**, 5196–5202 (2011).

[69] S. Mourdikoudis and L.M. Liz-Marzán, *Chem. Mater.*, **25**, 1465–1476 (2013).

[70] H. Kamo, H. Ishibahi, and T. Kobayashi, *J. Japan Soc. Colour Mater.*, **76**, 469–475 (2003).

[71] Q. Shen and J.F. Hartwig, *J. Am. Chem. Soc.*, **129**, 7734–7735 (2007).

[72] Y.S. Bao, M. Baiyin, B. Agula, M. Jia, and B. Zhaorigetu, *J. Org. Chem.*, **79**, 6715–6719 (2014).

[73] D. Guo, G. Xie, and J. Luo, *J. Phys. D. Appl. Phys.*, **47**, 1–25 (2014).

[74] H. Mateos, R.A. Picca, A. Mallardi, M. Dell'Aglio, A. De Giacomo, N. Cioffi, and G. Palazzo, *Appl. Sci.*, **10**, 1–12 (2020).

[75] M. Dell'Aglio, R. Gaudiuso, O. De Pascale, and A. De Giacomo, *Appl. Surf. Sci.*, **348**, 4–9 (2015).

[76] J.P. Sylvestre, S. Poulin, A. V. Kabashin, E. Sacher, M. Meunier, and J.H.T. Luong, *J. Phys. Chem. B*, **108**, 16864–16869 (2004).

[77] S. Barcikowski and G. Compagnini, *Phys. Chem. Chem. Phys.*, **15**, 3022–3026 (2013).

[78] M. De Anda Villa, J. Gaudin, D. Amans, F. Boudjada, J. Bozek, R. Evaristo Grisenti, E. Lamour, G. Laurens, S. Macé, C. Nicolas, I. Papagiannouli, M. Patanen, C. Prigent, E. Robert, S. Steydli, M. Trassinelli, D. Vernhet, and A. Lévy, *Langmuir*, **35**, 11859–11871 (2019).

[79] V. Merk, C. Rehbock, F. Becker, U. Hagemann, H. Nienhaus, and S. Barcikowski, *Langmuir*, **30**, 4213–4222 (2014).

[80] G. Palazzo, G. Valenza, M. Dell'Aglio, and A. De Giacomo, *J. Colloid Interface Sci.*, **489**, 47–56 (2017).

[81] M. Dell'Aglio, V. Motto-Ros, F. Pelascini, I.B. Gornushkin, and A. De Giacomo, *Plasma Sources Sci. Technol.*, **28**, 85017 (2019).

[82] M. Dell'Aglio and A. De Giacomo, *Appl. Surf. Sci.*, **515**, 146031 (2020).

[83] F. Taccogna, M. Dell'Aglio, M. Rutigliano, G. Valenza, and A. De Giacomo, *Plasma Sources Sci. Technol.*, **26**, 45002 (2017).

[84] J.W. Park and J.S. Shumaker-Parry, *J. Am. Chem. Soc.*, **136**, 1907–1921 (2014).

[85] D.B. Grys, B. De Nijs, A.R. Salmon, J. Huang, W. Wang, W.H. Chen, O.A. Scherman, and J.J. Baumberg, *ACS Nano*, **14**, 8689–8696 (2020).

[86] M. Bajaj, N. Wangoo, D.V.S. Jain, and R.K. Sharma, *Sci. Rep.*, **10**, 1–7 (2020).

[87] P. Slepička, N.S. Kasálková, J. Siegel, Z. Kolská, and V. Švorčík, *Materials (Basel).*, **13**, 1–22 (2020).

[88] J. Kimling, M. Maier, B. Okenve, V. Kotaidis, H. Ballot, and A. Plech, *J. Phys. Chem. B*, **110**, 15700–15707 (2006).

[89] Z.S. Pillai and P. V Kamat, *J. Phys. Chem. B*, **108**, 945–951 (2004).

[90] G.L. Hornyak, H.F. Tibbals, J. Dutta, and J.J. Moore, *CRC Press*, **1**, 1–1640 (2008).

[91] B.A. Zsembik, *Handb. Fam. Heal. Interdiscip. Perspect.*, **6**, 40–61 (2006).

[92] K.P. Tyas, P. Maratussolihah, S. Rahmadianti, and G.C.S. Girsang, *Arab. J. Chem. Environ. Res.*, **08**, 436–454 (2021).

[93] Y.-C. Yeh, B. Creran, and V.M. Rotello, *Nanoscale*, **4**, 1871–1880 (2012).

[94] S. Uibel, M. Takemura, D. Mueller, D. Quarcoo, D. Klingelhoefer, and D.A. Groneberg, *J. Occup. Med. Toxicol.*, **7**, 13 (2012).

[95] C. Contado, *Front. Chem.*, **3**, 1–20 (2015).

[96] C.W. Corti, R.J. Holliday, and D.T. Thompson, *Gold Bull.*, **35**, 111–117 (2002).

[97] A. Iwakoshi, T. Nanke, and T. Kobayashi, *Gold Bull.*, **38**, 107–112 (2005).

[98] F. Kuemmeth, K.I. Bolotin, S.F. Shi, and D.C. Ralph, *Nano Lett.*, **8**, 4506–4512 (2008).

[99] Z. He, Z. Zhang, and S. Bi, *Mater. Res. Express*, **7**, 1–13 (2020).

[100] H. Ouyang, Z. Liu, N. Li, B. Shi, Y. Zou, F. Xie, Y. Ma, Z. Li, H. Li, Q. Zheng, X. Qu, Y. Fan, Z.L. Wang, H. Zhang, and Z. Li, *Nat. Commun.*, **10**, 1–10 (2019).

[101] M. Zeng and Y. Zhang, *J. Mater. Chem. A*, **7**, 23301–23336 (2019).

[102] R. Rudolf, P. Majerič, D. Golub, and H.R. Tiyyagura, *Adv. Prod. Eng. Manag.*, **15**, 358–368 (2020).

[103] H.R. Tiyyagura, P. Majerič, M. Bračič, I. Anžel, and R. Rudolf, *Nanomaterials*, **11**, 1–13 (2021).

[104] Akzo Nobel, "Surface Chemistry General catalog", (n.d.).

[105] Kao Corporation, "Material Safety Data Sheet of AMIETs", (2014).

[106] C.G. van Ginkel, C.A. Stroo, and A.G.M. Kroon, *Tenside, Surfactants, Deterg.*, **30**, 213–216 (1993).

[107] J.B. St. Laurent, F. de Buzzaccarini, K. De Clerck, H. Demeyere, R. Labeque, R. Lodewick, and L. van Langenhove, *Elsevier Sci. B.V., Amsterdam*, **1**, 57–102 (2007).

[108] Petro Chem Trade., “Tallow Amine”, (2007).

[109] Floyd E. Friedli, *CRC Press*, **98**, 71–116 (2001).

[110] Tharwat F. Tadros, *Wiley VCH*, **1**, 399–430 (2005).

[111] R.J. Farn, *Blackwell Publ. Ltd*, **1**, 133–152 (2007).

[112] A. Tiehm, *Appl. Environ. Microbiol.*, **60**, 258–263 (1994).

[113] J.D. Desai and I.M. Banat, *Microbiol. Mol. Biol. Rev.*, **61**, 47–64 (1997).

[114] A. Franzetti, I. Gandolfi, G. Bestetti, and I. Banat, *Trends in Bioremediation and Phytoremediation (Research Signpost)*, **1**, 145–156 (2010).

[115] W. Virginia, *Jounal Polym. Sci.*, **57**, 51–57 (1960).

[116] Committee for Risk Assessment RAC Annex 1, *Eur. Chem. Agency*, **1**, 1–105 (2011).

[117] I.J. Boyer, C.L. Burnett, and B. Heldreth, *Cosmet. Ingred. Rev.*, **1**, 1–72 (2013).

[118] A.E. Ullmann, *Acad. Manag. Rev.*, **10**, 540–557 (1985).

[119] I. Boyer, C.L. Burnett, W.F. Bergfeld, D. V Belsito, R.A. Hill, C.D. Klaassen, D.C. Liebler, J.G.M. Jr, R.C. Shank, T.J. Slaga, P.W. Snyder, L.J. Gill, and B. Heldreth, *Int. J. Toxicol.*, **37**, 10–60 (2018).

[120] C.J. Alexander and M.M. Richter, *Anal. Chim. Acta*, **402**, 105–112 (1999).

[121] J.-L. Salager, *Lab. FIRP*, **2**, 1–50 (2002).

Chapter II Synthesis of aqueous polyoxyethylene alkyl amine functionalized gold nanoparticle

Abstract

The present section discusses the synthesis of AMIET-AuNPs made by reducing the gold salt with a non-ionic surfactant polyethoxylated alkyl amine (AMIET). These surfactants are switchable between the nonionic (unprotonated amine) and cationic (protonated amine) states when exposed to an aqueous phase less than pH 6 [1]. It has been used in various applications for many years, including emulsifiers for agriculture chemicals and bitumen, antistatic agents and dispersants, dyes, pigments, and detergents for textiles. In this study, however, AMIET was used as a reducing and capping agent to produce aqueous gold nanoparticles (AuNPs). It has been found that the AMIET can potentially reduce the gold salt and can be attached on the gold nanoparticle's surface which in turn stabilize the colloid. The AMIET has been shown to potentially reduce the gold salt and to attach to the surface of the gold nanoparticles, thereby stabilizing the colloid.

2.1 Introduction

AuNPs are undergoing a revolution [2] in terms of its multidisciplinary applications in both environmental [3,4], medical [5] and molecular sensing [6–9] due to their unique properties, such as quantum effect or fluorescence quenching [10–15]. The extent of these properties are strongly dependent on the size, morphology, and stabilization of nanoparticles, as well as the conditions under which they are synthesized.

The first attempt of colloidal gold synthesis by Faraday in 1857 involved the reduction of $AuCl_4$- ions with phosphorous and the addition of carbon sulfide as a stabilizer [16]. He noticed that optical properties of the ruby-red stable suspensions differed from those observed in the bulk or in the violet or green unstable states. He concluded that, in order to obtain the ruby-red stable colloids, it is important to maintain a certain gold/phosphorus ratio and to add sulfur in a controlled manner [17]. Later, Turkevich explored a variety of synthetic methods for obtaining AuNPs [18] and in 1973, Frens systematically developed methods to synthesize gold nanospheres of variable diameter using the citrate reduction process. However, the gold salts remain the main precursor as it has been since Faraday's research. Additionally, tetrachloroaurate in hydrate form ($HAuCl_4.xH_2O$) is the most commonly used precursor for the synthesis of AuNPs because of its complete solubility in common solvents such as water [19,20]. Nevertheless, unlike gold salt precursors, however, researchers have reportedly used different reducing agents and successfully produced AuNPs.

The preparation of AuNPs by conventional chemical reduction consists of two vital parts. In the first step, the reducing agents such as borohydrides, aminoboranes, hydrazine, formaldehyde, hydroxylamine, saturated and unsaturated alcohols, citric and oxalic acids, polyols, sugars, hydrogen peroxide, sulfites, carbon monoxide, hydrogen, acetylene, and monoelectronic reducing agents including electronrich transition-metal sandwich complexes. In the second step, stabilization occurs through the use of trisodium citrate dihydrate, sulfur ligands, phosphorous ligands, nitrogen-based ligands, oxygen-based ligands, dendrimers, polymers, and surfactant (especially cetyltrimethylammonium bromide, CTAB) [21]. Nevertheless, in many cases, a given reagent can simultaneously act as a capping and reducing agent.

AuNPs formed by reduction methods in an aqueous medium tend to be quasi-spheres [18]. As it has the smallest surface area, reduction is most often used to obtain AuNPs with this morphology [22]. Two steps are involved in the reduction method [23], nucleation, and successive growth. The process is referred to as in situ synthesis when the nucleation and successive take place simultaneously in a single step. If both steps are carried out in two distinct steps, then this process is termed as a seed-growth method. It is preferred to use in situ synthesis for the production of spherical or quasi-spherical AuNPs, and seed-growth method for the production of various sizes and shapes. However, the production of toxic by-products by chemical methods is a frequent issue that poses a threat to living organisms and the environment.

For the synthesis of AuNPs, reducing agents are typically used to convert Au ions into AuNPs [24]. However, thermolytic reduction at higher temperatures can be accomplished in two ways: (i) "heat up" approach- using a heating mantle or an oil bath to increase the temperature of the reaction mixture and (ii) through the so-called “hot-injection” technique, where a cold solution of precursor molecules is rapidly injected into a hot coordinating alkyl solvent [25]. Wang and Li have recently reported an improved hot-injection method which involves the simultaneous use of octadecylamine (ODA) [26].

The polyethoxylated alkyl amine is a long-chain tertiary alkyl amine that can act as an electron donor under elevated temperatures. Additionally, AMIET has more electron donating groups than han those of the primary alkylamine surfactants like oleylamine, ODA, and hexadecylamine [26]. As a result, the electron density of AMIET on nitrogen is increased to a greater extent. Consequently, AMIET could potentially reduce Au^{3+} to Au^{0}.

According to previous research on nanoparticle preparation methodologies, nanoparticles can be synthesized using both hydrophilic and hydrophobic solvents [27] but the preparation of the desired particles in organic solvents require more complex and meticulous steps due to the law solubility of gold salts in organic phase [28] and the difficulty in controlling the size and shape of AuNPs [29]. Conversely, aqueous phase synthesis is increasingly prevalent because it is more simple, rapid, and environmentally friendly [30]. Moreover, there are many well-defined

preparation procedures for synthesizing gold nanoparticles in aqueous media [31]. AuNPs are thus most easily and economically synthesized in water when considering their applications.

The present study has therefore prepared gold nanoparticles in aqueous media through a single step synthesis by the reduction of tetra chloroauric (III) using polyethoxylated alkyl amine that serves as a reducing agent as well as capping ligand. The results indicate that only specific ranges of AMIET concentration can produce gold nanoparticles with less residual organic matter and a clear ruby red appearance. It was also observed that each AMIET-AuNP contains particles of different sizes. However, this polydisperse AMIET-AuNPs exhibit sufficient surface plasmon resonance, meaning it may have potential applications.

2.2 Experimental

2.2.1 Materials and methods

Hydrogen tetrachloroaurate (III) tetrahydrate ($HAuCl_4.4H_2O$) was obtained from Fujifilm Wako pure chemicals Industries Ltd. Japan and used as received. The polyethoxylated alkyl amines (AMIET320, AMIET302, AMIET102, AMIET105A and AMIET105) used for the synthesis of Gold nanoparticles (AuNPs) were sourced from Kao corporation, Japan. Ultrapure water (UPW) with a resistance of ~18.2 MΩ.cm was used for final cleaning and as a solvent throughout the experiments. Prior to use, the glass wares were immersed overnight in 5% cica clean solution and sonicated twice with UPW for 15 minutes, followed by drying at 100 ºC for 3 hours in oven.

2.2.2 Preparation of Au^{3+} aqueous solution

1g of $HAuCl_4.4H_2O$ was dissolved in 50 ml of UPW to yield 48.56 mM of Au^{3+} aqueous solution, resulting in a yellow color homogeneous solution.

2.2.3 Preparation of gold nanoparticle's colloid

Gold nanoparticles were successfully prepared through chemical reduction at a high temperature. Initially, AMIET and ultrapure water were heated in a three-naked round bottom flask. Once the temperature reached 80 ºC, a certain amount of 48.56 mM Au^{3+} aqueous solution (yellow color) was added to the flask, similar to the hot injection technique. Following a few minutes, the entire

solution turned wine red, indicating the reduction of gold chloride with the surfactant and the formation of gold colloid. During this stage, the mixture was allowed to reflux for one hour ensuring complete completion of reaction while maintaining the temperature at 80 ºC and stirring rate at 100 rpm. Afterwards, the heat was turned off and the mixture was allowed to cool to room temperature with continuous stirring. Finally, the synthesized gold nanoparticles were collected in a clean glass container and labelled as shown in Table-2. An illustration of the entire procedure is shown in Fig-2.1, and the amounts of reactants used are outline in Table-2.

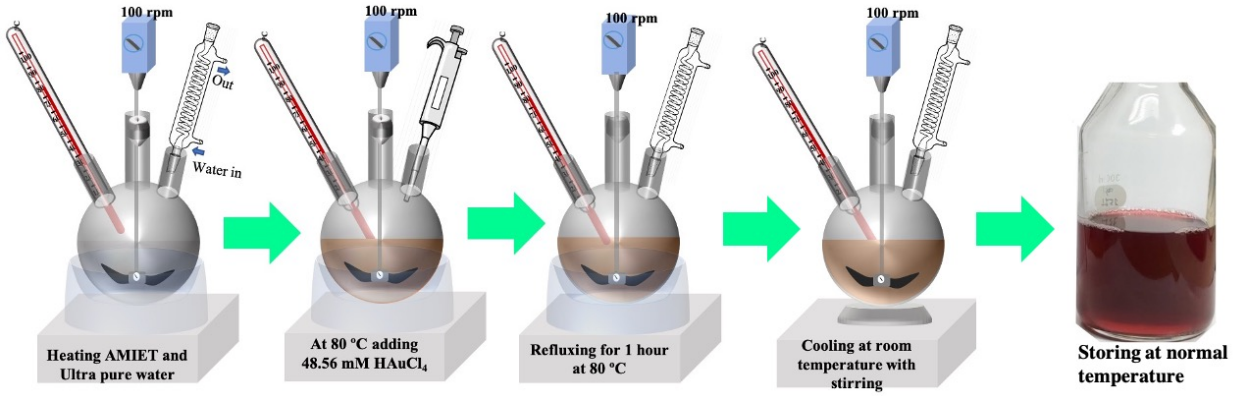

Fig-2.1 Representation of the synthesis rout of AMIET functionalized gold nanoparticles

Table-2 Amount of reactants in the synthesis of AMIET coated AuNPs

Surfactant	Qty. AMIET	Qty. $HAuCl_4$	Qty. UPW	AuNPs
AMIET 320	0.8 ml	48.56 mM, 2.5 ml	300 ml	AMIET 320-AuNPs
AMIET 302	0.4 g	48.56 mM, 1.5 ml	200 ml	AMIET 302-AuNPs
AMIET 105	1.0 ml	48.56 mM, 2.5 ml	300 ml	AMIET 105-AuNPs
AMIET 105A	1.0 ml	48.56 mM, 2.5 ml	300 ml	AMIET 105A-AuNPs
AMIET 102	0.3 ml	48.56 mM, 2.5 ml	300 ml	AMIET 102-AuNPs

2.2.4 Characterization

The absorption spectra of gold nanoparticles were recorded with a JASCO V-670 double beam UV-vis spectrometer using 1 cm path length semi-micro (Q-204, AS ONE) quartz cuvette within the range of 290 nm to 740 nm and the base baseline correction was performed with corresponding solvent and used as a reference. Zeta potential measurements were performed using laser Doppler electrophoresis with Zetasizer Nano ZS (Malvern). The pH of solutions was measured using a pH meter (Mettler Toledo). JEOL JEM 2010 was used for transmission electron microscopy (TEM) analysis. The NMR (Nuclear Magnetic Resonance) spectra were recorded using an Agilent NMR-VNMRS 500 spectrometer spectra were recorded using Agilent-NMR-vnmrs 500 spectrometer. TEM imaging of drop cast nanoparticles prepared from aqueous AMIET-AuNPs may not reflect their dispersion state because drying affects the dispersion. Therefore, we employed an alternate sample preparation approach for TEM to produce solution derived specimens; to prepare the aqueous sample, a few drops of the colloid were placed on the bright side of a copper grid, coated with elastic carbon film (ELA-C10 STEM Cu100P, OKENSHOJI, Japan), and then gently touched with ethanol on a glass slide gently with a tweezer in order to diffuse the particles through the grid.

2.3 Results and Discussion

2.3.1 Formation of gold nanoparticles and UV-visible spectra

An almost immediate change in color from light yellow to red was observed when $HAuCl_4 \cdot 3H_2O$ was added to AMIET, which indicated that the reduction of Au was effective [32–34]. UV-vis

Fig-2.2 Tyndall effect created by the prepared AMIET-AuNPs

spectra of the obtained Au colloid solution show the typical absorption band as expected due to the presence of gold nanoparticles (AuNPs) [34]. Furthermore, the formation of gold nanoparticles in the resulting colloids is further established by the wine red color, indicating light absorption within the visible spectrum and tyndall effect resulting from scattering of light upon interacting with particles in the solution, as displayed in Fig-2.2.

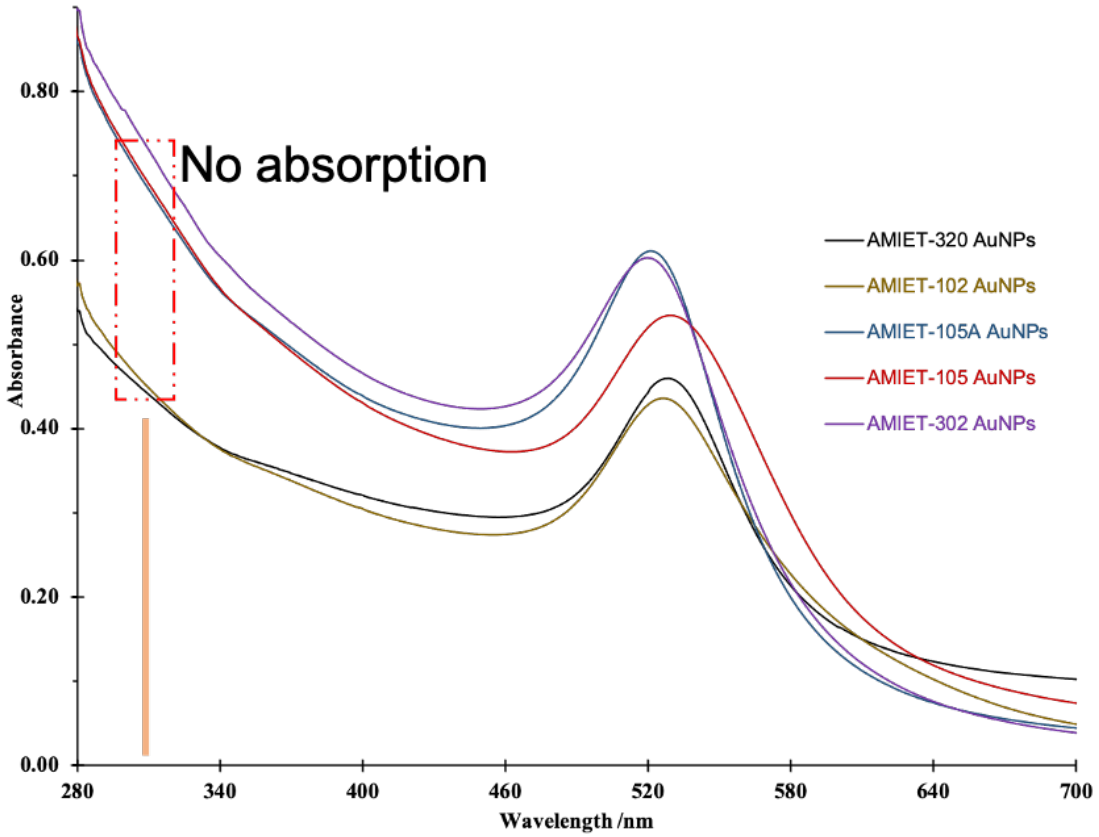

Fig-2.3 UV-Visible spectra of synthesized AMIET-AuNPs

Surface plasmon resonance (SPR) occurs typically in a range of 520 to 540 nm for spherical gold nanoparticles [35,36]. Thus, the peak around 525 nm as seen in Fig-2.3 is attributed to the characteristic surface plasmon resonance absorption of spherical AuNPs that only absorb light in the blue-green region and transmit red light efficiently, resulting in the wine-red color of the colloid. A striking feature of the extinction spectrum is that it results the combination of absorption and scattering components [37–42]. Total extinction caused by all absorption produces sharp band

SPR peaks that also represent the spherical particle [43–45]. In this study, all prepared AMIET-AuNPs shows SPR peaks within the range of 520 to 530 nm, suggesting the formation of spherical or quasi spherical shaped particles [46,47]. Peak broadening may be due to the fact that AMIET-AuNPs are not uniform, rather they are polydisperse [48].

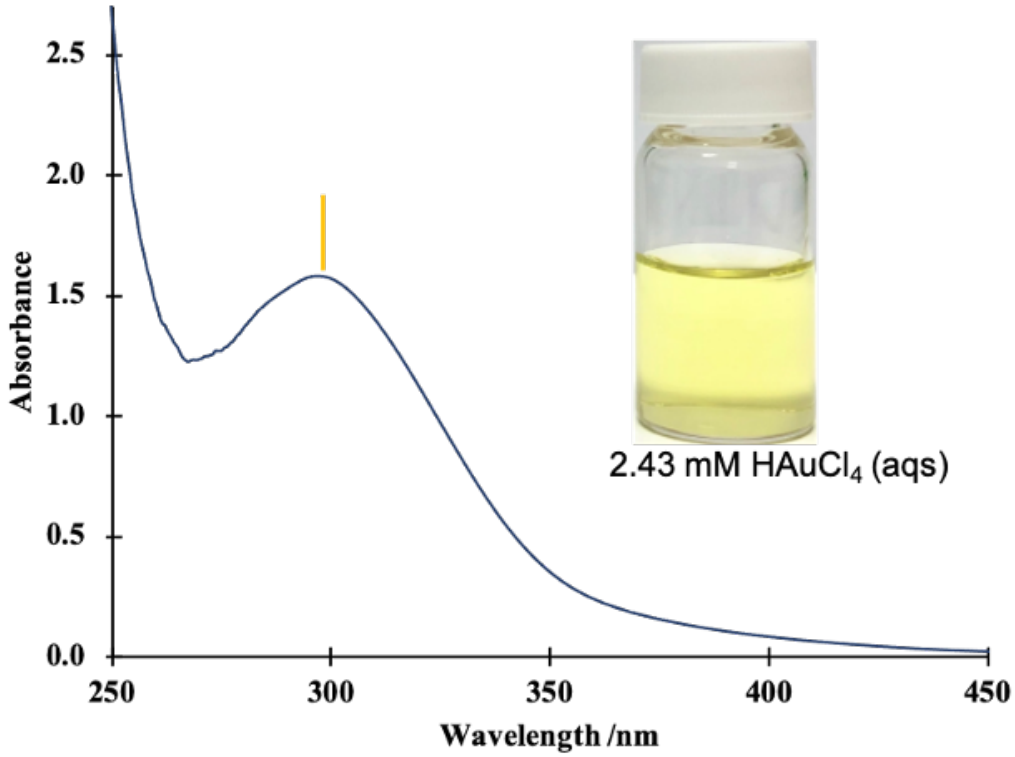

Fig-2.4 Characteristic UV-Vis peak of aqueous Au^{3+}

Moreover, the complete conversion of Au^{3+} to Au^{0} is also ensured by the spectra of resulting AMIET-AuNP as there is no peak around ~300 nm which is the characteristic peak of Au^{3+} due to ligand metal charge transfer and as shown by the UV-vis spectrum of aqueous Au^{3+} solution as in Fig-2.4 [49].

2.3.2 Morphology by Transmission Electron Microscopy (TEM)

It is clearly visible from the TEM images that the gold nanoparticles are spherical in shape with a wide range of sizes. According to the size distribution histogram processed with ImageJ software,

the average calculated diameter ranges from 4 to 24 nm. Observing their distinct appearance, it can be deduced that the AuNPs synthesized are not covered or capped with residues, which indicates a smooth surface. As illustrated in Fig-2.5, the particle sizes in the TEM micrograph are 2-12 nm for AMIET 302-AuNP, 4-20 nm for AMIET 320-AuNPs, 4-18 nm for AMIET 105-AuNPs, 6-24 nm for AMIET 105A-AuNPs and 6-22 nm for AMIET 102-AuNPs. It is noticeable that the large particle with a size of about 15 nm appears to consist of many smaller particles to form an aggregate-like structure in the TEM microgram of AMIET 102-AuNPs as indicated in Fig-4(e). A reliable particle count is impossible in such situations with or without touching particles being ignored. This can be attributed to either the poor nature of TEM sample preparation or the inherent tendency of the nanoparticles to aggregate [50].

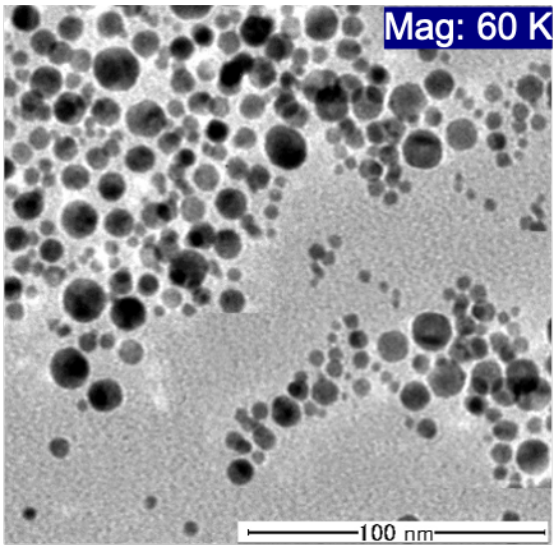

(a)

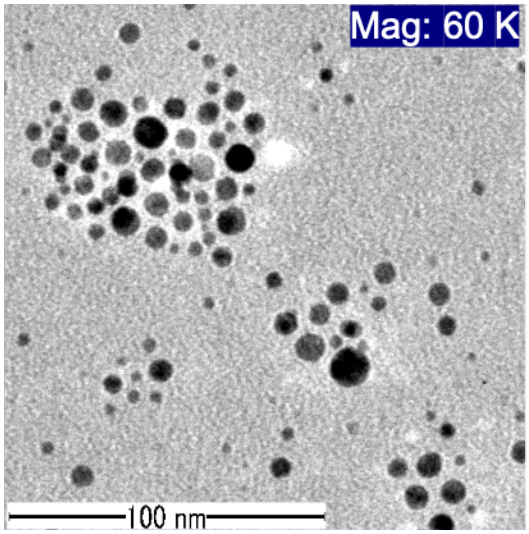

(b)

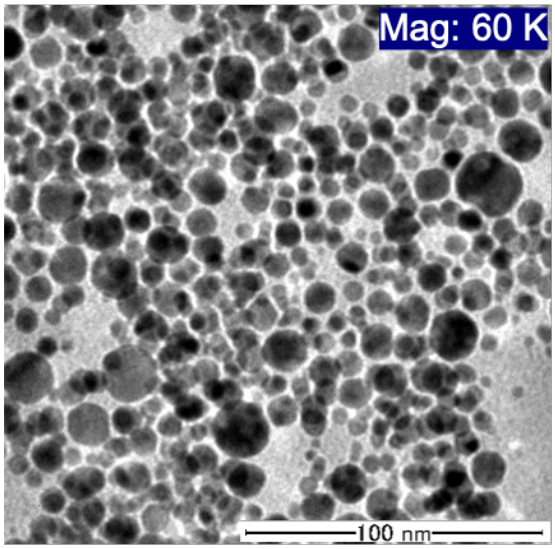

(c)

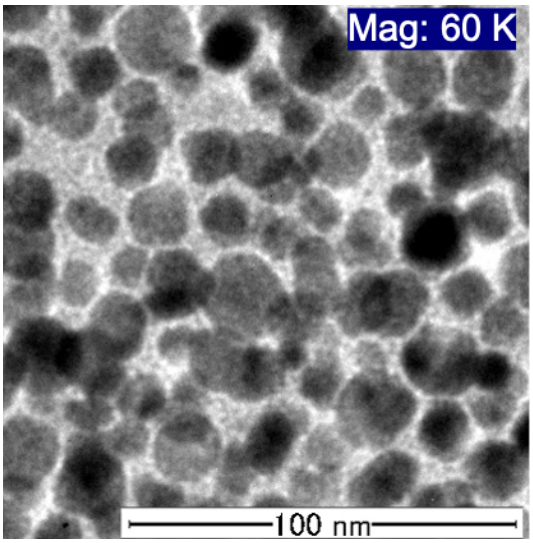

(d)

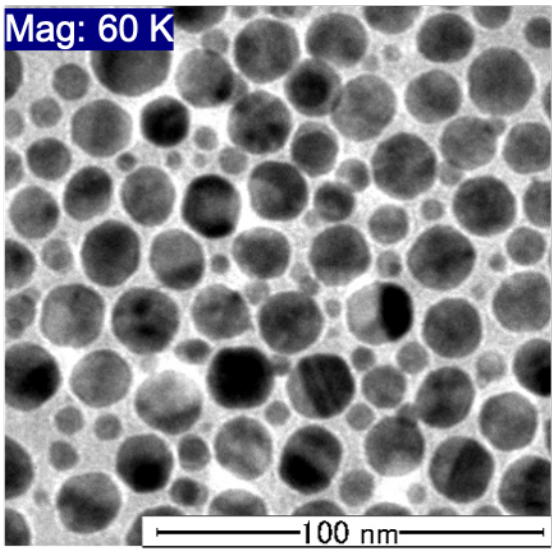

(e)

Fig-2.5 TEM images of five AMIET-AuNPs (a) AMIET 320-AuNPs (b) AMIET 302-AuNPs (c) AMIET 105-AuNPs (d) AMIET 105A-AuNPs (e) AMIET 102-AuNPs

2.3.2 Characterization of ^{1}H NMR spectroscopy

By using ^{1}H NMR, it is possible to directly study molecules that are bound to the surface of these nanoparticles [51]. Since nanomaterials are typically inhomogeneous and have low solubility, solution NMR is often negated by their inefficiency [52]. In addition, when attached to a solid particle, solution NMR signals of molecules bound to nanomaterials become broad and less intense compared to free organic molecules [53]. However, in this section we will highlight the presence

of ^{1}H peak at the ~ 0-4 ppm, which corresponds to the long chain alkyl carbon as evident by Fig-2.6 as an example. The Fig-2.6 also demonstrates the approximate ^{1}H peak assignment of AMIET. According to ^{1}H NMR, the synthesized AuNPs are coated with AMIET; therefore, they are referred to as in situ AMIET functionalized AuNPs.

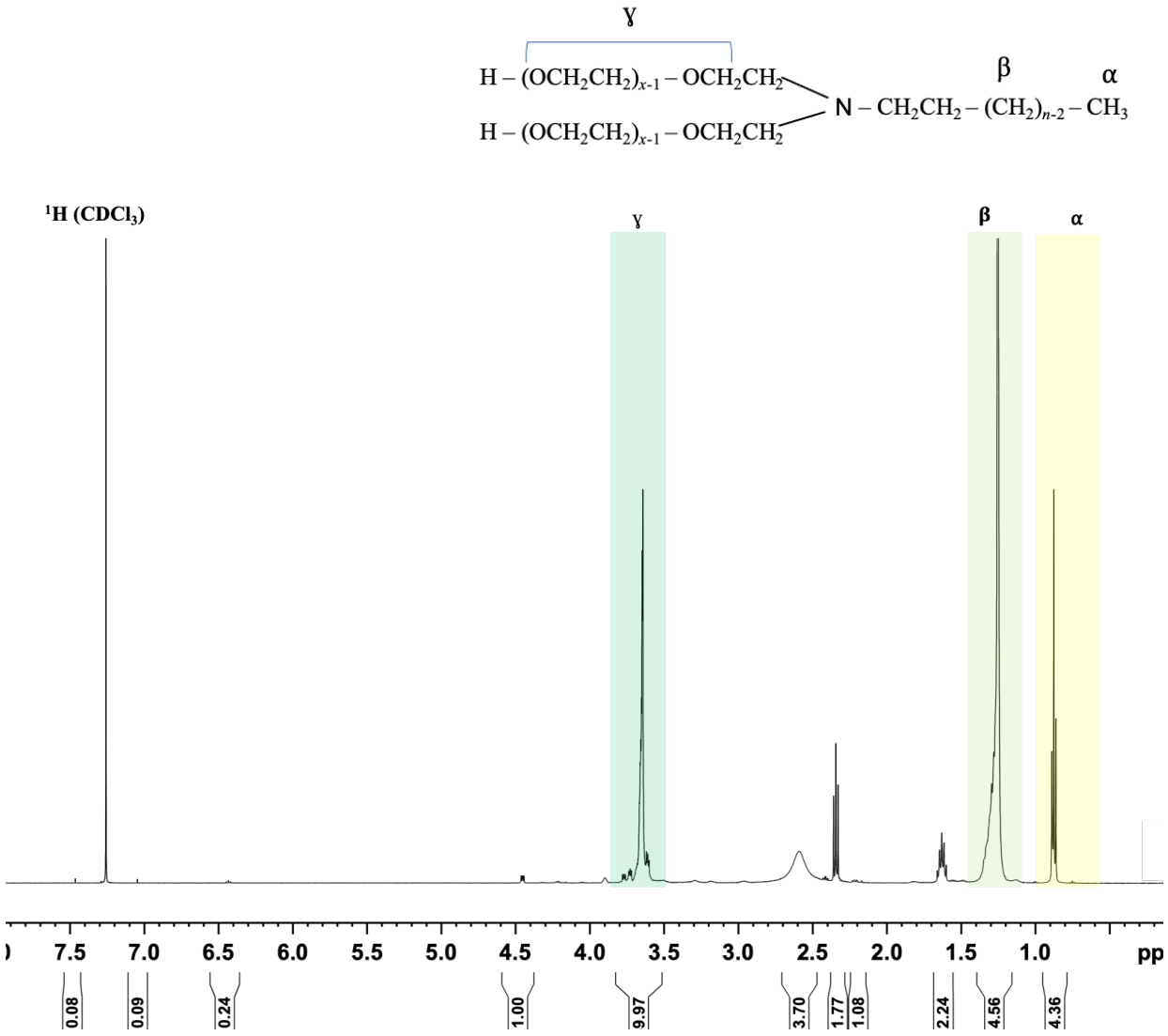

Fig-2.6 1H NMR spectrum of AMIET 320-AuNPs

2.4 Conclusion

Our work investigated a facile method for synthesizing AMIET coated gold nanoparticles using chemical reduction and hot injection procedures. It was found that the quality of gold nanoparticles colloid produced was highly dependent on the ratio of gold precursor and AMIET. It was therefore very important to ensure the right ratio during the synthesis of AuNPs using this method. Although polydispersity is a concern, the experimental results are in good agreement with our predictions. The outcomes could pave the way for simple process design to offer large-scale production of AMIET-AuNPs without the need for complex manufacturing processes and equipment.

2.5 Reference

[1] Y. Chen, A.S. Elhag, B.M. Poon, L. Cui, K. Ma, S.Y. Liao, P.P. Reddy, A.J. Worthen, G.J. Hirasaki, Q.P. Nguyen, S.L. Biswal, and K.P. Johnston, *SPE J.*, **19**, 249–259 (2013).

[2] F.J. Heiligtag and M. Niederberger, *Mater. Today*, **16**, 262–271 (2013).

[3] S. Rahmati, W. Doherty, A. Amani Babadi, M.S. Akmal Che Mansor, N.M. Julkapli, V. Hessel, and K. Ostrikov, *Micromachines*, **12**, 719 (2021).

[4] S.E. Lohse, N.S. Abadeer, M. Zoloty, J.C. White, L.A. Newman, and C.J. Murphy, *ACS Sustain. Chem. Eng.*, **5**, 11451–11458 (2017).

[5] A.J. Mieszawska, W.J.M. Mulder, Z.A. Fayad, and D.P. Cormode, *Mol. Pharm.*, **10**, 831–847 (2013).

[6] G. Liu, M. Lu, X. Huang, T. Li, and D. Xu, *Sensors (Switzerland)*, **18**, 1–16 (2018).

[7] T. Uchida, T. Yoshikawa, M. Tamura, T. Iida, and K. Imura, *J. Phys. Chem. Lett.*, **7**, 3652–3658 (2016).

[8] C. Matricardi, C. Hanske, J.L. Garcia-Pomar, J. Langer, A. Mihi, and L.M. Liz-Marzán, *ACS Nano*, **12**, 8531–8539 (2018).

[9] A. Balčytis, Y. Nishijima, S. Krishnamoorthy, A. Kuchmizhak, P.R. Stoddart, R. Petruškevičius, and S. Juodkazis, *Adv. Opt. Mater.*, **6**, 1–29 (2018).

[10] V. V. Apyari, S.G. Dmitrienko, and Y.A. Zolotov, *Sensors Actuators, B Chem.*, **188**, 1109–1115 (2013).

[11] A.S. Thakor, J. Jokerst, C. Zavaleta, T.F. Massoud, and S.S. Gambhir, *Nano Lett.*, **11**, 4029–4036 (2011).

[12] M. Hojeij, N. Younan, L. Ribeaucourt, and H.H. Girault, *Nanoscale*, **2**, 1665–1669 (2010).

[13] S. Eustis and M.A. El-Sayed, *Chem. Soc. Rev.*, **35**, 209–217 (2006).

[14] D. Pissuwan, T. Niidome, and M.B. Cortie, *J. Control. Release*, **149**, 65–71 (2011).

[15] Y. Zhang, W. Chu, A.D. Foroushani, H. Wang, D. Li, J. Liu, C.J. Barrow, X. Wang, and W. Yang, *Materials (Basel).*, **7**, 5169–5201 (2014).

[16] M. Faraday, *Phil. Trans. R. Soc.,* **147**, 145–181 (1857).

[17] A. Jimenez-Ruiz, P. Perez-Tejeda, E. Grueso, P.M. Castillo, and R. Prado-Gotor, *Chem. - A Eur. J.*, **21**, 9596–9609 (2015).

[18] B. Mehravani, A.I. Ribeiro, and A. Zille, *Nanomaterials*, **11**, 1067 (2021).

[19] R. Rudolf, B. Friedrich, S. Stopić, I. Anžel, S. Tomić, and M. Čolić, *J. Biomater. Appl.*, **26**,

595–612 (2010).

[20] M. Shariq, B. Friedrich, B. Budic, N. Hodnik, F. Ruiz-Zepeda, P. Majerič, and R. Rudolf, *Chem. Open*, **7**, 533–542 (2018).

[21] R. Herizchi, E. Abbasi, M. Milani, and A. Akbarzadeh, *Artif. Cells, Nanomedicine, Biotechnol.*, **44**, 596–602 (2016).

[22] L. de Freitas, G.H.C. Varca, J.G. Dos Santos Batista, and A. Benévolo Lugão, *Nanomaterials*, **8**, 939 (2018).

[23] E.C.B.A. Alegria, A.P.C. Ribeiro, M. Mendes, A.M. Ferraria, A.M. Botelho do Rego, and A.J.L. Pombeiro, *Nanomaterials*, **8**, 6–10 (2018).

[24] H. seok Kim, Y.S. Seo, K. Kim, J.W. Han, Y. Park, and S. Cho, *Nanoscale Res. Lett.*, **11**, 230–239 (2016).

[25] S. Mourdikoudis and L.M. Liz-Marzán, *Chem. Mater.*, **25**, 1465–1476 (2013).

[26] D. Wang and Y. Li, *Inorg. Chem.*, **50**, 5196–5202 (2011).

[27] N.A. Sapoletova, S.E. Kushnir, A.E. Kushnir, P.B. Kocherginskaya, P.E. Kazin, and K.S. Napolskii, *RSC Adv.*, **6**, 112409–112412 (2016).

[28] V. V Terekhin, I.N. Senchikhin, O. V Dement'eva, and V.M. Rudoy, *Colloid J.*, **77**, 511–519 (2015).

[29] S. Thawarkar, T.C. Nirmale, S. More, J.D. Ambekar, B.B. Kale, and N.D. Khupse, *Langmuir*, **35**, 9213–9218 (2019).

[30] X. Wang, S. Xu, J. Zhou, and W. Xu, *J. Colloid Interface Sci.*, **348**, 24–28 (2010).

[31] A. López-Millán, P. Zavala-Rivera, R. Esquivel, R. Carrillo, E. Alvarez-Ramos, R. Moreno-Corral, R. Guzmán-Zamudio, and A. Lucero-Acuña, *Appl. Sci.*, **7**, 273 (2017).

[32] P. Nalawade, T. Mukherjee, and S. Kapoor, *Adv. Nanoparticles,* **2**, 78–86 (2013).

[33] R. Fenger, E. Fertitta, H. Kirmse, A.F. Thünemann, and K. Rademann, *Phys. Chem. Chem. Phys.*, **14**, 9343–9349 (2012).

[34] P.J. Babu, P. Sharma, S. Saranya, R. Tamuli, and U. Bora, *Nanomater. Nanotechnol.*, **3**, 1–7 (2013).

[35] M. Murawska, A. Skrzypczak, and M. Kozak, *Acta Phys. Pol. A*, **121**, 888–892 (2012).

[36] P. Rao and R. Doremus, *J. Non. Cryst. Solids*, **203**, 202–205 (1996).

[37] J.X. Xu, K. Siriwardana, Y. Zhou, S. Zou, and D. Zhang, *Anal. Chem.*, **90**, 785–793 (2018).

[38] G.T. Vasilyuk, V.F. Askirka, A. V Lavysh, S.A. Kurguzenkov, V.M. Yasinskii, O.I.

Kobeleva, T.M. Valova, A.O. Ayt, V.A. Barachevsky, V.N. Yarovenko, M.M. Krayushkin, and S.A. Maskevich, *J. Appl. Spectrosc.*, **84**, 770–779 (2017).

[39] A. Spangenberg, R. Métivier, R. Yasukuni, K. Shibata, A. Brosseau, J. Grand, J. Aubard, P. Yu, T. Asahi, and K. Nakatani, *Phys. Chem. Chem. Phys.*, **15**, 9670–9678 (2013).

[40] D. Kim and Y. Kim, *Catalysts*, **11**, 413 (2021).

[41] B.J. Liu, K.Q. Lin, S. Hu, X. Wang, Z.C. Lei, H.X. Lin, and B. Ren, *Anal. Chem.*, **87**, 1058–1065 (2015).

[42] A.D. Kondorskiy and V.S. Lebedev, *Opt. Express*, **27**, 11783 (2019).

[43] J. Grand, B. Auguié, and E.C. Le Ru, *Anal. Chem.*, **91**, 14639–14648 (2019).

[44] G.Y. Yao, Q.L. Liu, and Z.Y. Zhao, *Catalysts*, **8**, 236 (2018).

[45] A.B. Taylor, J. Kim, and J.W.M. Chon, *Opt. Express*, **20**, 5069 (2012).

[46] A.S. Dileseigres, Y. Prado, and O. Pluchery, *Nanomaterials*, **12**, 292 (2022).

[47] A. Aji, S.J. Santosa, and E.S. Kunarti, *Indones. J. Chem.*, **20**, 413–421 (2020).

[48] A.K. Sahu, A. Das, A. Ghosh, and S. Raj, *Nano Express*, **2**, 1–34 (2021).

[49] S.R. King, J. Massicot, and A.M. McDonagh, *Metals (Basel).*, **5**, 1454–1461 (2015).

[50] S. Mourdikoudis, R.M. Pallares, and N.T.K. Thanh, *Nanoscale*, **10**, 12871–12934 (2018).

[51] F. Du, B. Zhang, H. Zhou, B. Yan, and L. Chen, *TrAC - Trends Anal. Chem.*, **28**, 88–95 (2009).

[52] M. Alvaro, C. Aprile, B. Ferrer, and H. Garcia, *J. Am. Chem. Soc.*, **129**, 5647–5655 (2007).

[53] X. Liu, M. Yu, H. Kim, M. Mameli, and F. Stellacci, *Nat. Commun.*, **3**, 1182–1189 (2012).

Chapter III Phase transfer of *in-situ* AMIET functionalized gold nanoparticles from aqueous to organic solvents

Abstract

This section demonstrates a feasible and reliable phase transfer protocol for dispersed spherical gold nanoparticles to water immiscible organic solvents based on the coagulation and flocculation of the dispersed particles through a liquid-liquid interface. Initially, the colloidal aqueous dispersion is destabilized by adjusting the pH towards the nanoparticle's isoelectric pH in order to modify the interfacial energy and area that lead to particle separation from the liquid. Moreover, it is noteworthy that at this unstable state, the AuNPs spontaneously transfer their phases regardless of the density of nonaqueous solvents. We further explore a mechanistic view of this phase transfer phenomenon by considering the orientation of the hydrophilic-hydrophobic moiety depending on the nearby solvent nature. It is suggested that the surface bound ligand shell can undergo conformational changes based on the solvents around the particles that favor the particles to phase transfer. Interestingly the ^{1}H NMR spectra of AMIET-AuNPs in both media verify this fact. Moreover, TEM images and absorption spectra before and after phase transfer show that the particles retain their original morphology. This makes it suitable for a wide range of applications.

3.1 Introduction

Metallic nanoparticles (NPs) such as Au, Ag, Ru, Pd etc. differ markedly from their bulk counterparts because of their unique size and shape-dependent optical, electrical and thermal properties that results from their large surface area, large surface energies, plasmonic excitation, quantum confinement and a large number of coordination sites [1]. These unique properties could potentially have great impacts on electronic [2], textile [3], catalyst [4], biomedicine [5], fuel cell [6], and other applications. Amongst metal nanoparticles, gold nanoparticles have attracted remarkable interest as it shows a strong absorption of electromagnetic waves in the visible region due to surface plasmon resonance, chemical inertness and highly stable dispersion [7]. The optoelectronic properties of gold nanoparticles make it a versatile material for the use in broad range of applications such as sensory probes, electronic conductors, therapeutic agents, organic photovoltaics, drug delivery and catalysis [8]. Moreover, the optical and electronic properties of AuNPs can be tuned by changing their size, shape, surface chemistry which in turn broaden the application fields. Though the synthesis of AuNPs in water is widely used convenient and economical method, organic dispersion AuNPs is also essential for extending its application. However, it is noteworthy to mention that the usage of nanoparticles in memory elements requires the incorporation of metallic NPs that are free from the contact of water as well as dispersed in an organic matrix [9,10] the organic dispersion is also mandatory for the formation of monolayer of AuNP thin film to weaken the interfacial energy between metal NPs [11,12]. Furthermore, in organic catalysis, solution-processible opto-electronic applications and composite materials, the nanoparticles require to be dispersed and stabilized in non-aqueous liquid phase [13]. Therefore, the transfer of gold nanoparticles specially from aqueous to water immiscible organic solvent is often required in order to increase their applications , as well as to take the advantages of the preparation process in water. However, the critical issue of the phase transfer of colloidal nanoparticles is their colloidal stability [14]. It is often challenging to transfer the nanoparticle from a stable colloid system to another phase, where the particle are at first not able to disperse. Though numerous promising approaches have been carried out for successful phase transfer of nanoparticles from aqueous to organic phase, one of major drawback of those techniques is either to exploiting post synthesis ligand exchange[15] or the addition of cosolvents [16] or employing ionic-liquids [17,18] which may disrupt the integrity of nanoparticles in second solvent. An increasing number of studies have been found in using various methods for phase transfer. For

instance, centrifugation method was extensively studied by J. park et al. [19] that is only useful for the organic solvents that are denser than water and pH-sensitive zwitterionic amphiphiles were used for the recovery and redispersion of AuNPs [20,21], Y. Imura et al. showed a reversible phase transfer by changing the pH of the colloid [22] and the reusability of pH- responsive gold AuNPs catalyst are well investigated by Chakraborty and Christopher [23]. Despite of their success, there are still a number of critical issues including the incomplete transfer with few residual particles remaining in the aqueous phase, the transferred nanoparticles are not fully dispersed in second solvents but rather agglomerate into larger clusters, and the long-term colloidal stability of the transferred particles in nonaqueous solvents during storage is usually questionable. Additionally, most ligand exchange processes are applicable to a very limited types of nanoparticles [13,24]. Therefore, it is necessary to find a more general and robust phase transfer strategy for dispersion of the synthesized AuNPs in organic phase.

We investigated phase transfer of AMIET-AuNPs using three strategies in this study. These strategies include: Method-A: allowing some days with vigorous shaking 3-4 times daily; Method-B: centrifugation; and Method-C: pH triggered phase transfer. It is notable that both method A and B have the same concerns as mentioned in the highlighted literature. Furthermore, in many instances no phase transfer was observed even after a month. Thus, the first two methods are not consistent and reliable for successful phase transfer.

Therefore, we will demonstrate a straight forward effective phase transfer method of laboratory synthesized AMIET-AuNP without the addition of any specific chemical. The goal of this study is to establish a robust and repeatable phase transfer methodology for AMIET-AuNP. However it was observed that the phase transfer of AMIET functionalized AuNPs is strongly influenced by the particle's surface charge and its dispersion pH. It was also observed that only in a narrow pH regime, quantitative phase transfer of in-situ AMIET functionalized gold nanoparticles occurs as the van der Waals attractive force surpasses the electrical double layer repulsive force hereby affecting the colloidal stability in aqueous dispersion. Hence, this study aims to destabilize the aqueous colloidal system by changing its pH in order to obtain nearly zero surface-charged particles that will be stable in nonaqueous phase. Consequently, complete phase transfer was rapidly achieved at the state known as isoelectric pH [25], at which the AuNPs tend to coagulate

or flocculate. Moreover, it is noteworthy that at this unstable state, the AuNPs spontaneously transfer their phases irrespective of the density of nonaqueous solvents as shown in Fig-3.1. It is suggested that the surface bound ligand shell can undergo conformational changes depending on

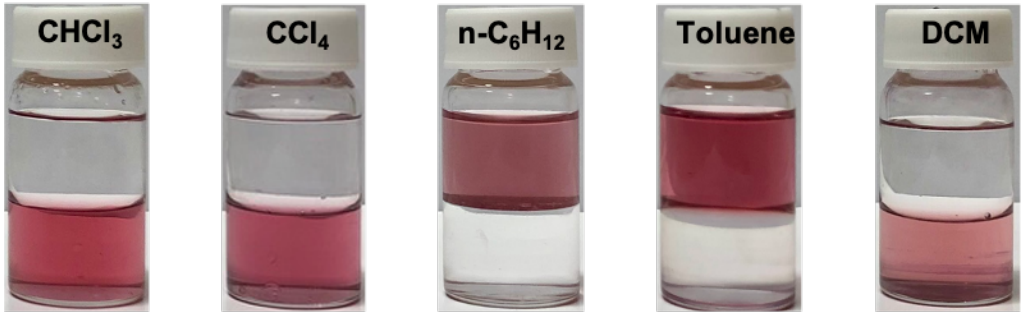

Fig-3.1 Illustration of phase transfer of AMIET-AuNPs, irrespective of solvents density

the surrounding solvents that favors the particles for phase transfer [26][27]. Moreover, it has been found that the AMIET-AuNP after transferring to chloroform is readily dispersed in various organic solvents. Though the morphology of AMIET-AuNPs in different organic solvents has not been examined in this study but it was confirmed by ultraviolet–visible spectroscopy and scanning transmission electron micrographs that the particles preserve their size and morphology, while transferring to chloroform. Furthermore, the ligand arrangement in both phases or the orientational changes of surface bound AMIET has been explained and well supported by their nuclear magnetic resonance spectra.

3.2 Experimental

3.2.1 Materials and methods

Previously synthesized *in-situ* polyethoxylated alkyl amine functionalized aqueous gold nanoparticles such as AMIET 320-AuNPs, AMIET 302-AuNPs, AMIET 105-AuNPs, AMIET 105A-AuNPs and AMIET 102-AuNPs have been taken as the starting materials. Chloroform ($CHCl_3$) from FUJIFILM Wako Pure Chemical Corporation was used as received. Sodium hydroxide (Kanto Chemical Co. Inc.), 37% hydrochloric acid (Kanto Chemical Co. Inc.), and chloroform (FUJIFILM Wako Pure Chemical Corporation) were also used as received for pH adjustment. Ultrapure water obtained by Merck Direct-Q UV was used for final cleaning of glass wares and as a solvent throughout the experiments. Prior to use, the glass wares were immerged

overnight in 5% cica clean (Kanto Chemicals) solution and sonicated with ultrapure water twice for 15 minutes followed by drying for 3 hours at 100 ºC in an drying oven.

3.2.2 Phase transfer method

Method A- 5 ml of chloroform was added to the 5 ml of AuNP solution with vigorous shaking and allowing few days with shaking 3-4 times daily to observe the phase transfer process.

Method B- 5 ml of chloroform was added to the 5 ml of AuNP solution and was centrifuged twice 80 minutes using100 ×100 RPM rotation.

Method-C- pH of AMIET-AuNP colloids were adjusted to 4 , 5, 6, 7, 8, 9, 10 using 0.01 M HCl or 0.01 M NaOH (aq) and their zeta potential were measured. pH adjustment can be demonstrated by the Fig-3.2. The zeta potential vs pH was plotted in order to define the isoelectric point of the

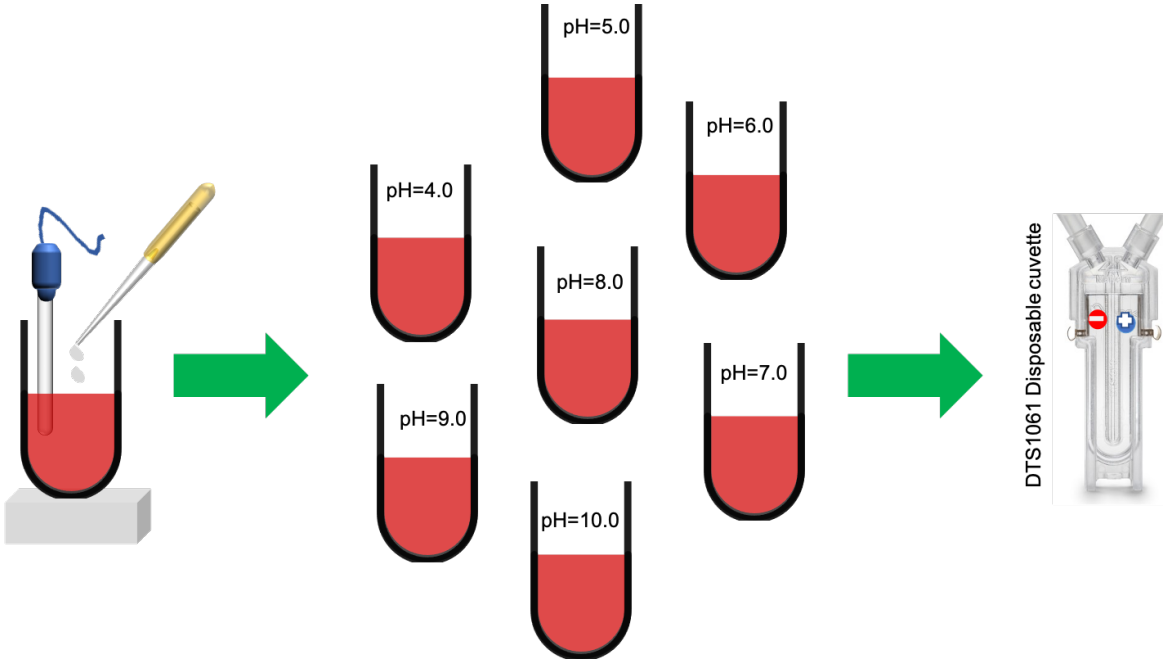

Fig-3.2 pH adjustment and zeta potential measurement for IEP determination

nanoparticle. As the pH of colloidal AuNP was adjusted to its isoelectric point it shows rapid phase transfer upon the addition of organic solvents. Method A, B and C can also be clearly represented by the illustration as shown in Fig-3.3.

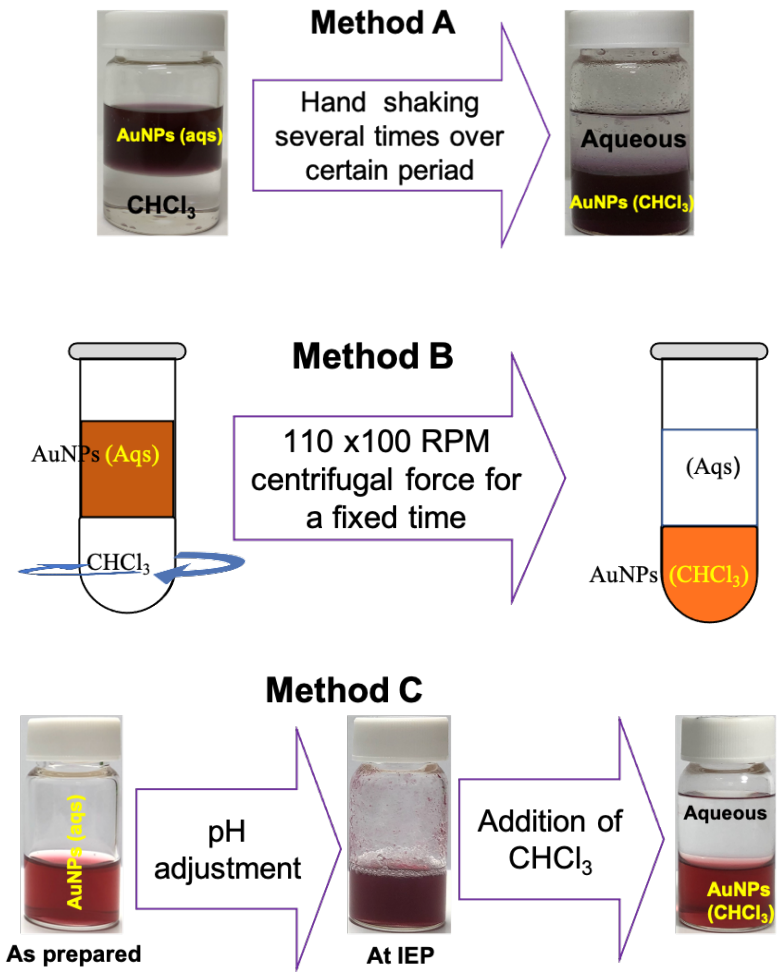

Fig-3.3 Three strategies for phase transfer of aqueous AMIET-AuNPs to organic phase

3.2.3 Characterization

Zeta potential were recorded three readings for each sample at 25 ºC using DTS1061-disposable cuvette by the instrument (Malvern Zetasizer nano ZS) functioned with at a fixed scattering angle of 173º under the 4 mW He-Ne laser operating at wavelength of 633 nm. The UV-visible measurement of AMIET-AuNPs before and after phase transfer were recorded using JASCO V-670 double beam UV-vis spectrometer with 1 cm path length semi micro (Q-204, AS ONE) quartz cuvette within the range of 300 nm to 700 nm and baseline correction was done with corresponding solvent and used as a reference. TEM imaging of samples prepared by drop casting is not representative of the dispersed state of the nanoparticles owing to drying effects. Therefore, we have applied an alternative TEM sample preparation route to produce solution derived specimens; the aqueous sample was prepared by placing a few drops of the colloid on bright side of a copper

grid, coated with an elastic carbon film (ELA-C10 STEM Cu100P, OKENSHOJI, Japan) and then touched gently on a little drop of ethanol on a glass slide with the help of a tweezer in order to diffuse the particles through the grid properly; while TEM sample of the chloroform dispersed AuNPs has been prepared by direct drop casting method. The both techniques can be illustrated as shown in Fig-3.4.

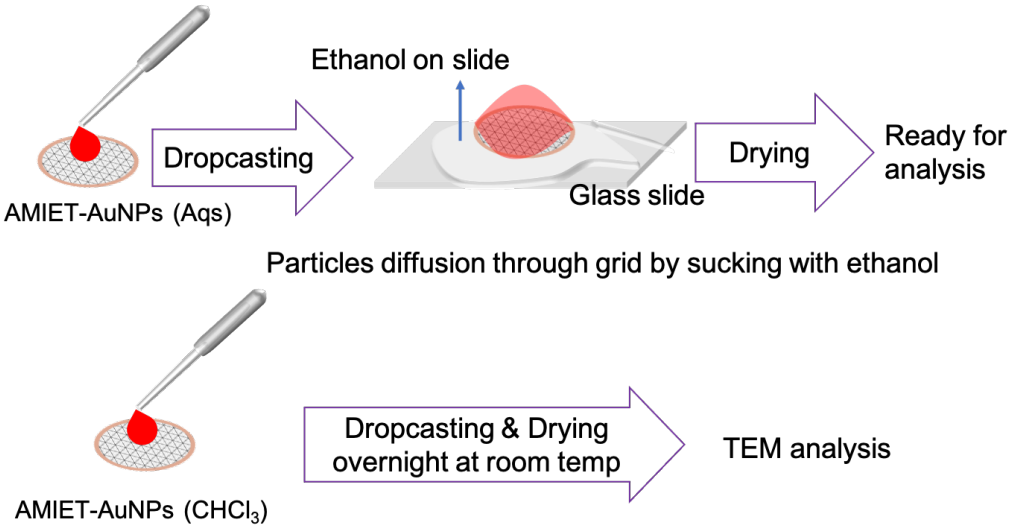

Fig-3.4 AMIET-AuNPs deposition technique on TEM grid

Afterwards, the grid was dried overnight at room temperature because wet sample will degrade high-vacuum inside the column causing undesirable contamination of microscope. Then the well dried samples were used for TEM imaging at 200 kV accelerating voltage and the images were processed using ImageJ software. Nanoparticles were sampled randomly (N) 100 particles for constructing a histogram based on their size. In order to understand the ligand arrangement on the particle surface upon phase transfer the NMR analysis was carried out. In the preparation of NMR sample, the aqueous AMIET-AuNPs was centrifuged and D_2O was added to the sedimented part which results sufficient shimming to take the NMR spectrum. The chloroform dispersed AMIET-AuNP was deuterated by drying 2 ml of the particle at room temperature and dispersed in 2 ml of $CDCl_3$. NMR data were processed by Bruker's Topspin software. The solvent exchange for both phases dispersed AMIET-AuNPs is simply illustrated by the Fig-3.5.

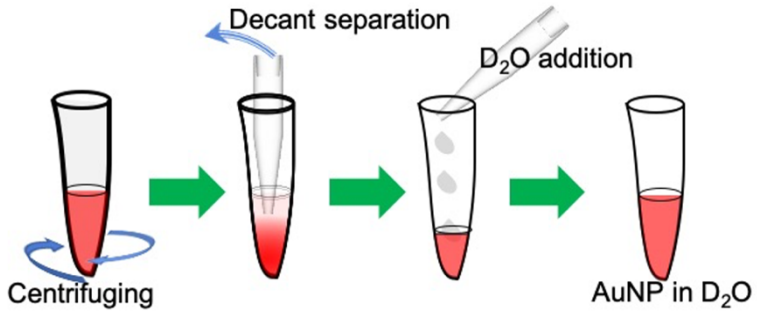

H_2O to D_2O exchange techniques

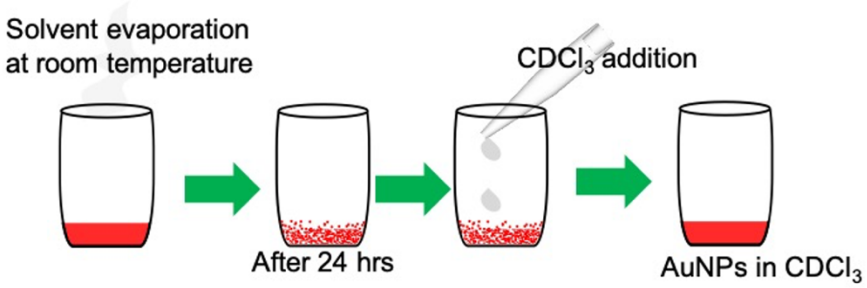

$CHCl_3$ to $CDCl_3$ exchange techniques

Fig-3.5 Solvent exchange for NMR sample preparation

3.3 Results and Discussion

3.3.1 Determination of isoelectric point of AMIET-AuNPs

The factors affecting the zeta potential (ZP) includes pH, ionic strength and concentration of the nano-colloid . However, pH is the most leading parameter in ZP measurements of NPs in aqueous medium. The plot of zeta potential as a function of pH is shown in Fig-3.6 for different AMIET coated AuNPs. The pH of the colloid at which the ZP value is zero i.e. the point where the graph goes through zero is called the isoelectric point (IEP). Therefore, the derived IEPs from the plots 3.6 are 5.4 for AMIET 320-AuNP, about 7.9 for AMIET 302-AuNPs, AMIET 105-AuNPs, AMIET 105A-AuNPs, and 9.0 for AMIET 102-AuNPs. It is noticeable that the obtained IEP value is not absolute for the particular AMIET-AuNPs, a subtle change that could not be controlled by any means during the synthesis of any of the AMIET coated AuNPs would deviate from the derived IEP value. Therefore, it is important to determine the isoelectric point of each freshly prepared AuNPs even if it is reduced by the same AMIET. However, in the unstable zone with ZP

value -30 mV to +30 mV; the Vander Waals attraction overcomes the electrostatic repulsion thus particles tend to agglomerate, and as the pH reached to its IEP, the particles are likely to be agglomerated or coagulated and prone to transfer to another non-polar solvents, and the different stages observed overtime is demonstrated by the Fig-3.7. Conversely, in the stable region shown by the green marked zone, the particles are stable and showing no significant phase transfer.

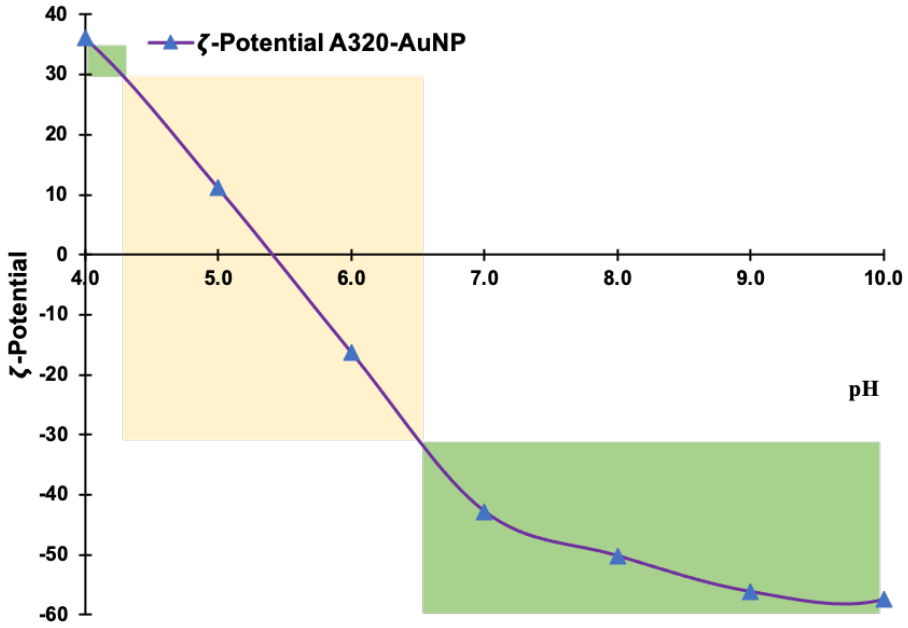

Fig-3.6.1 Zeta potential vs pH plot of AMIET 320- AuNPs

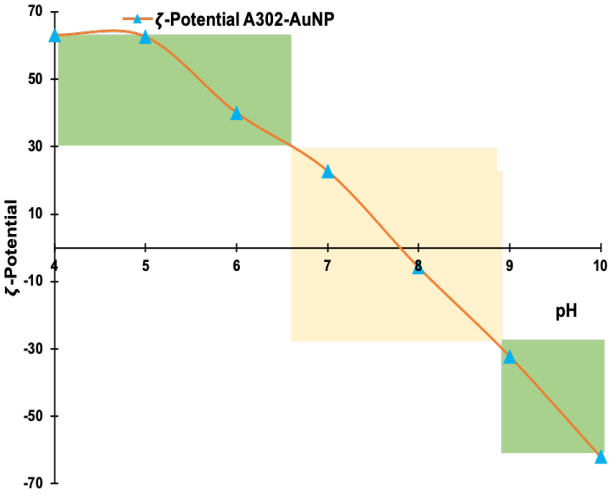

Fig-3.6.2 plot of AMIET 302- AuNPs

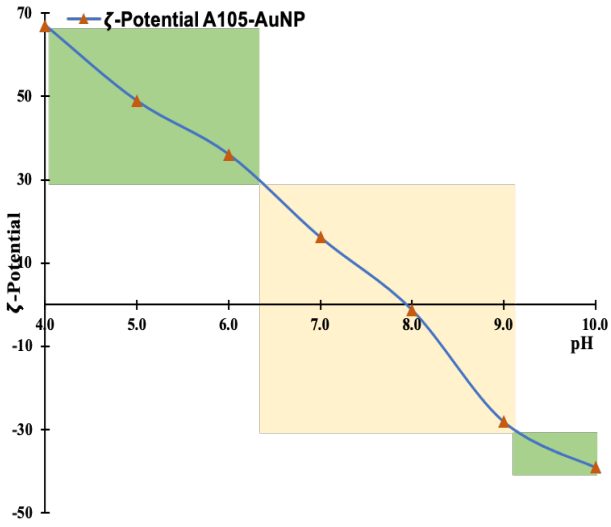

Fig-3.6.3 plot of AMIET 105- AuNPs

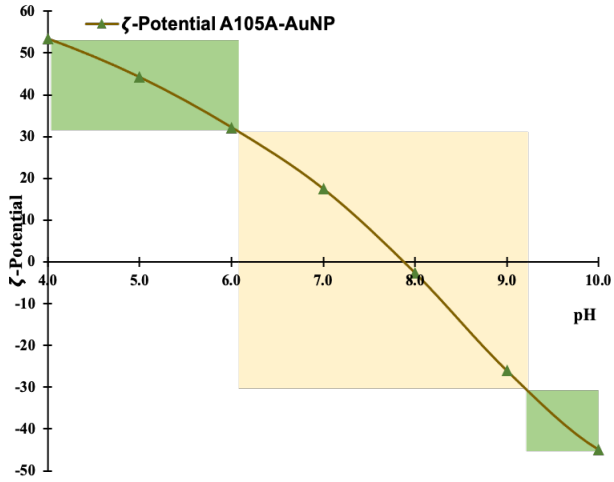

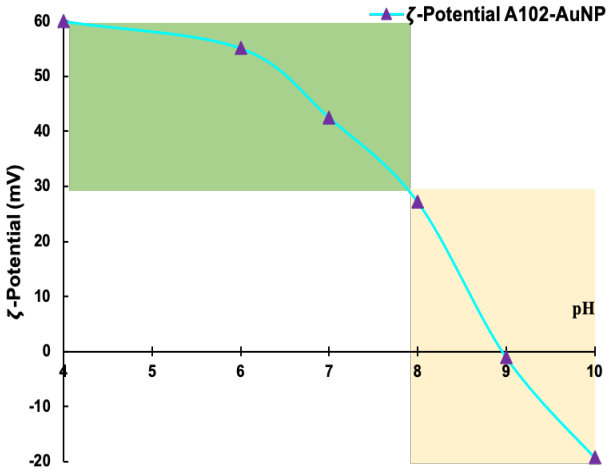

Fig-3.6.4 plot of AMIET 105A- AuNPs

Fig-3.6.5 plot of AMIET 102- AuNPs

Fig-3.6 Zeta potential versus pH plot of AMIET-AuNPs for determination of isoelectric pH (IEP)

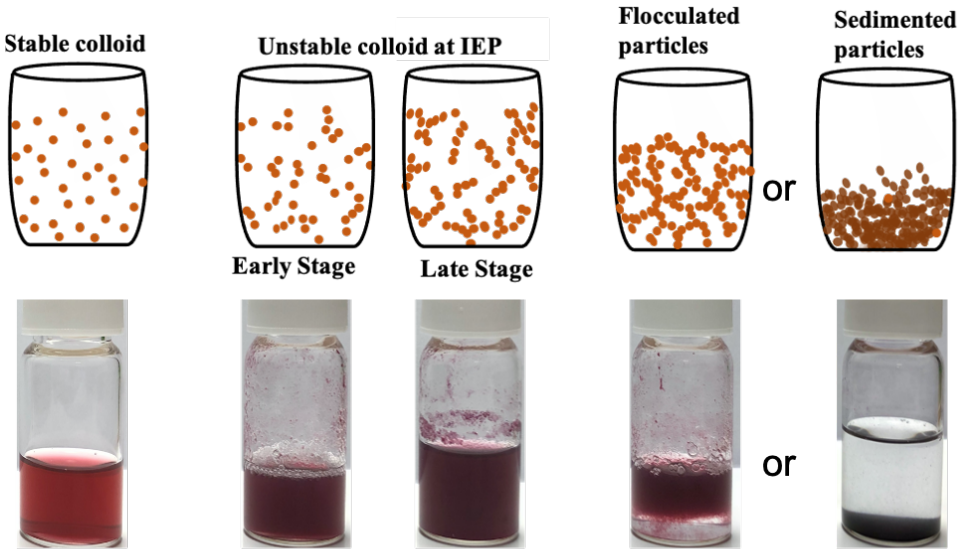

Fig-3.7 The observed phenomena over time after adjusting the pH to IEP

3.3.2 Phase Transfer to organic solvents

The phase transfer by applying the method A, it was observed that the holding period for phase transfer is always different regardless of the synthesis experiments as well as the phase transfer experiments. Even in some cases, the phase transfer is not occurred at all without any obvious reason. However, in this way the transfer phenomenon was not well understood initially.

The phase transfer using second method has a strong correlation with the first method. Though the transfer is enhanced by the centrifugal force, it is not always repeatable for freshly synthesized identical AMIET-AuNPs within the same condition. Moreover, The pattern or the dispersion mechanism would be more or less identical for these two methods. However, the phase transfer using the method-A shows that more than 90% particles are moving towards the chloroform phase after 7 days as show in Fig-3.8, but the complete transfer is not occurred even after a long period of time. Although. Fig-3.8 shows a comparison of phase transfer using first two methods and their

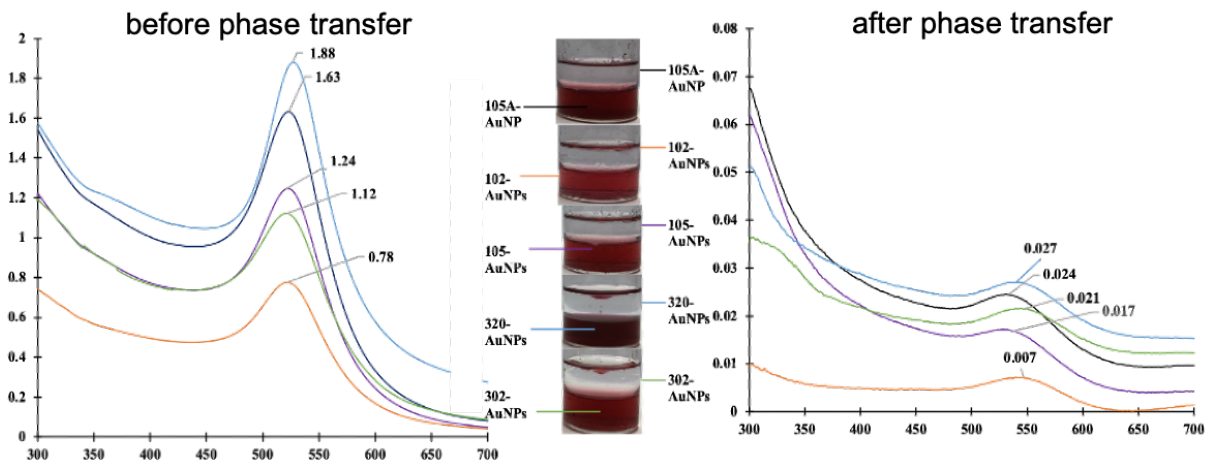

Fig-3.8 Spectra of AMIET-AuNPs with their appearance in aqueouses phases (after 7 days)

phase transfer efficiency. Though 95% transfer efficiency has been presented in the Fig-3.8, but the important breakthrough is that most of the cases the transfer is not complete and clear; even in sometimes there is no transfer at all. Moreover, it is considerable observation that the appearance of aqueous phase after phase transfer is not enough suitable for UV-vis measurement that is evident by the image presented in Fig-3.8 and Fig-3.9. Moreover method-A and method-B are not justifiable for organic solvents that are less dense than water. Furthermore, there are some discrepancies in dispersing the transferred AuNPs in other organic solvents; which was overcome by the later method so called pH triggered phase transfer method described as method-C.

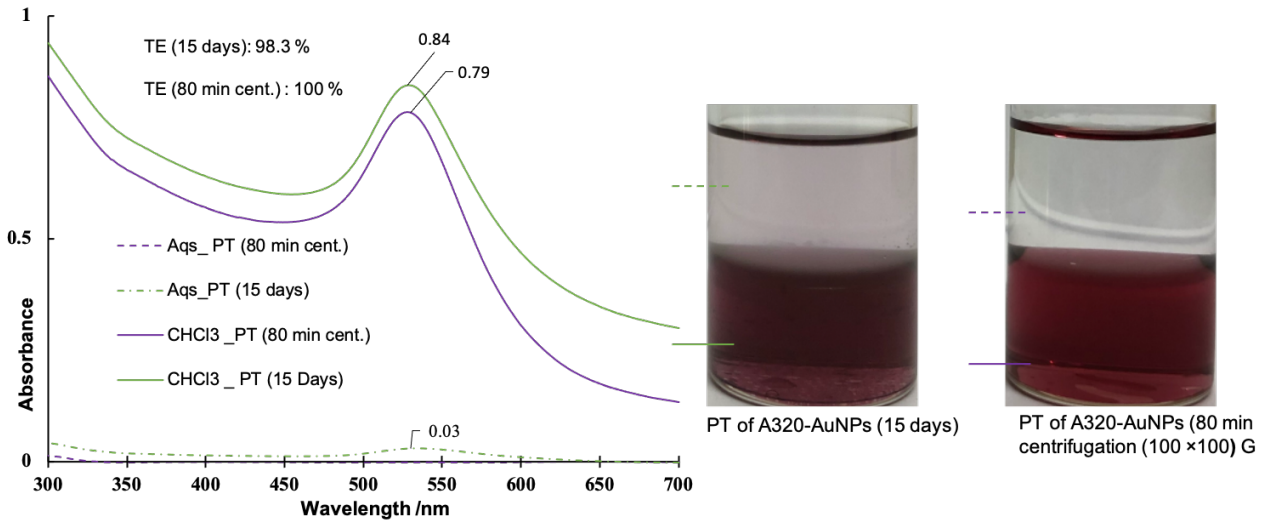

Fig-3.9 Comparison of AuNPs phase transfer efficiency by method A & B with appearances

The investigation carried out in this research revealed that there is no evidence to claim the repeatability and consistency of phase transfer using the above first two methods. Therefore, it has

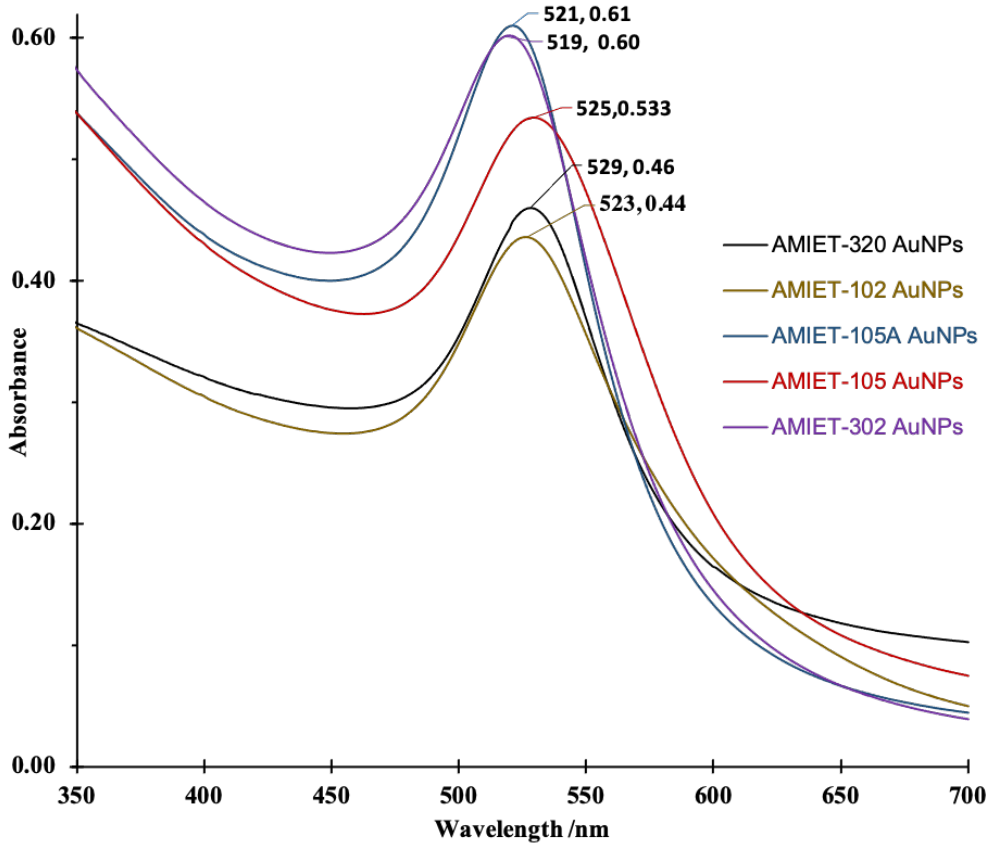

Fig-3.10 Spectra of AMIET-AuNPs before phase transfer

been projected to search an alternative approach and finally it is confirmed that the AMIET functionalized AuNP efficiently transfer to the organic phase when the colloids have zero zeta potential i.e isoelectric pH. At the isoelectric point, the AuNPs can easily be transferred to chloroform and concentrated by more than 10 times. Nevertheless, the AuNPs at their IEP may go under coagulation, flocculation, granulation or even become just cloudy depending on the nature of colloids as clearly demonstrated in Fig-3.7. However, complete transfer is occurred at this unstable state immediately after the addition of organic solvents regardless of the size of the particles and the density of the organic solvents. The complete transfer of Au NPs was confirmed by the UV−vis analysis of the aqueous phase before and after the transfer process as demonstrated by Fig-3.10 and 3.11.

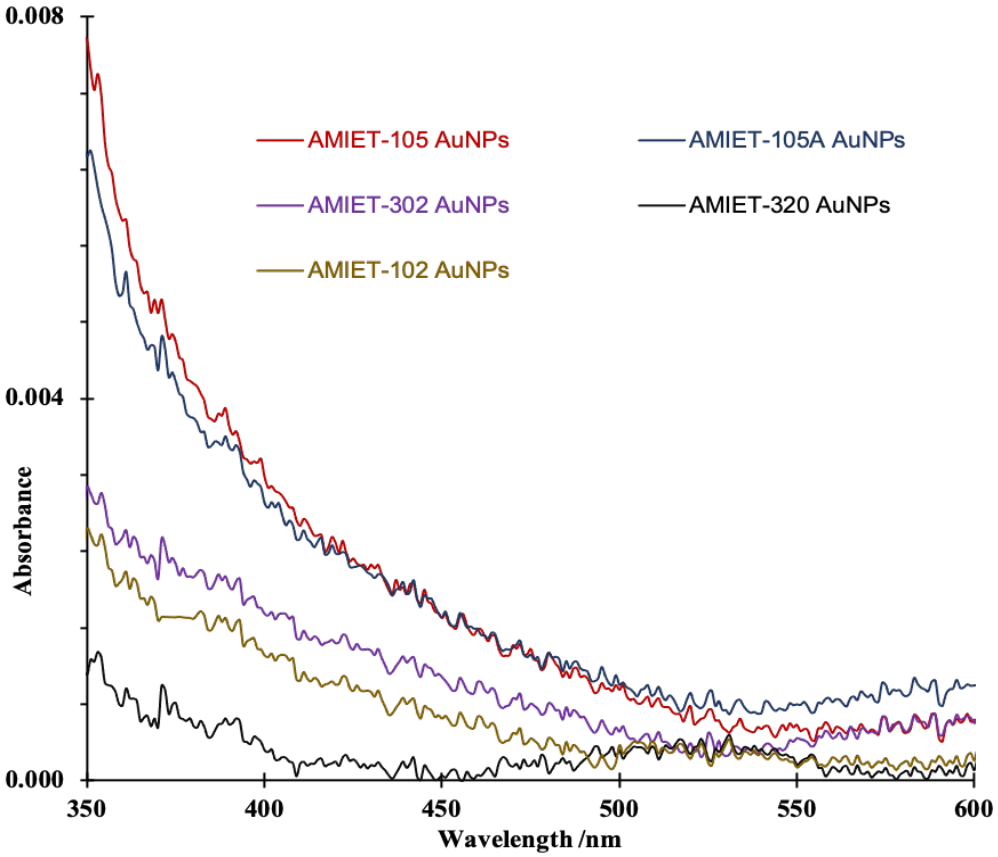

Fig-3.11 Spectra of AMIET-AuNPs after phase transfer

No absorption around ~ 525 nm was observed after phase transfer, indicating the absence of AuNPs in the aqueous layer. As the refractive index of the solvents increases after phase transfer (ηwater = 1.33 ; ηchloroform = 1.45) a small red shift about ~ 3 nm is usual and observed [28] as

in Fig-3.12 and 3.13. But a large ~ 10 nm red shift was noticed for AMIET 302-AuNP and AMIET 102-AuNPs; it is probably due to their higher dispersibility towards the organic solvents than water, along with the increase of solvent refractive index. Though particle size for AMIET 302-AuNPs is comparatively smaller than other AMIET-AuNPs, no difference was noticed in transferring the particle to organic phase using pH triggered method. The evidence indicates that the method is functionable regardless of particle size though further experimental investigations are needed to justify for ≥ 50 nm particles. However, it is anticipated that there is little aggregation in AMIET 302-AuNP and AMIET 102-AuNP in aqueous phase due to the lower HLB value 5.1 and 6.3 of their corresponding surfactants.

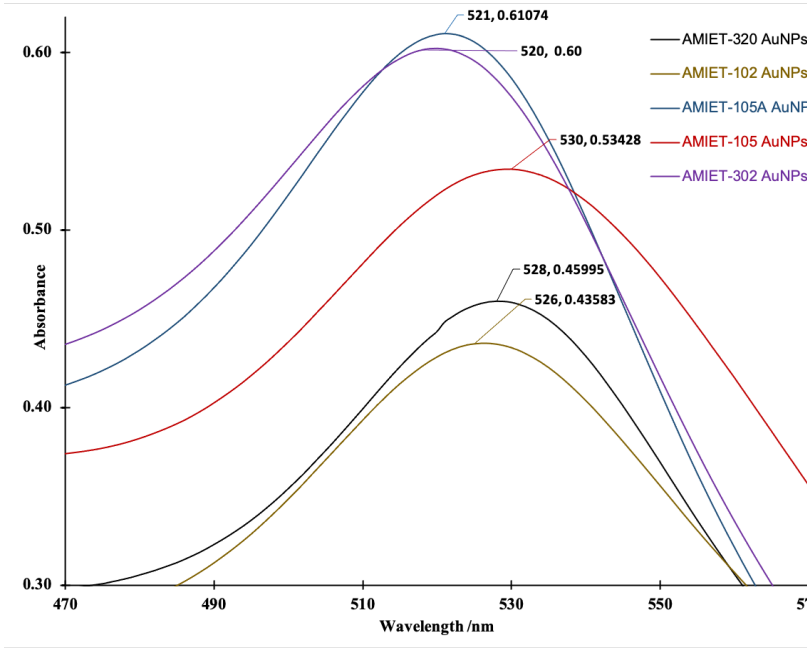

Fig-3.12 SPR peak in aqueous phase

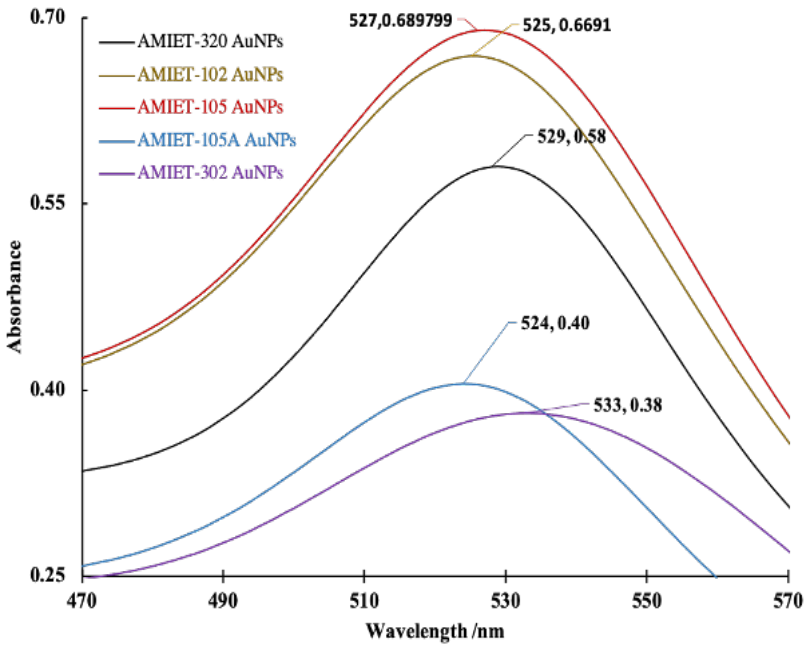

Fig-3.13 SPR peak in chloroform phase

This fact is also supported by the formation of the blackish precipitation of AMIET 102-AuNPs and agglomeration state observed for AMIET 302 about 30 days later from the synthesis.

In order to avoid the phase behavior complexity of water and different organic solvents, another way to disperse the AMIET- AuNPs in different organic solvents is to dry the phase transferred

NPs by evaporating the $CHCl_3$ at room temperature and dispersed in the desired organic solvents. Nevertheless, the stability of AuNPs in organic solvents is not investigated in this framework but the evidence of our observation points direct towards the idea that the directly transferred AuNPs in organic solvents is more stable than the dispersion of dried gold NPs in different organic solvents.

3.3.3 Morphology study through Transmission Electron Microscopy (TEM)

TEM measurements have also been employed to provide more reliable information on the size and spatial arrangement of the gold nanoparticles [29]. The gold nanoparticle synthesized in the present way are spherical having diameters from 4 to 24 nm. It has been confirmed that the synthesized AuNPs are not capped or covered by any residues that indicates surface of the particles is smooth. In TEM micrograph of AMIET 302-AuNP, AMIET 102-AuNPs where the large particle with a size of about 12 nm appears to consist of many smaller particles forming and aggregate like shape. In such cases, reliable particle counting is not possible with or without touching particles being ignored. This is due to either the poor nature of TEM sample preparation or the inherent tendency of the nanoparticles to aggregate [30]. However, after phase transfer, the chloroform dispersed AMIE-AuNP is not quantitatively showing any adverse effect on the size, shape and morphology of the nanoparticle [31]. TEM morphology of AMIET-AuNPs before and after phase transfer along with their size distribution is presented in Fig-3.14.1-5.

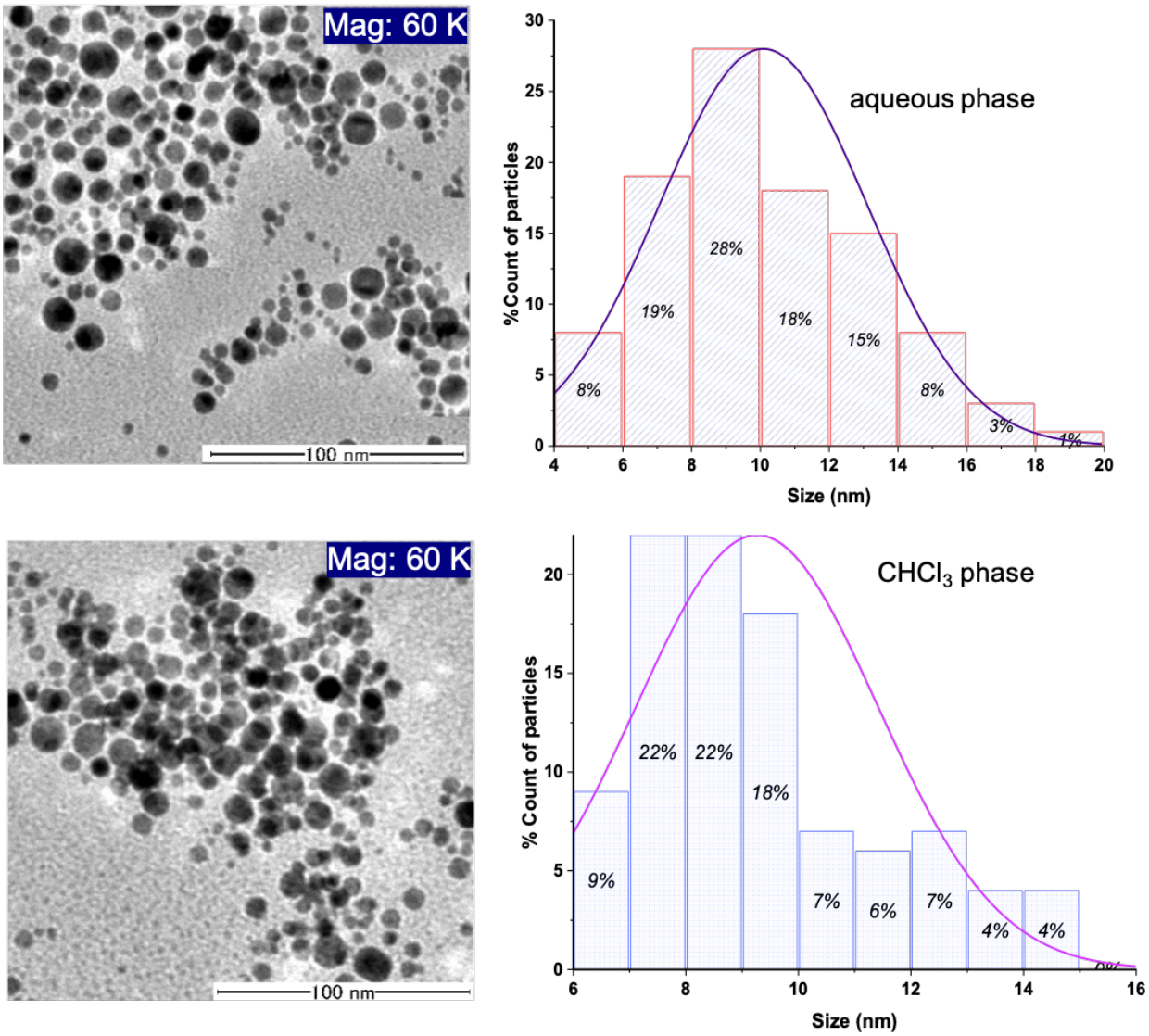

Fig-3.14.1 TEM images of AMIET 320-AuNP and associated size distribution histograms

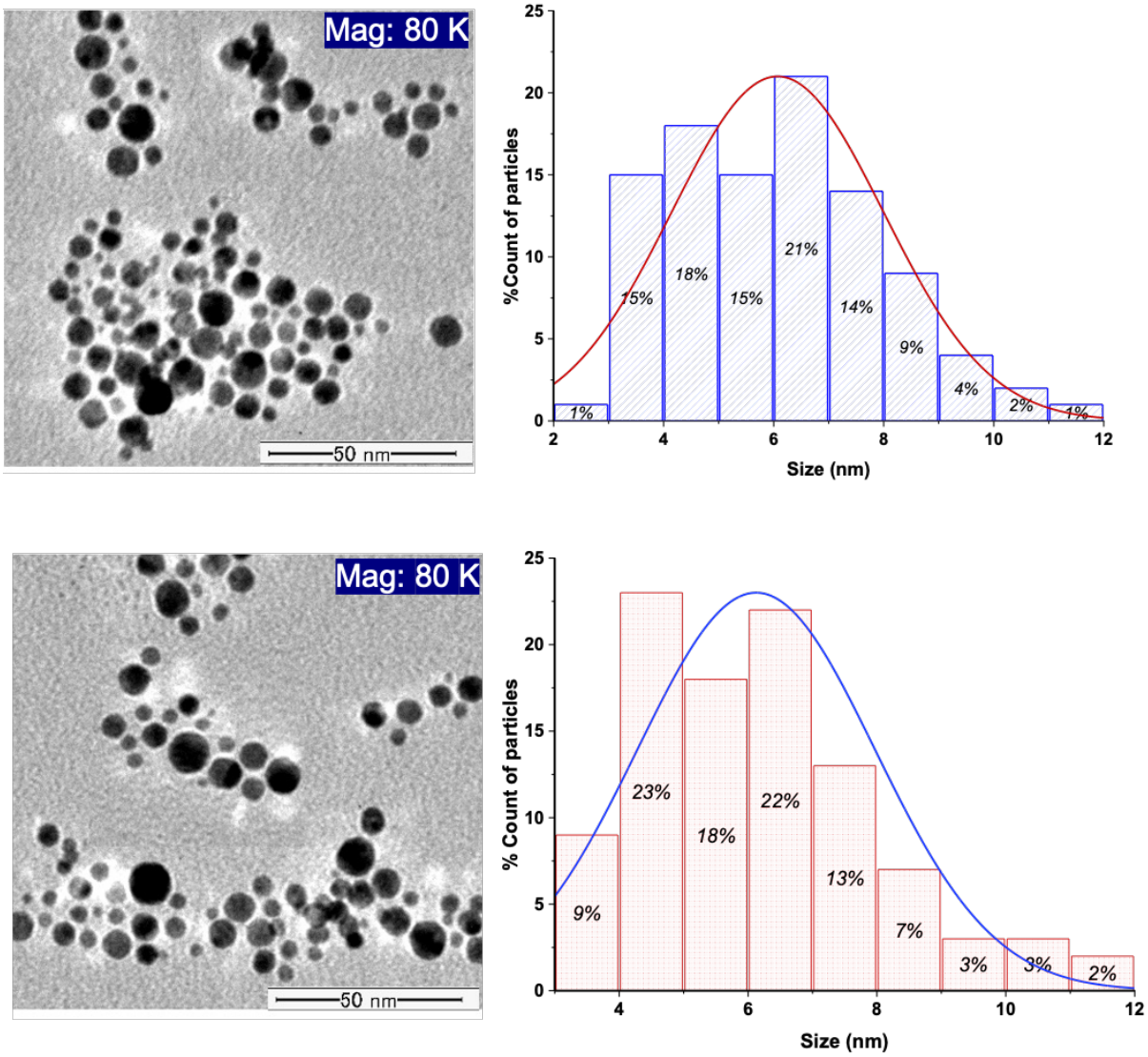

Fig-3.14.2 TEM images of AMIET 302-AuNP and associated size distribution histograms

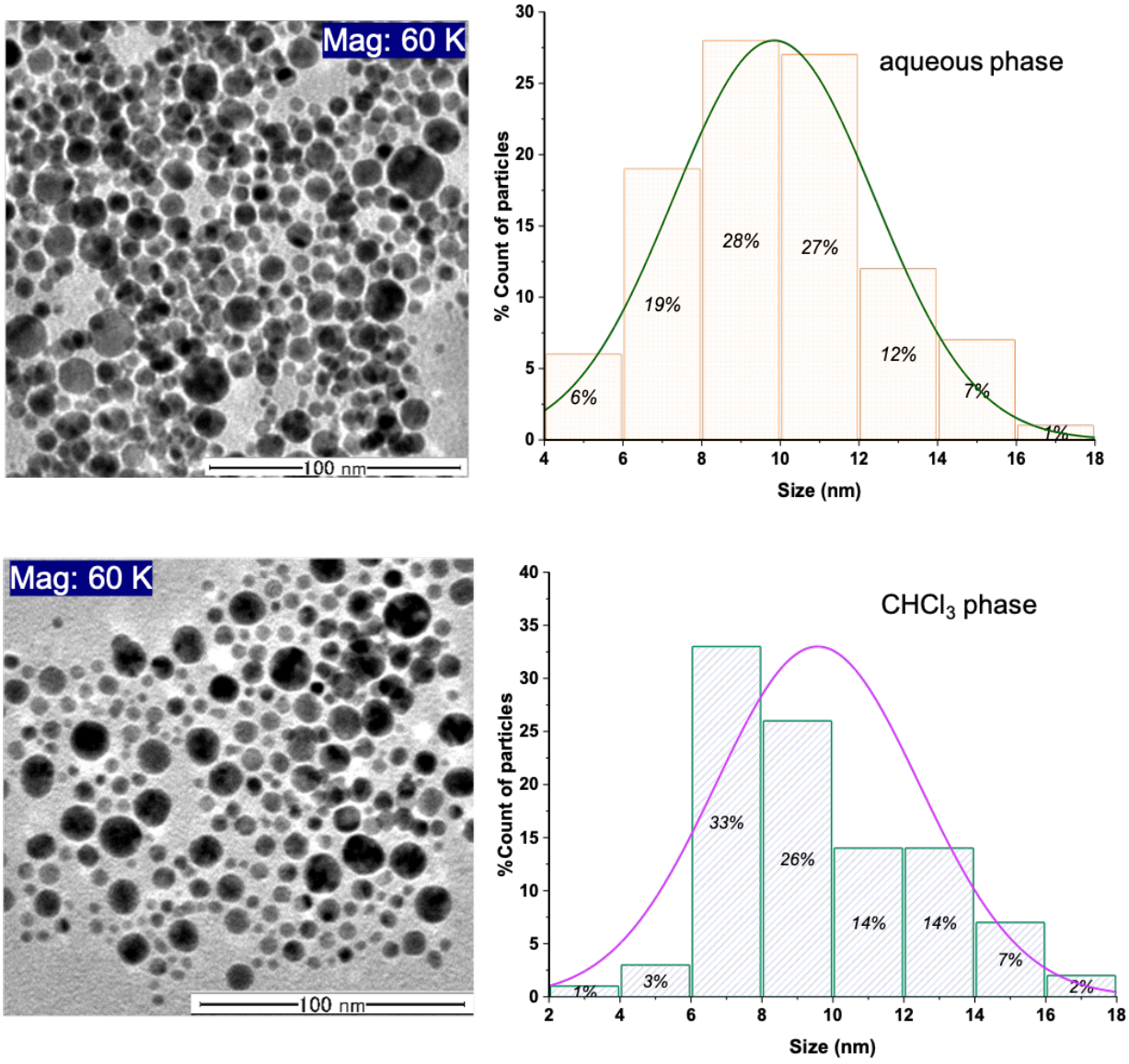

Fig-3.14.3 TEM images of AMIET 105-AuNP and associated size distribution histograms

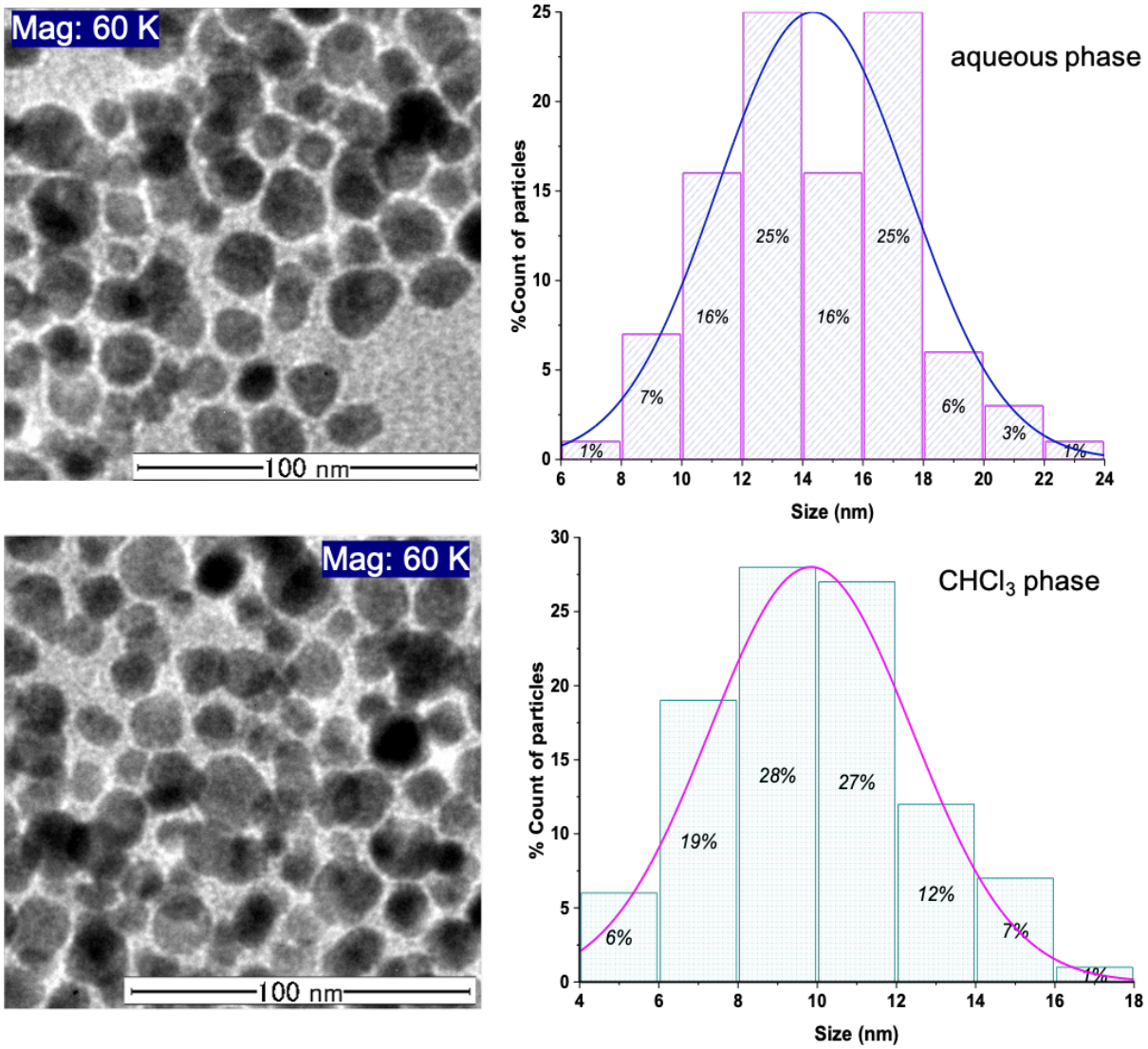

Fig-3.14.4 TEM images of AMIET 105A-AuNP and associated size distribution histograms

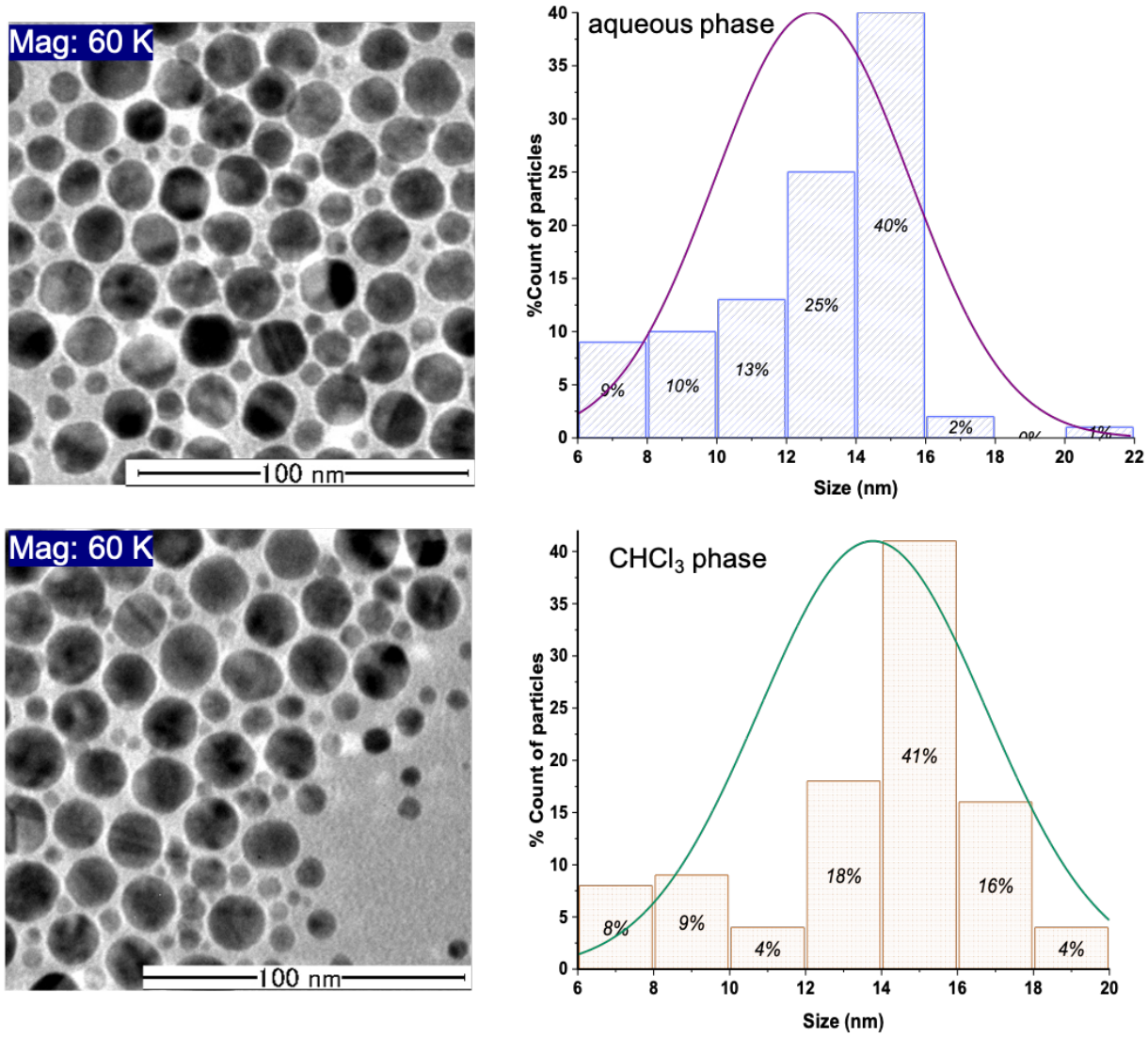

Fig-3.14.5 TEM images of AMIET 102-AuNP and associated size distribution histograms

3.3.4 Characterization surface-bound AMIETs on AuNP by ^{1}H NMR

The spatial information on the surface bound ligand in both phases can explained by the NMR spectra [32,33] as presented in Fig- 3.15.1-5. Important difference can be appreciated between ^{1}H spectrum of AMIET-AuNPs dissolved in d-chloroform ($CDCl_3$) and that of the same particles suspended in d-water (D_2O). AuNPs dissolved in $CDCl_3$ show most of their functional group α and β peaks in the aliphatic region in the upfield that are considerably below 3.5 ppm. The AuNPs

suspended in d-water, however, did not exhibit any significant signals related to aliphatic functional groups.

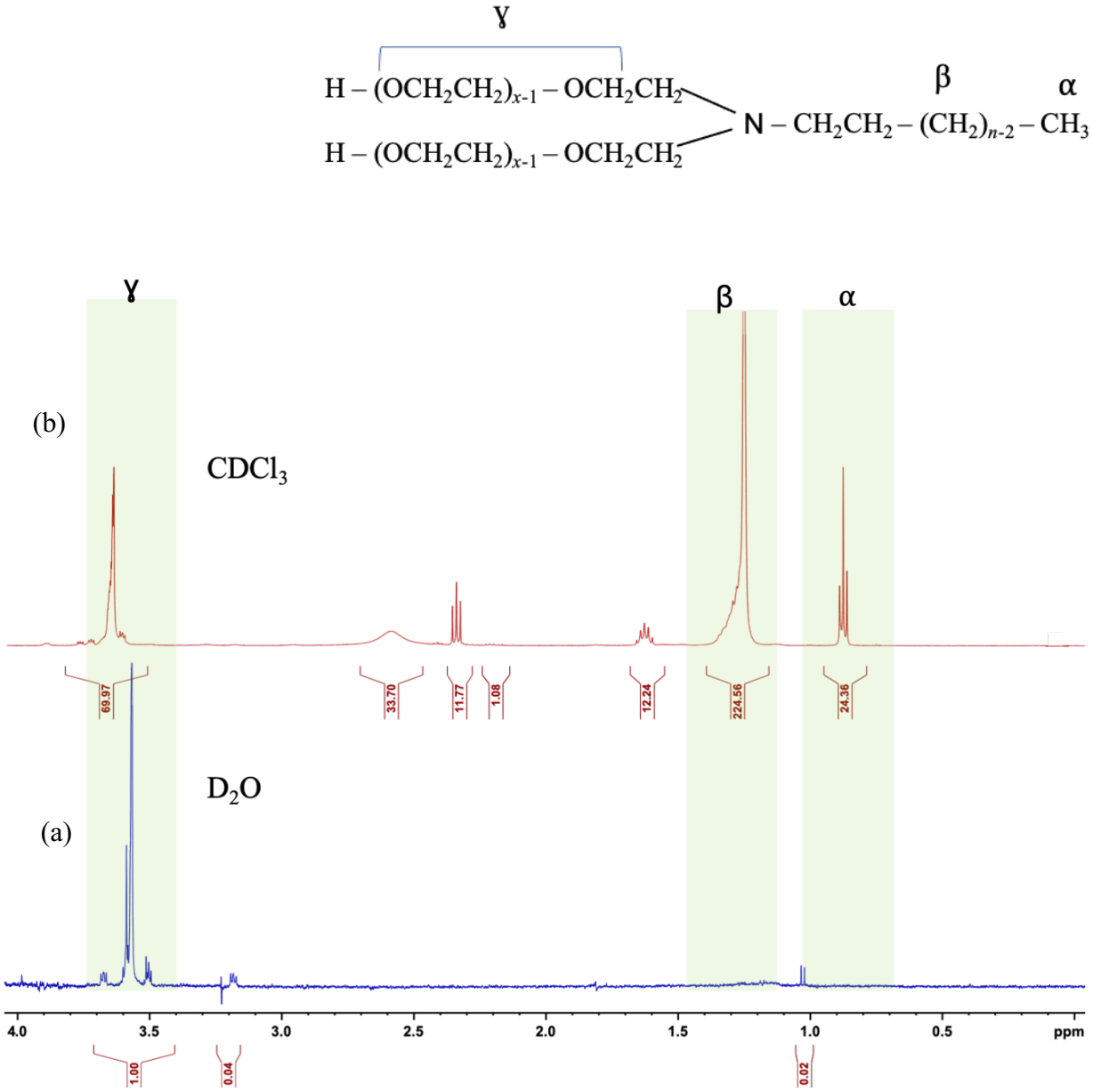

Fig-3.15.1 ^{1}H NMR spectra of AMIET 320-AuNPs, before **(a)** and after phase transfer **(b)**

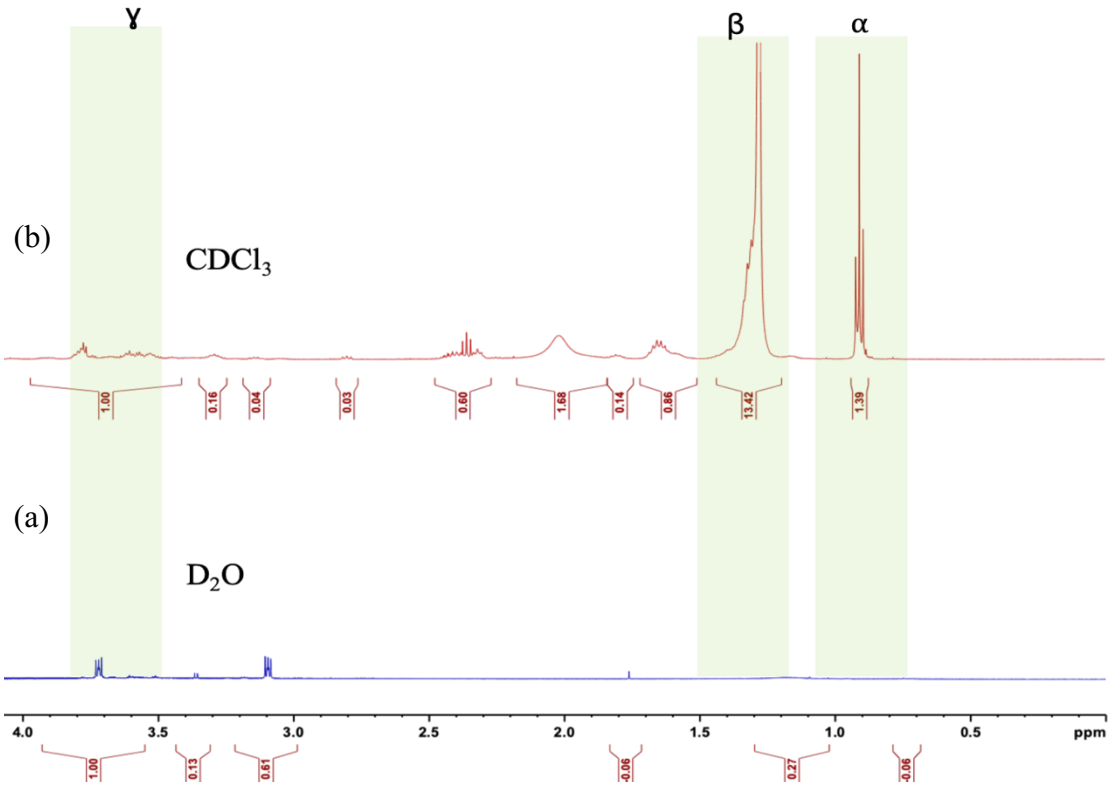

Fig-3.15.2 ^{1}H NMR spectra of AMIET 302-AuNPs before **(a)** and after phase transfer **(b)**

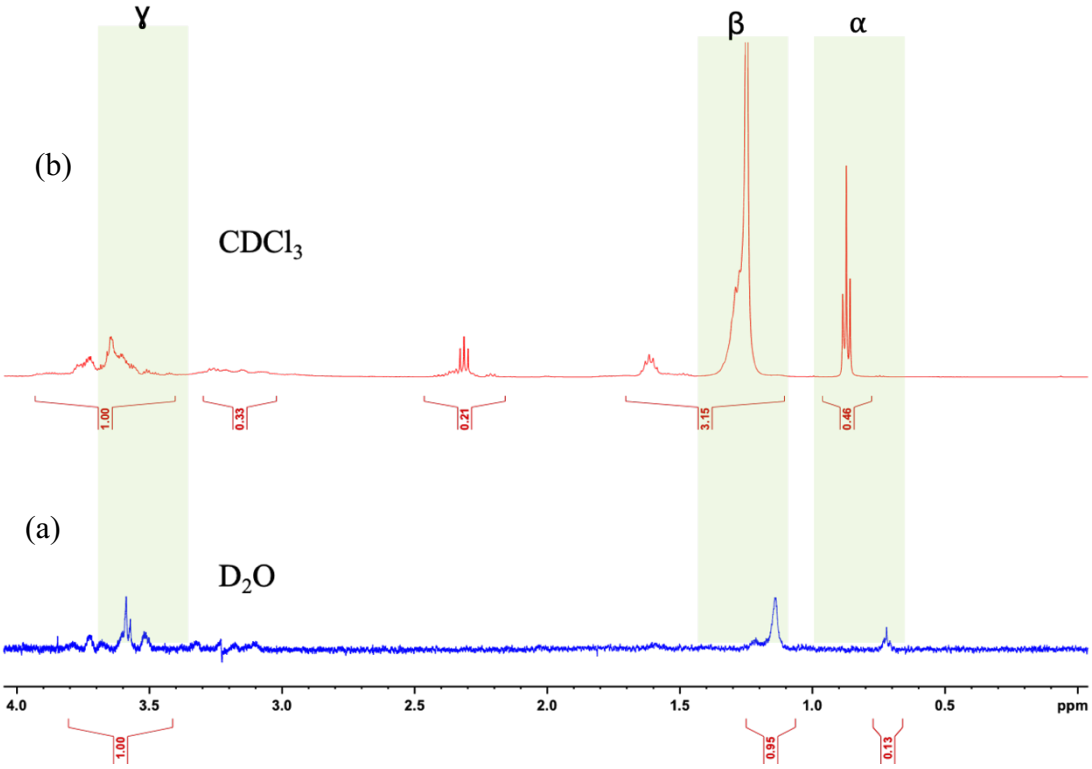

Fig-3.15.3 ^{1}H NMR spectra of AMIET 105-AuNPs, before **(a)** and after phase transfer **(b)**

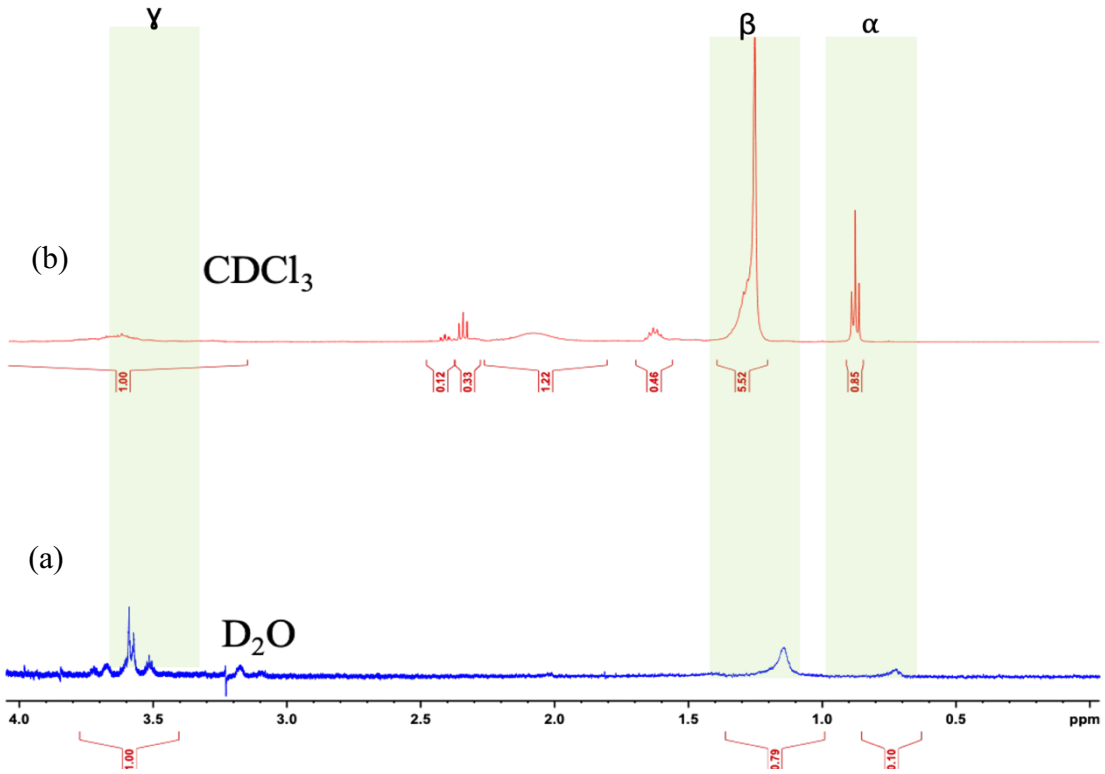

Fig-3.15.4 ^{1}H NMR spectra of AMIET 105A-AuNPs before **(a)** and after phase transfer **(b)**

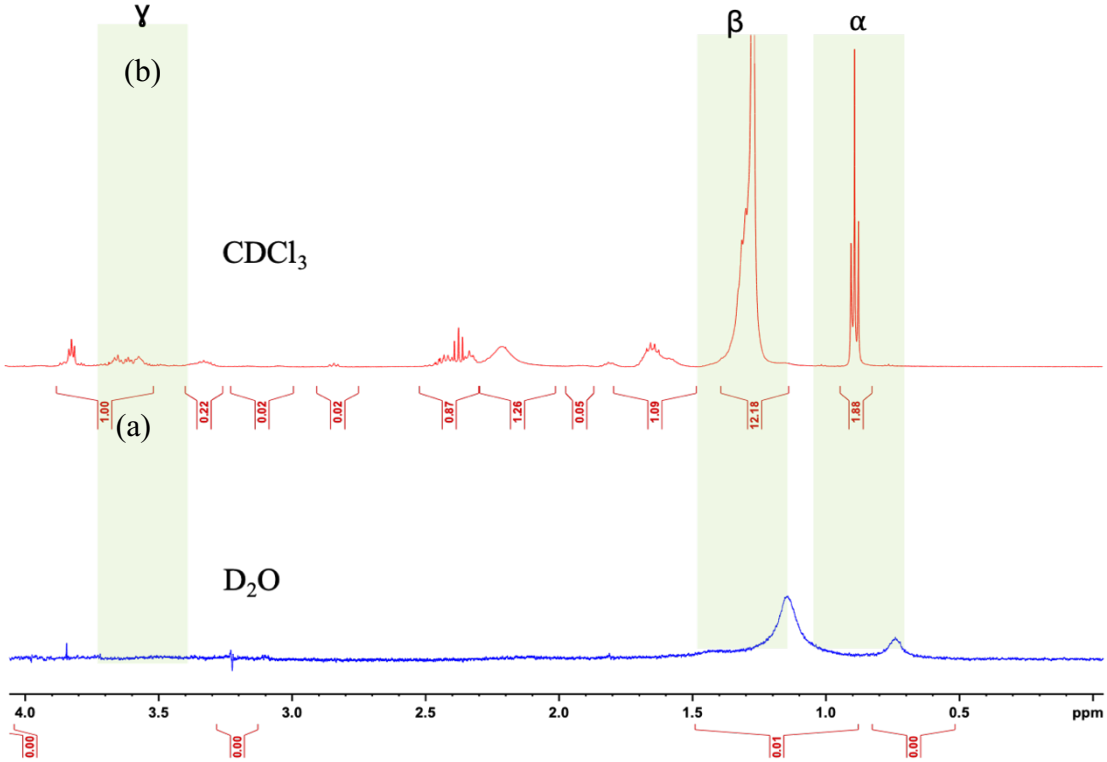

Fig-3.15.5 ^{1}H NMR spectra of AMIET 102-AuNPs, before **(a)** and after phase transfer **(b)**

No signal of aliphatic protons in this dispersion strongly suggests that the hydrophobic moiety (long alkyl chain) is being repelled by the solvent environment and these molecules tend to orient themselves at the nanoparticle surface as represented by the ligand arrangement in both phases shown in Fig-3.16. Thus, no significant peak at high field (shielded) region is observed in the NMR spectra of these compounds because free rotation of proton in solution is not feasible due to strong metal-ligand interaction. However, it is worth noting that, though the polyethylene-oxide chain is

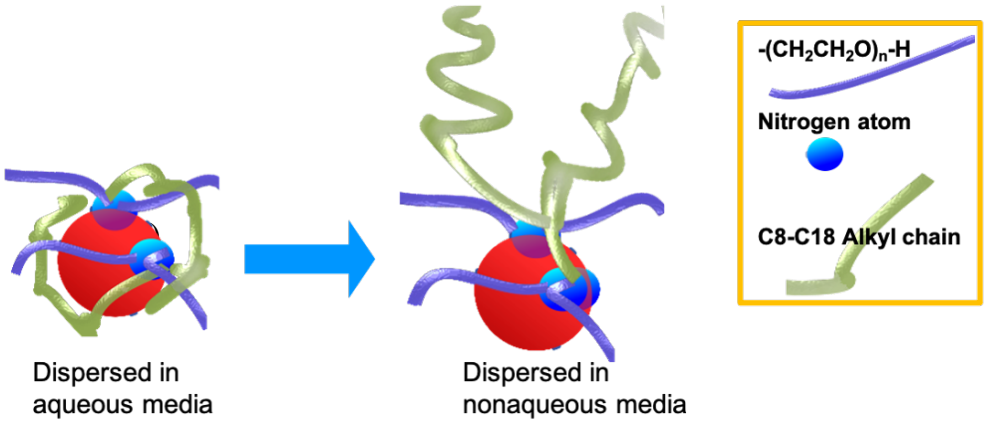

Fig-3.16 representation of proposed surface bound ligand arrangement in both phase

known as globally hydrophilic, each ethoxy/ (EO) group contains 2 methylene (-CH_2-) units which are hydrophobic [34,35]. Thus, it can be said that poly EO group is not an extremely hydrophilic and this characteristic makes it soluble in organic solvent too. Moreover, the terminal proton of polyoxyethylene chain does not show any peak due to either it has been exchanged with deuterium or restricted by forming hydrogen bond with solvent. On the other hand, during the dispersion in chloroform alkyl moiety is being attracted toward solvents and making the dispersion feasible as well as ensuring nanoparticles stability in chloroform [36]. Consequently, a number of proton signals are observed at up field region. In this case, though the hydrophilic ethoxy group is repelled by the solvent environment, but due to the dual nature of poly ethoxy chain it may produce rotational motion enough to generate as weak proton (as denoted by ɣ) peak at around 3.5 ppm as shown in the NMR spectra. Moreover, a distinguishable difference may be noted between the ɣ peaks for AMIET 320-AuNPs and those for other AMIET-AuNPs. This could be related to the presence of larger numbers of ethoxy groups, since AMIET 320 contains 20 ethoxyelene groups which are more numerous than the other AMIETs.

3.4 Conclusion

Using a comparative study, a straightforward cutting edge approach has been demonstrated for transferring of aqueous AMIET-AuNP into organic that can preserve the shape and size, as evidenced by UV-vis spectra and TEM analysis. This method has been successfully demonstrated to be consistent, systematic, reproducible, and independent of particle size and density of second solvent. The plasmon peaks remained unchanged after the phase transfer except for red shifts caused by the change in medium. They also remained narrow in their band width, suggesting that the AuNPs were well dispersed in the transferred medium. TEM images after phase transfer did not show any additional aggregation. The current work not only confirms the emerging role of AMIET ligands, but also suggests AMEIT will be useful in direct synthesis of gold nanoparticles as well as for phase transfer and stabilization of the gold nanoparticles in the future. Our current strategy may confer multiple possibilities for phase transfer of other nonionic surfactant coated metal nanoparticles. This approach is believed to provide multiple opportunities for phase transfer of other nonionic surfactant-coated metallic nanoparticles.

3.5 References

[1] I. Khan, K. Saeed, and I. Khan, *Arab. J. Chem.*, **12**, 908–931 (2019).

[2] L.M. Sousa, L.M. Vilarinho, G.H. Ribeiro, A.L. Bogado, and L.R. Dinelli, *R. Soc. Open Sci.*, **4**, 170675 (2017).

[3] L.C. Giannossa, D. Longano, N. Ditaranto, M.A. Nitti, F. Paladini, M. Pollini, M. Rai, A. Sannino, A. Valentini, and N. Cioffi, *Nanotechnol. Rev.*, **2**, 307–331 (2013).

[4] L. Liu and A. Corma, *Chem. Rev.*, **118**, 4981–5079 (2018).

[5] G. Chen, I. Roy, C. Yang, and P.N. Prasad, *Chem. Rev.*, **116**, 2826–2885 (2016).

[6] A.J. Stephen, N. V Rees, I. Mikheenko, and L.E. Macaskie, *Front. Energy Res.*, **7**, 1–13 (2019).

[7] N. Li, P. Zhao, and D. Astruc, *Angew. Chemie - Int. Ed.*, **53**, 1756–1789 (2014).

[8] J. Zhang, L. Mou, and X. Jiang, *Chem. Sci.*, **11**, 923–936 (2020).

[9] K. Soliwoda, E. Tomaszewska, B. Tkacz-Szczesna, M. Rosowski, G. Celichowski, and J. Grobelny, *Polish J. Chem. Technol.*, **16**, 86–91 (2014).

[10] K. Ranoszek-Soliwoda, M. Girleanu, B. Tkacz-Szczęsna, M. Rosowski, G. Celichowski, M. Brinkmann, O. Ersen, and J. Grobelny, *J. Nanomater.*, **1**, 1–10 (2016).

[11] A.B. Serrano-Montes, D. Jimenez de Aberasturi, J. Langer, J.J. Giner-Casares, L. Scarabelli, A. Herrero, and L.M. Liz-Marzán, *Langmuir*, **31**, 9205–9213 (2015).

[12] J. Zhou, X. Cao, L. Li, X. Cui, and Y. Fu, *Nanomater. (Basel, Switzerland)*, **9**, 1468 (2019).

[13] M. Cao, Q. Liu, M. Chen, P. Yang, Y. Xu, H. Wu, J. Yu, L. He, X.-H. Zhang, and Q. Zhang, *RSC Adv.*, **7**, 25535–25541 (2017).

[14] W. Yu and H. Xie, *J. Nanomater.*, **435873**, 1–17 (2012).

[15] T. Honold, D. Skrybeck, K.G. Wagner, and M. Karg, *Langmuir*, **33**, 253–261 (2017).

[16] S. Kittler, S.G. Hickey, T. Wolff, and A. Eychmüller, *Zeitschrift Fur Phys. Chemie*, **229**, 235–245 (2015).

[17] M. Qu, S. Chen, W. Ma, J. Chen, K. Kong, F. Zhang, H. Li, Z. Hou, and X.-M. Zhang, *Langmuir*, **32**, 13746–13751 (2016).

[18] S. Thawarkar, T.C. Nirmale, S. More, J.D. Ambekar, B.B. Kale, and N.D. Khupse, *Langmuir*, **35**, 9213–9218 (2019).

[19] J.O. Park, S.-H. Cho, J.-S. Lee, W. Lee, and S.Y. Lee, *Chem. Commun.*, **52**, 1625–1628 (2016).

[20] C. Morita-Imura, K. Zama, Y. Imura, T. Kawai, and H. Shindo, *Langmuir*, **32**, 6948–6955 (2016).

[21] A. Popowich, Q. Zhang, and X.C. Le, *J. Environ. Sci.*, **38**, 168–171 (2015).

[22] Y. Imura, C. Morita, H. Endo, T. Kondo, and T. Kawai, *Chem. Commun.*, **46**, 9206–9208 (2010).

[23] S. Chakraborty and C.L. Kitchens, *J. Phys. Chem. C*, **123**, 26450–26459 (2019).

[24] N.F.A. van der Vegt and D. Nayar, *J. Phys. Chem. B*, **121**, 9986–9998 (2017).

[25] S. Surawanvijit, M. Kim, and Y. Cohen, *NSTI-Nanotech 2010*, **3**, 591–593 (2010).

[26] S. Sekiguchi, K. Niikura, Y. Matsuo, and K. Ijiro, *Langmuir*, **28**, 5503–5507 (2012).

[27] L.M. Rossi, J.L. Fiorio, M.A.S. Garcia, and C.P. Ferraz, *Dalt. Trans.*, **47**, 5889–5915 (2018).

[28] M. Wielgus, M. Gordel, M. Samoć, and W. Bartkowiak, *Acta Phys. Pol. A*, **130**, 1380–1384 (2016).

[29] S.G. Booth, A. Uehara, S.Y. Chang, J.F.W. Mosselmans, S.L.M. Schroeder, and R.A.W. Dryfe, *J. Phys. Chem. C*, **119**, 16785–16792 (2015).

[30] S. Mourdikoudis, R.M. Pallares, and N.T.K. Thanh, *Nanoscale*, **10**, 12871–12934 (2018).

[31] C. Amgoth, A. Singh, R. Santhosh, S. Yumnam, P. Mangla, R. Karthik, T. Guping, and M. Banavoth, *RSC Adv.*, **9**, 33931–33940 (2019).

[32] L.E. Marbella and J.E. Millstone, *Chem. Mater.*, **27**, 2721–2739 (2015).

[33] M. Lista, D.Z. Liu, and P. Mulvaney, *Langmuir*, **30**, 1932–1938 (2014).

[34] J.-L. Salager, R. Antón, J. Bullón, A. Forgiarini, and R. Marquez, *Cosmetics*, **7**, 57 (2020).

[35] J.-L. Salager, *Lab. FIRP*, **2**, 1–50 (2002).

[36] E. Pramauro and E. Pelezetti, *Elsevier B.V.*, **31**, 1–91 (1996).

Chapter IV Facile removal of surfactant of concentrated AMIET-AuNPs after phase transfer and its dispersion to various organic solvents

Abstract

Nanocrystal colloid synthesis presents a serious challenge when removing surfactants from nanoparticles due to the colloidal nature of the particles. Furthermore, these ligands are inseparable since they are formed simultaneously during synthesis. This section describes how to remove excess surfactant from AMIET-AuNPs by using a simple washing method after phase transfer. Our method utilizes the dual nature of ethoxy chains (-CH_2CH_2-O-), which facilitates the accumulation of unbound reactants at the interface of organic and water by vigorous shaking and washing with fresh water. Though this method need to be repeated numerous times to achieve the desired cleanliness, but it is free of laborious instruments and chemicals. Thereby, this simple method can reduce the interruption caused by uncleaned AMIET-AuNPs for further investigation, such as fabrication and dispersion in organic solvents. Furthermore, ^{1}H NMR and UV-Visible spectra of AMIET-AuNPs dispersed in different organic solvents indicate that this simple, inexpensive and effective technique can achieve sufficient purification.

4.1 Introduction

The synthesized polyethoxylated alkyl amine functionalized gold nanoparticles (AMIET- AuNPs) can be concentrated at least 10 times in organic solvent by using the pH triggered phase transfer method (the details have been discussed in chapter III) . As the gold nanoparticles were prepared with AMIET surfactants, it is expected to have excess organic ligands along with good and poor packing surfactants even after phase transfer as colloidal nanoparticles are usually capped with organic ligands used in the synthesis [1]. These molecules play an important role to stabilize the nanoparticles and prevent against aggregation [2]. Moreover, the shape [3,4] and size [5,6] can be controlled modulating the nanoparticle growth kinetics with the use of the surfactants [7,8]. use of ligands during synthesis has also a dramatic effect on the resulting crystal structure, dispersion.[9] In spite of these useful role, the bulky surfactants surrounding nanoparticles create barriers for many applications including catalysis [10]. However, A number of possible drawbacks might be encountered with colloidal nanoparticles containing excess surfactant. That includes the interactions occurring at the interface and between the constituents lead to the formation of different aggregated structures [11,12], significant decrease in their activity, reproducibility problem in catalytic study due to blocking the access of reactants to the active sites [13]. The presence of residual surfactants on the NP surface might also impair further functionalization when the latter is desired such as for medical applications or film formation [14]. The presence of organic molecules/surfactants in nanoparticles' dispersions may hamper the formation of film on air-water interface and the deposition onto solid substrates. Therefore the usefulness of these gold nanoparticles relies on the ability to remove the residual surfactant while maintaining original morphology [15]. Consequently, several surfactant removal methods, such as ligand exchange with small carboxylate or amine ligands [16], thermal annealing [1,17] UV-ozone/plasma treatments [18], high temperature calcination [13] (~450 ºC), Dialysis [19] have been reported in attempts to liberate active sites. However, these methods are not effective for strongly bound surfactants like phosphines, which are a common component of nanocrystal syntheses [20,21], and can lead to improper cleaning, contaminate with undesirable impurities under the strict condition used for individual process [17].

G. Li et al. demonstrated that high temperature calcination always require a higher temperature than the ligand desorption temperature and the oxide-supported gold nanoparticles, but it can

completely removes the protecting ligands on the gold nanoparticles [22]. So calcination is preferable when ligand-off particles is desired. Moreover, Coutanceau et al. observed the sintering problem while removing polyethylene glycol−dodecylether ligand from Pt NPs by a thermal annealing at 200 °C under H_2/Ar atmosphere [23]. Notably, thermal annealing could produce other intermediates or byproducts by decomposing the organic ligands that could also hamper the activity of the nanoparticles [24]. To overcome the limitations of thermal calcination, dialysis can be a useful method. However, dialysis is time-consuming and sometimes fails to remove unwanted thiols completely. M. Jansen et al. [25] attempted to isolate and clean diglyme-protected gold nanoparticles by standard centrifugation and redispersion procedure, but they found some irreversible coalesce and it is no longer dispersible. However, it is possible to remove unattached water soluble-ligands such as polyvinylpyrrolidone, cetyltrimethylammonium bromide, sodium acetate by thoroughly washing with water for few cycles. But, the oil-soluble ligands such as oleylamine, triphenylphosphine, dodecanethiol require more cycles, perhaps due to the strong coordination interaction between the ligands and nanoparticles [26,27].

Therefore, it is critical to establish a proper procedure of surfactant removal and surface cleaning, without changing the particle size and morphology that is sufficient for the application of colloidal NPs in nanofabrication. In order to avoid the complexity associated with each method, herein we demonstrate a simple and facile washing method to remove residual surfactant from the AMIET functionalized gold nanoparticles after transferring to chloroform. This method is basically conceptualized from the liquid-liquid extraction technique. ^{1}H NMR of cleaned AMIET-AuNPs shows that this method can effectively separate the unbound AMIET. The nature and properties of the gold core were found to influence chemical shifts of nuclei close to the gold core [28].

It also observed that the AMIET-AuNPs are readily dispersible in various organic solvents with enhanced stability comparing to the uncleaned AMIET-AuNPs. Additionally, the effect of dispersing media of the nanoparticles were investigated by their UV-visible absorption measurement. However, it is noteworthy that the effect of changes in the refractive index of the surrounding medium is more difficult to demonstrate from an experimental point of view, because of the very high susceptibility of nanoparticles to aggregate in aqueous and organic solvents. A red shift in the SPR peak with increasing the solvent dielectric constant was observed only if metal surface do not complex with solvent or ligand [28]. Moreover, G. Ertas et al. [29] extensively

studied the effects of solvent refractive index on the surface plasmon resonance of gold nanoparticles and demonstrates that the SPR shift does not rely merely on the refractive index of dispersing solvents rather depending on interaction of the particles surface with the surrounding environment, peak position may be changed. Only if there is no significant interaction, red shift was reported with increasing the refractive index of solvents and vice versa. More explicitly, the SPR of metallic nanoparticles depends sensitively on nanoparticles geometry and its dielectric surrounding environment [30]. Becasuse, The optical cross sections of the nanoparticles acts as a function of energy, that strongly effects the surface plasmon peak position and width. So it is a complicated issue to conclude the effect of solvent refractive index on metallic nanoparticles from the experimental point of view. However, The visual appearance in various organic solvent and their UV-Visible spectra confirms the dispersion of AMIET-AuNPs in different organic media.

4.2 Experimental

4.2.1 Materials and methods

AuNPs after phase transfer such as AMIET 320-AuNPs, AMIET 302-AuNPs, AMIET 105-AuNPs, AMIET 105A-AuNPs and AMIET 102-AuNPs dispersed in chloroform have been taken as the starting materials. Chloroform ($CHCl_3$), super dehydrated n-hexane (C_6H_{12}) and carbon tetrachloride (CCl_4) from FUJIFILM Wako Pure Chemical Corporation; dichloromethane (CH_2Cl_2) and toluene (C_6H_5-CH_3) from Kanto Chemical Co. Inc. were used as received as further dispersing solvents. Ultrapure water by Merck Direct-Q UV was used as washing solvent. Prior to use, the glass wares were immerged overnight in 5% cica clean solution and sonicated with UPW twice for 15 minutes followed by drying for 3 hours at 100 ºC in drying oven.

4.2.2 Surfactant removal method

Ultra-pure water was added to the concentrated AMIET-AuNPs dispersed in chloroform. The mixture was vigorously shacked and settled for about 30 mins, then the complete separation between water and chloroform phase was noticed and a layer of AMIET was also observed at the interface with naked eye. Then the water and the AMIET layer were removed using a micropipette. As long as the layer was noticed, the washing was continuously repeated. The procedure can also be represented by the Fig-4.1.

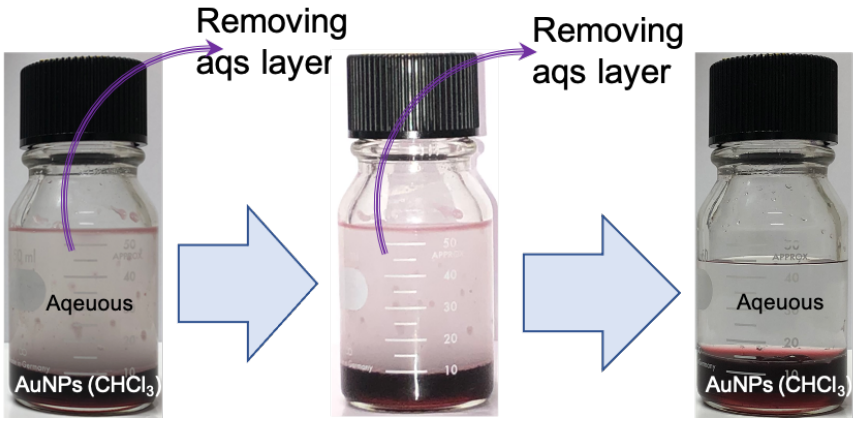

Fig-4.1 Representation of surfactant removal procedure with improved appearance

4.2.3 Dispersion technique after purification

2 ml of cleaned AMIET gold nanoparticles were dried in five cleaned 15 ml glass vials overnight at the room temperature. Then 7 ml of chloroform, di-chloromethane, n-hexane, toluene and carbon tetrachloride was added to the five vials, and their appearance were recorded by camera. The drying and dispersion can be demonstrated by Fig-4.2.

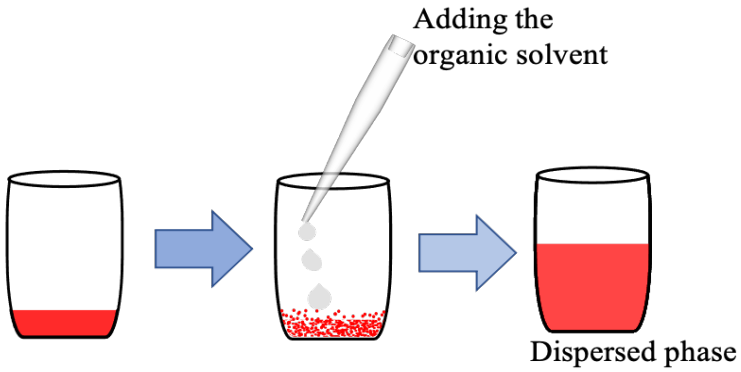

Fig-4.2 Representation of dispersion of AMIET-AuNPs after drying

4.2.4 Characterization

The absorption spectra of gold nanoparticles dispersed in different organic solvents were recorded using JASCO V-600 double beam UV-vis spectrometer with 1 cm path length semi micro (Type 18-F/Q/10, Starna scientific) quartz cuvette within the range of 290 nm to 740 nm and baseline correction was done with corresponding solvent and used as a reference. Proton Nuclear magnetic resonance (NMR) spectra were recorded using an Agilent-NMR-vnmrs 500 spectrometer in order to monitored the change after applying the removal procedure. ^{1}H NMR sample was prepared by drying at room temperature and dispersed with d-chloroform ($CDCl_3$).

4.3 Results and Discussion

4.3.1 ^{1}H NMR spectra observation

The amount of organic ligand before and after cleaning was assessed via ^{1}H NMR spectroscopy. (Fig-4.3.1-5.) It is noticeably observed that a sharp decrease in the intensity of the peak between 3.5~4.0 ppm corresponding to ethoxy (-CH_2CH_2-O-) group for all AMIET-AuNPs after passing through the removal procedure. This is due to dual nature of ethoxy group because it contains 2 hydrophobic methylene (-CH_2-) units that allows the AMIET molecule to form a layer at the interface during each repeated washing and removal of that layer may cause the less intense peak at the region. Moreover, some 1H peak corresponding related with inner alkyl groups, observed between 1.5 ppm ~ 2.5 ppm are either disappeared or diminished; that suggests our cleaning method can also remove some poorly bound ligand on AuNPs. Furthermore, the signal of terminal methyl (CH_3-) peak at ~0.83 ppm and the adjacent methylene (-CH_2-) peak at ~1.25 ppm are also displayed with reduced intensity after cleaning. The observation explicitly reveals the applying method is capable to remove the residual ligand as well as some poorly attached organic to the AuNPs [31,32].

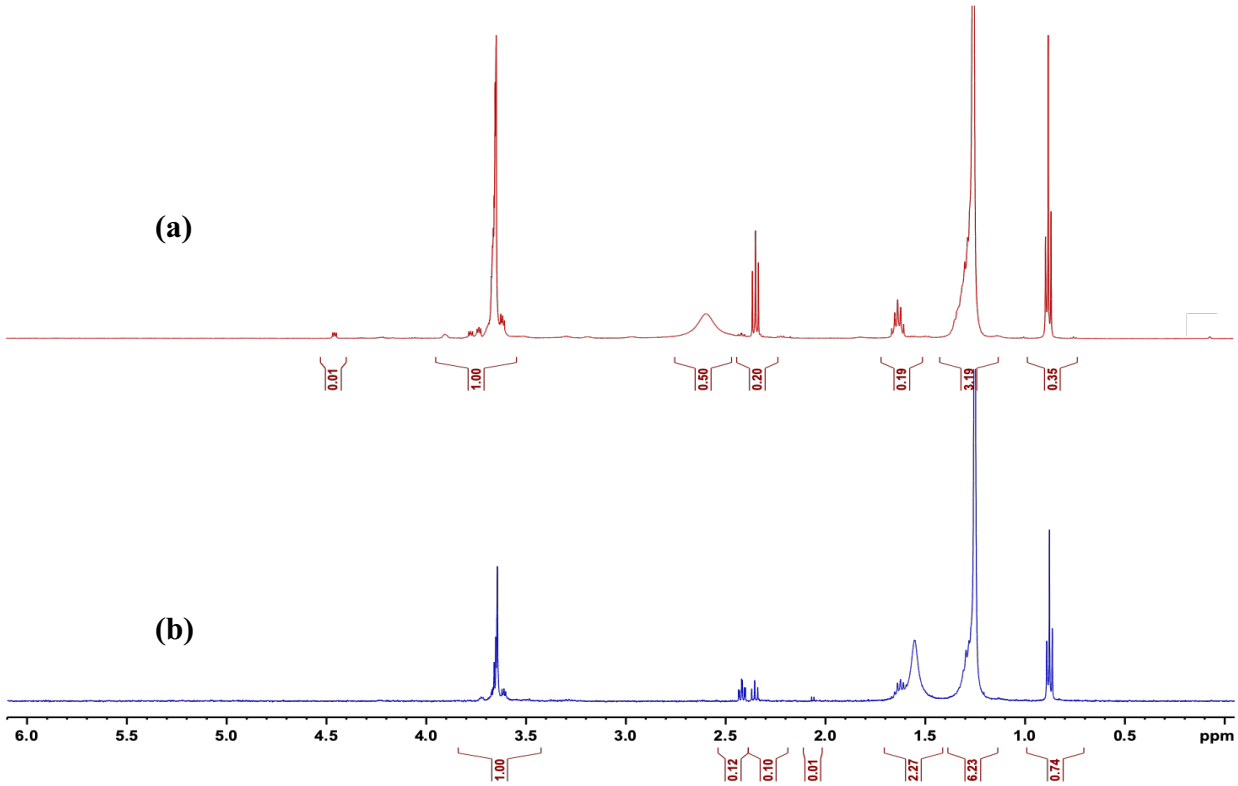

Fig-4.3.1 ^{1}H NMR spectra of AMIET 320-AuNPs in $CDCl_3$ before **(a)** and after cleaning **(b)**

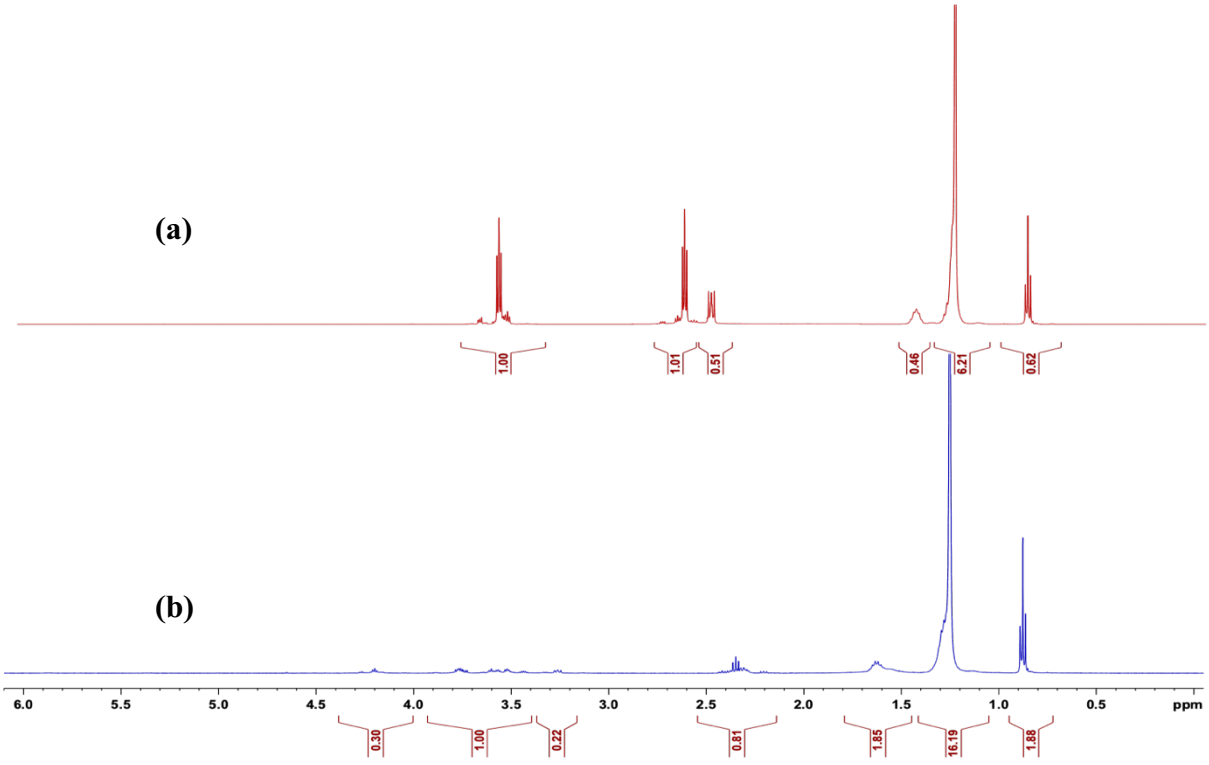

Fig-4.3.2 ^{1}H NMR spectra of AMIET 302-AuNPs in $CDCl_3$ before **(a)** and after cleaning **(b)**

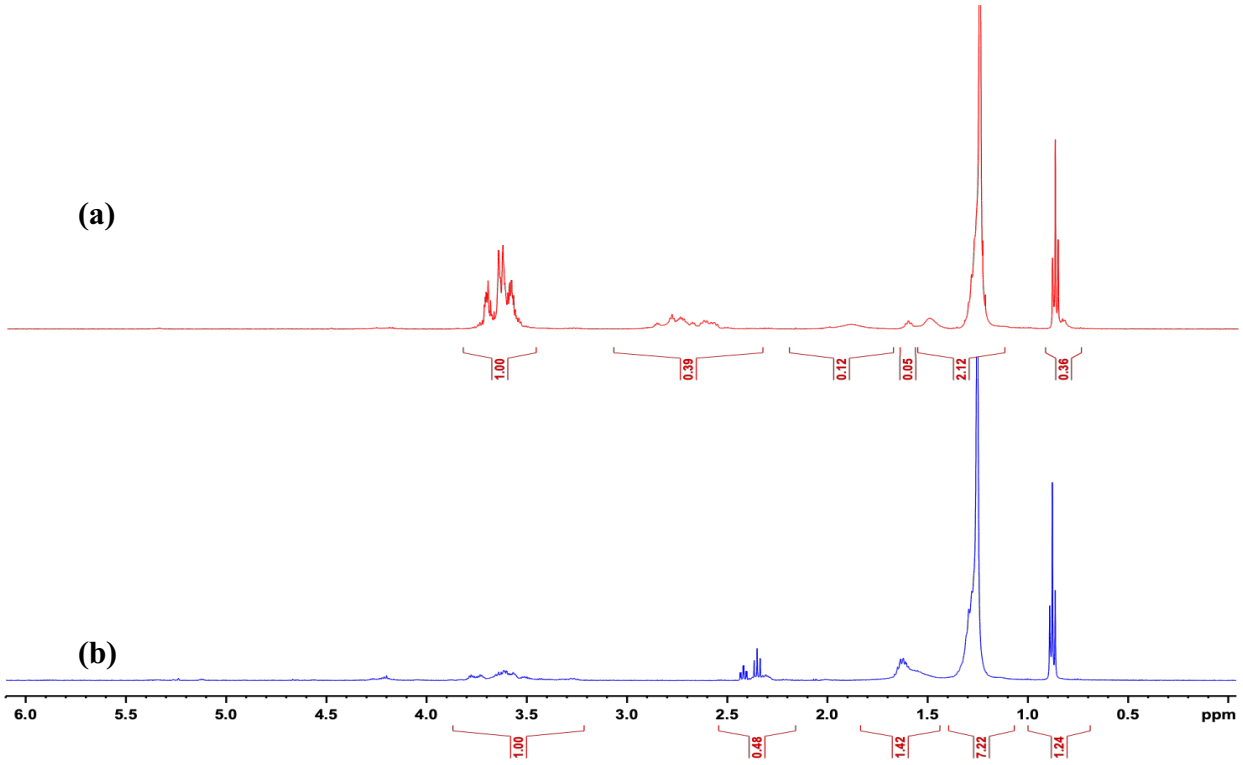

Fig-4.3.3 ^{1}H NMR spectra of AMIET 105-AuNPs in $CDCl_3$ before **(a)** and after cleaning **(b)**

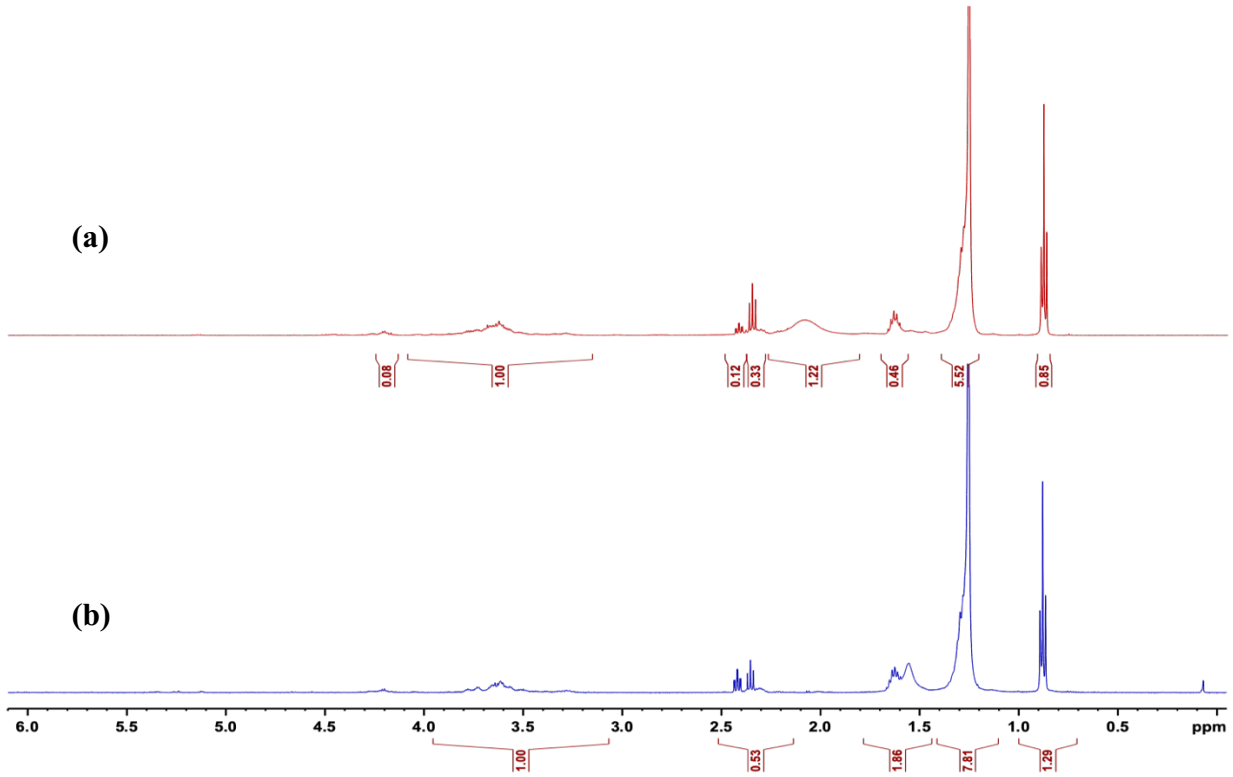

Fig-4.3.4 ^{1}H NMR spectra of AMIET 105A-AuNPs in $CDCl_3$ before **(a)** and after cleaning **(b)**

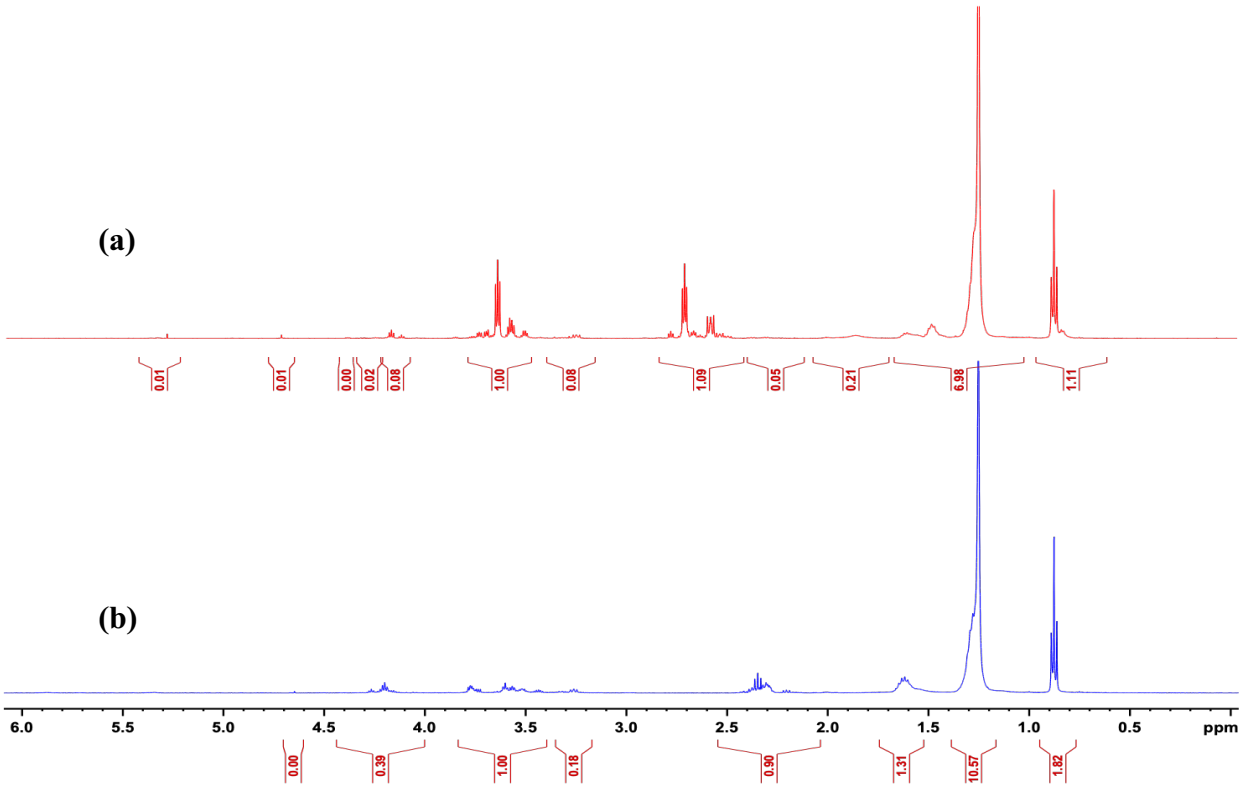

Fig-4.3.5 ^{1}H NMR spectra of AMIET 102-AuNPs in $CDCl_3$ before **(a)** and after cleaning **(b)**

4.3.2 Appearance of dispersion and UV-Vis spectra in various solvents

The visual observation and the photo images in Fig-3.5.1-5 clearly demonstrates that the AMIET-AuNPs can be transferred into a variety of organic solvents without suffering any significant coagulation. It is also noticed that the dispersions of an individual AMIET-AuNPs in five different organic solvents are almost identical regarding to its color. The variation of surface plasmon peak position five AMIET-AuNPs when dispersed in the same solvent is due to the interaction and particle size of different AMIET-AuNPs. However, if no particular interaction functions then a red shift is generally observed with increasing the refractive index of surrounding media [29] and the dispersion of AMIET 302-AuNPs and AMIET 102-AuNPs in terms of refractive index of the solvents bears a close resemblance to the fact as shown by the derived plot in Fig-4.4; whereas for other AMIET-AuNPs the effect of refractive index of solvents is not conceivable. The refractive indices of use solvents such as water, n-hexane [33], dichloromethane [34], chloroform, carbon

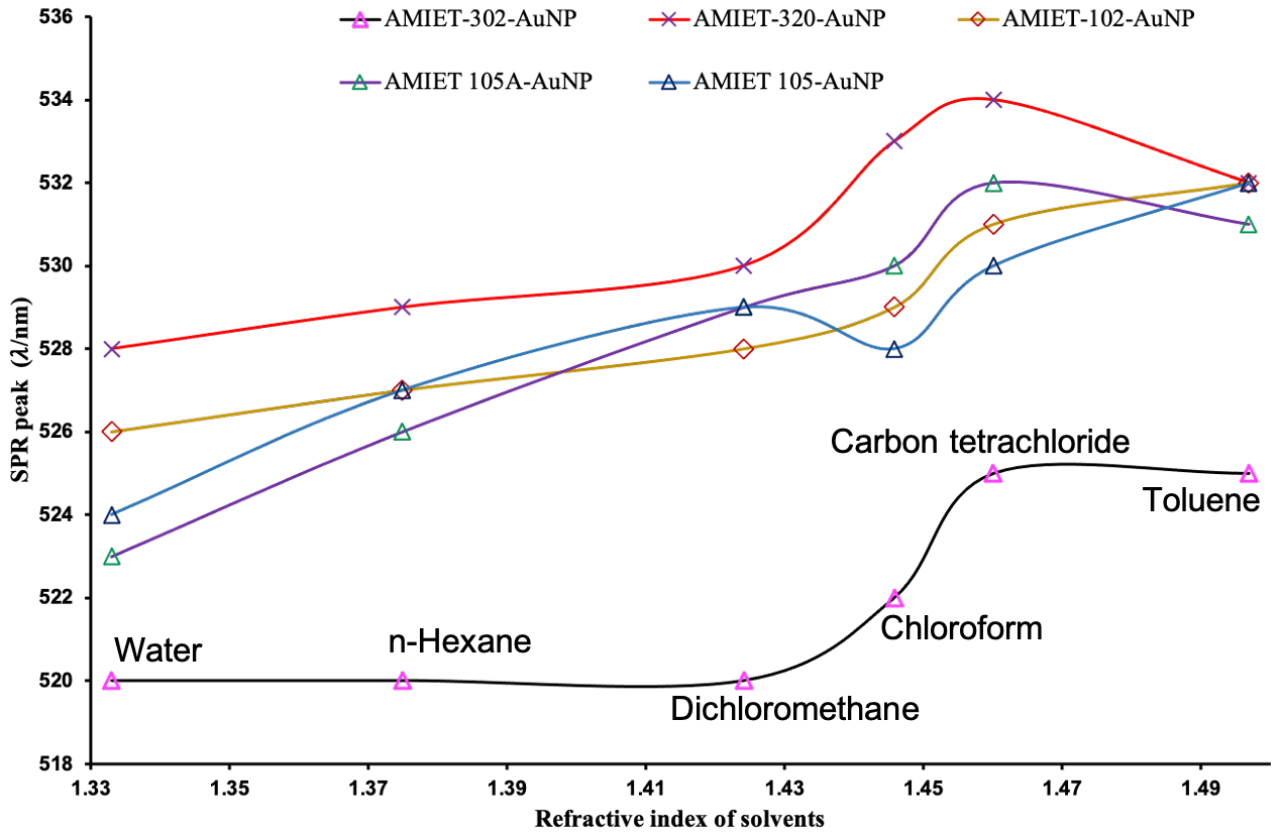

Fig-4.4 The effect of refractive index of solvents on the SPR peak position

tetrachloride and toluene [35] are 1.333, 1.396, 1.442, 1.446, 1.461 and 1.496 respectively. Moreover, no previous experimental evidence claim the clear correlation of nanoparticle's dispersion regarding to the refractive of solvents because of the complexity in interaction with nanoparticle surface and ligand in various solvents. Therefore, we consider it is not unjustifiable to draw a concrete conclusion about the effect of refractive index of solvents on AMIET-AuNPs. However, in this work it is ensured that the AMIET- AuNPs can be redispersed in various organic solvent after drying, and they do not aggregate irreversibly. The physical appearance along with their surface plasmon peak while dispersing in 5 different organic solvents can be presented as in Fig-4.5.1-5.

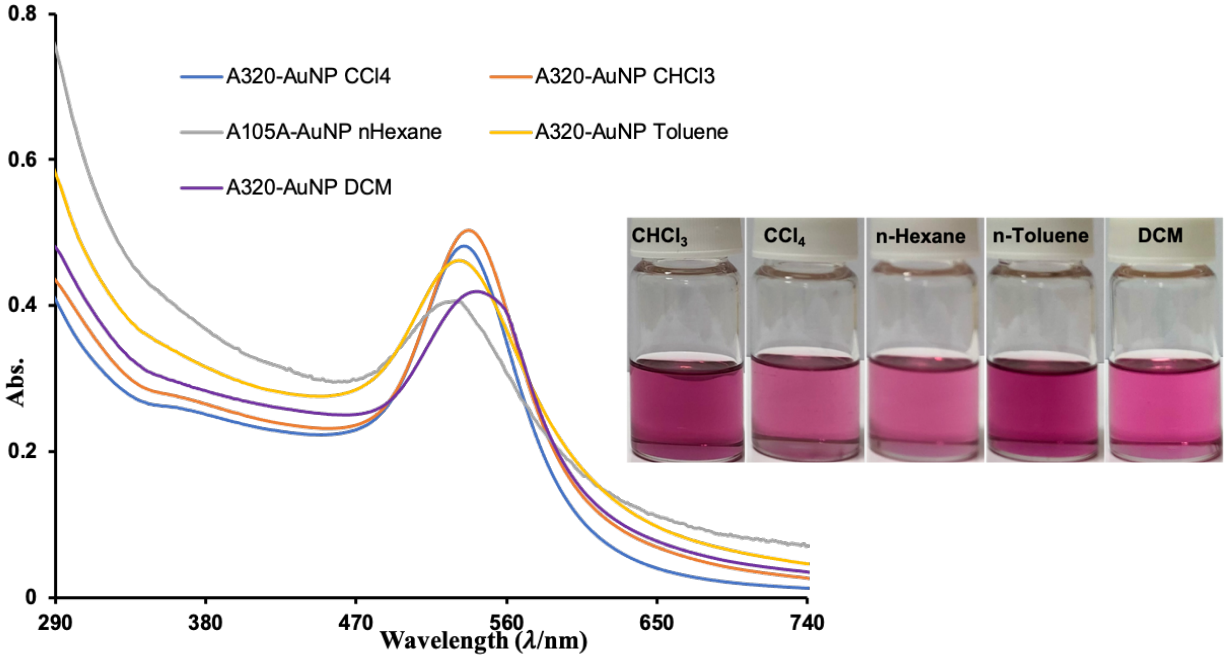

Fig-4.5.1 Visual appearances and UV-vis spectra of AMIET 320-AuNPs in 5 organic solvents

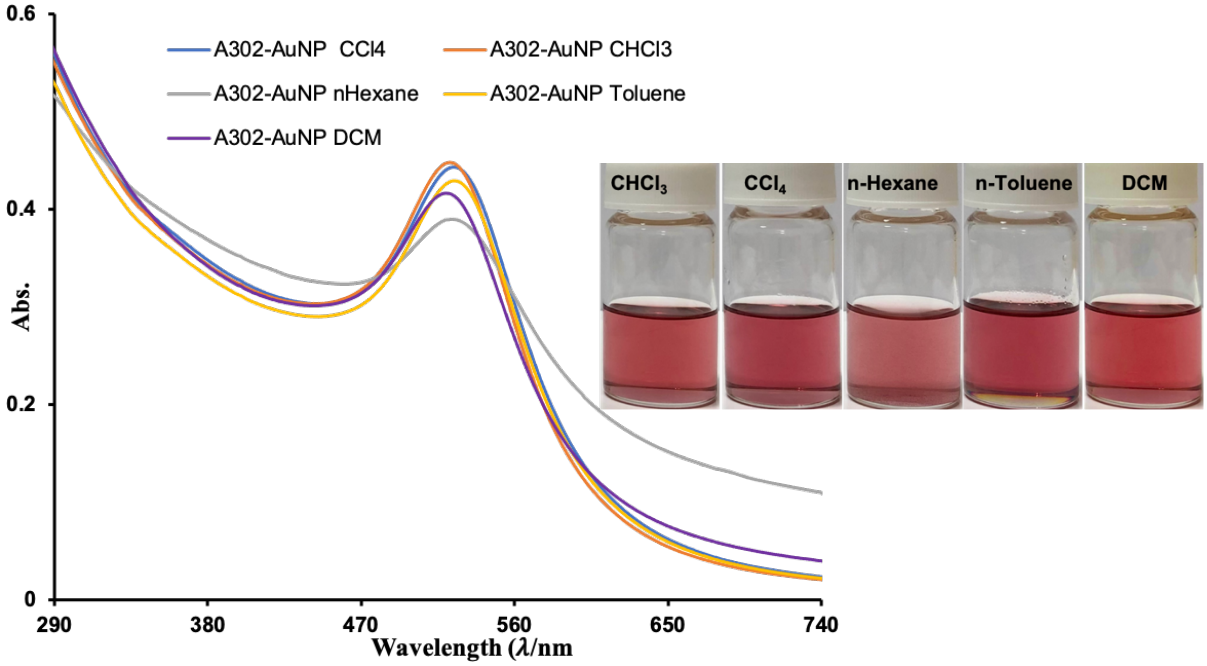

Fig-4.5.2 Visual appearances and UV-vis spectra of AMIET 302-AuNPs in 5 organic solvents

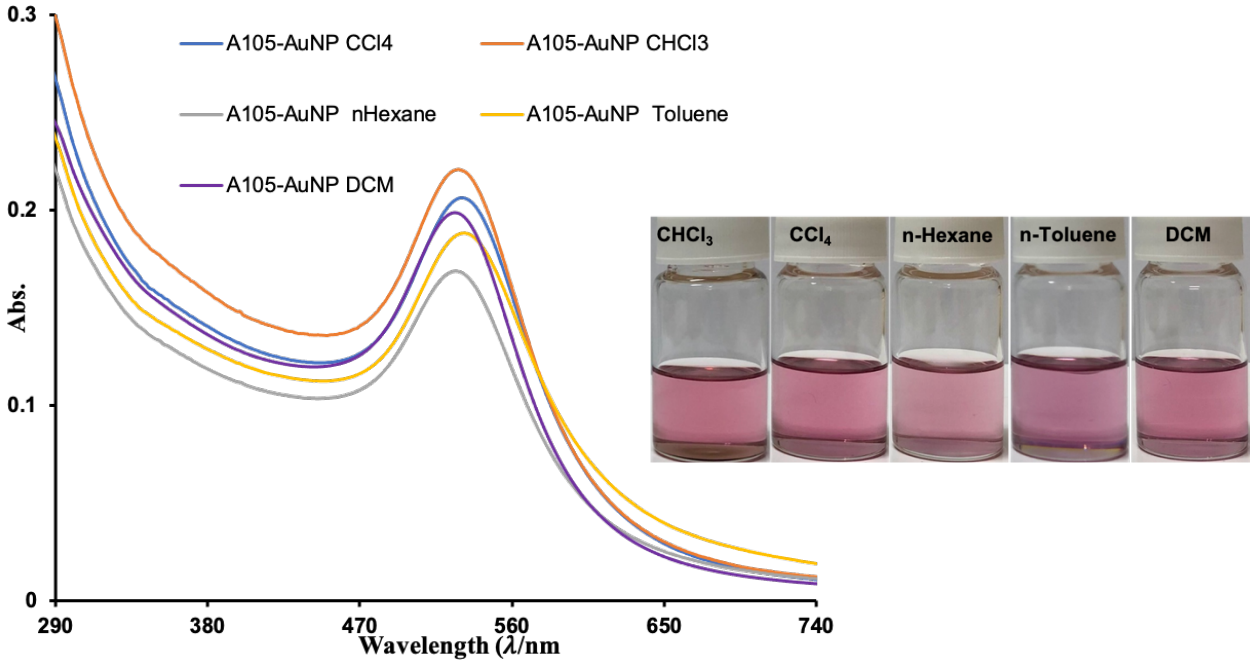

Fig-4.5.3 Visual appearances and UV-vis spectra of AMIET 105-AuNPs in 5 organic solvents

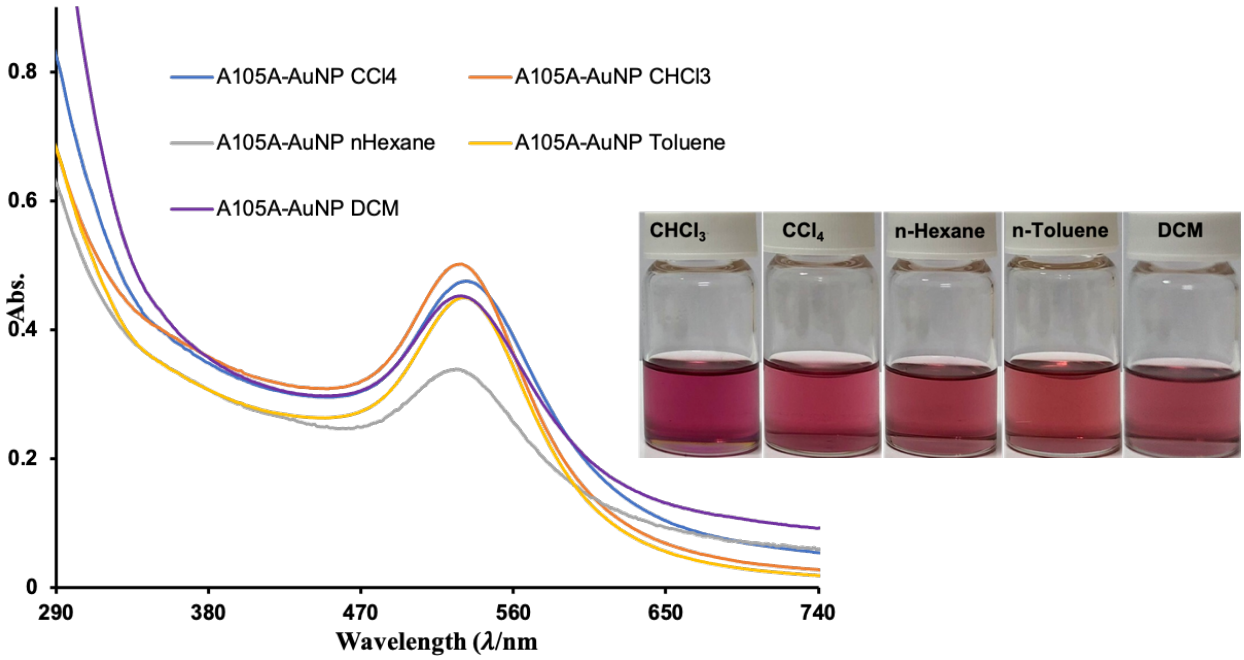

Fig-4.5.4 Visual appearances and UV-vis spectra of AMIET 105A-AuNPs in 5 organic solvents

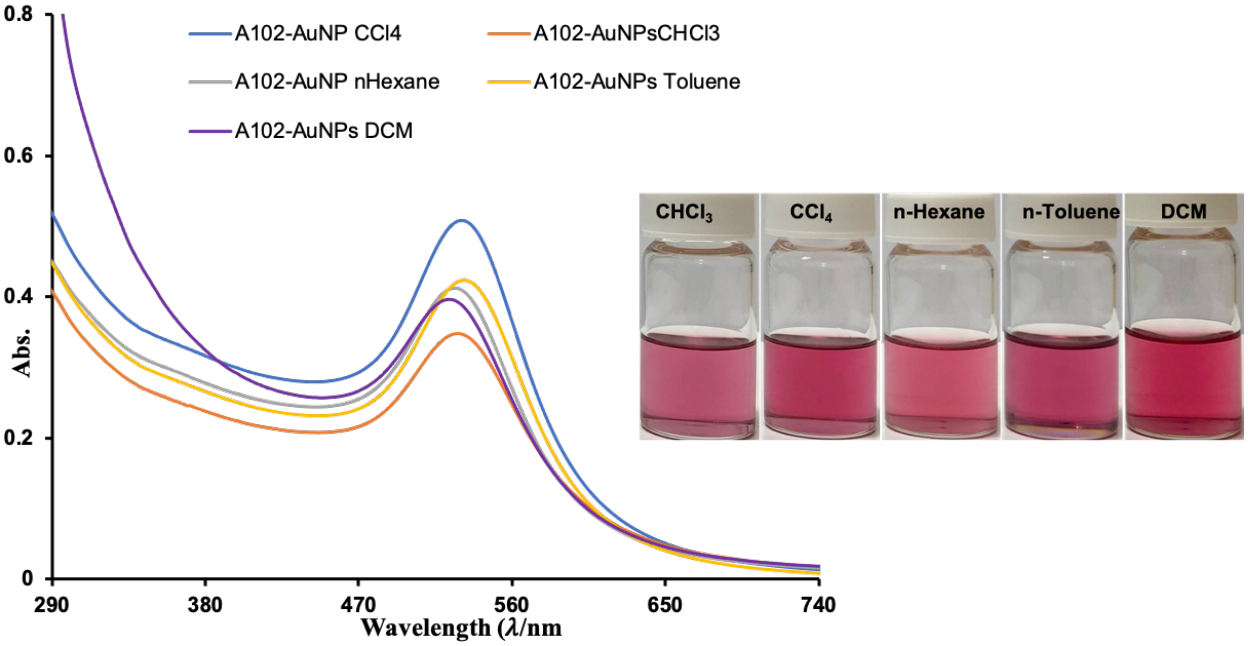

Fig-4.5.4 Visual appearances and UV-vis spectra of AMIET 102-AuNPs in 5 organic solvents

4.4 Conclusion

This study found a cutting edge solution for removing the residual organic from the AMIET-AuNPs without using laborious tools and chemicals . Moreover, the findings of this approach have considerable managerial implications. It is anticipated that this research will help to eliminate potential problems that may arise with size or shape separations. Overall, this techniques can be applied at least as the primary cleaning before proceeding for further extensive purification.

4.5 References

[1] D. Li, C. Wang, D. Tripkovic, S. Sun, N.M. Markovic, and V.R. Stamenkovic, *ACS Catal.*, **2**, 1358–1362 (2012).

[2] P. Trogadas, N. Kapil, G.M.A. Angel, S. Kühl, P. Strasser, D.J.L. Brett, and M.-O. Coppens, *J. Mater. Chem. A*, 24283–24289 (2021).

[3] D. Liu, X. Xu, Y. Du, X. Qin, Y. Zhang, C. Ma, S. Wen, W. Ren, E.M. Goldys, J.A. Piper, S. Dou, X. Liu, and D. Jin, *Nat. Commun.*, **7**, 1–8 (2016).

[4] S.L.A. Bueno, J.T.L. Gamler, and S.E. Skrabalak, *ChemNanoMat*, **6**, 783–789 (2020).

[5] P. Iyengar, J. Huang, G.L. De Gregorio, C. Gadiyar, and R. Buonsanti, *Chem. Commun.*, **55**, 8796–8799 (2019).

[6] D. Gao, H. Zhou, J. Wang, S. Miao, F. Yang, G. Wang, J. Wang, and X. Bao, *J. Am. Chem. Soc.*, **137**, 4288–4291 (2015).

[7] T.H. Yang, Y. Shi, A. Janssen, and Y. Xia, *Angew. Chemie - Int. Ed.*, **59**, 15378–15401 (2020).

[8] Y. Liu, N.O. Weiss, X. Duan, H.-C. Cheng, Y. Huang, and X. Duan, *Nat. Rev. Mater.*, **1**, 1–17 (2016).

[9] A. Heuer-Jungemann, N. Feliu, I. Bakaimi, M. Hamaly, A. Alkilany, I. Chakraborty, A. Masood, M.F. Casula, A. Kostopoulou, E. Oh, K. Susumu, M.H. Stewart, I.L. Medintz, E. Stratakis, W.J. Parak, and A.G. Kanaras, *Chem. Rev.*, **119**, 4819–4880 (2019).

[10] P. Godbold, G. Johnson, A.D. Obi, R. Brown, S. Hwang, R.J. Gilliard, and S. Zhang, *J. Am. Chem. Soc.*, **143**, 2644–2648 (2021).

[11] K. Bhattacharjee, K. Biswas, and B.L.V. Prasad, *J. Phys. Chem. C*, **124**, 23446–23453 (2020).

[12] I. Kanelidis and T. Kraus, *Beilstein J. Nanotechnol.*, **8**, 2625–2639 (2017).

[13] Z. Niu and Y. Li, *Chem. Mater.*, **26**, 72–83 (2014).

[14] J. Quinson, *Front. Nanotechnol.*, **3**, 1–6 (2021).

[15] A.M. Dattelbaum, M.L. Amweg, J.D. Ruiz, L.E. Ecke, A.P. Shreve, and A.N. Parikh, *J. Phys. Chem. B*, **109**, 14551–14556 (2005).

[16] Z. Zhang, M. Chi, G.M. Veith, P. Zhang, D.A. Lutterman, J. Rosenthal, S.H. Overbury, S. Dai, and H. Zhu, *ACS Catal.*, **6**, 6255–6264 (2016).

[17] M. Cargnello, C. Chen, B.T. Diroll, V.V.T. Doan-Nguyen, R.J. Gorte, and C.B. Murray, *J.*

Am. Chem. Soc., **137**, 6906–6911 (2015).

[18] Y. Kang and C.B. Murray, *J. Am. Chem. Soc.*, **132**, 7568–7569 (2010).

[19] C. Urata, Y. Aoyama, A. Tonegawa, Y. Yamauchi, and K. Kuroda, *Chem. Commun.*, **34**, 5094–5096 (2009).

[20] Y. Zhang, N. Li, Z. Zhang, S. Li, M. Cui, L. Ma, H. Zhou, D. Su, and S. Zhang, *J. Am. Chem. Soc.*, **142**, 8490–8497 (2020).

[21] C. Liu, Z. Ma, M. Cui, Z. Zhang, X. Zhang, D. Su, C.B. Murray, J.X. Wang, and S. Zhang, *Nano Lett.*, **18**, 7870–7875 (2018).

[22] G. Li and R. Jin, *Nanotechnol. Rev.*, **2**, 529–545 (2013).

[23] S. Brimaud, C. Coutanceau, E. Garnier, J.-M. Léger, F. Gérard, S. Pronier, and M. Leoni, *J. Electroanal. Chem.*, **602**, 226–236 (2007).

[24] M. Crespo-Quesada, J.-M. Andanson, A. Yarulin, B. Lim, Y. Xia, and L. Kiwi-Minsker, *Langmuir*, **27**, 7909–7916 (2011).

[25] M. Schulz-Dobrick, K.V. Sarathy, and M. Jansen, *J. Am. Chem. Soc.*, **127**, 12816–12817 (2005).

[26] A. Heuer-Jungemann, N. Feliu, I. Bakaimi, M. Hamaly, A. Alkilany, I. Chakraborty, A. Masood, M.F. Casula, A. Kostopoulou, E. Oh, K. Susumu, M.H. Stewart, I.L. Medintz, E. Stratakis, W.J. Parak, and A.G. Kanaras, *Chem. Rev.*, **119**, 4819–4880 (2019).

[27] J. Ding, L. Bu, S. Guo, Z. Zhao, E. Zhu, Y. Huang, and X. Huang, *Nano Lett.*, **16**, 2762–2767 (2016).

[28] K.G. Thomas, J. Zajicek, and P. V Kamat, *Langmuir*, **18**, 3722–3727 (2002).

[29] G. Ertas and S. Suzer, *J. Nanosci. Nanotechnol.*, **7**, 4333–4338 (2007).

[30] S.F. Sweeney, G.H. Woehrle, and J.E. Hutchison, *J. Am. Chem. Soc.*, **128**, 3190–3197 (2006).

[31] R. La Spina, V. Spampinato, D. Gilliland, I. Ojea-Jimenez, and G. Ceccone, *Biointerphases*, **12**, 1–9 (2017).

[32] I. Kulu, R. Huang, B. Kalyanaraman, and V.M. Rotello, *MethodsX*, **7**, 1–5 (2020).

[33] I.Z. Kozma, P. Krok, and E. Riedle, *J. Opt. Soc. Am. B*, **22**, 1479–1485 (2005).

[34] S. Valkai, J. Liszi, and I. Szalai, *J. Chem. Thermodyn.*, **30**, 825–832 (1998).

[35] S. Kedenburg, M. Vieweg, T. Gissibl, and H. Giessen, *Opt. Mater. Express*, **2**, 1588–1611 (2012).

Chapter V Deposition of AMIET-AuNPs on solid substrate

Abstract

Formation of gold nanoparticles thin film at the air-water interface and its deposition on solid substrate remains challenging. In this study, the organic dispersed AMIET-AuNPs were used for the formation of monolayer films and the deposition onto silicon wafer was performed using Langmuir-Blodget (LB) technique. However, it is found that the immobilization of AuNPs is maximum when the substrate is dipped shortly in dilute hydrogen fluoride solution prior to film deposition. Moreover, 3-mercaptopropyl trimethoxysilane (MPTMS) functionalized silicone surface has also been used to deposit the AMIET-AuNPs in order to have a proper understanding of the immobilization. Film characterization was performed by atomic force microscopy investigation. The developed system is likely to predict the effectiveness gold nanoparticles deposition onto Si substrate using LB technique.

5.1 Introduction

Thin films of gold nanoparticles are gaining recognition and use in various products and applications including displays, sensors and energy storage. the immobilization of gold nanoparticles onto solid substrates has grown amongst researchers across the fields of chemistry, materials science, optics, photonics and medicine. gold nanoparticles offer benefits over other metallic nanoparticles due to its chemically stability [1,2] and bioconjugation capability [3–7]that yields highly functional surfaces compatible for various application. Since the localized surface plasmon resonance of gold nanoparticles is affected by the local environment and interparticle interactions [8–11], the immobilization state of gold nanoparticles on the surface dictates the particle-enhanced surface properties [12,13]. Therefore, the proper controlling of immobilization of gold nanoparticles is crucial to obtain the desired surface properties. Successful immobilization of gold nanoparticles is till challenging [14] and critical because the films are thermodynamically unstable compared to macroscopic films of larger grain sizes [15].

A variety of methods exist to incorporate gold nanoparticles onto solid substrates, which can be classified into two categories: direct formation [16–19]of nanoparticles on the surface, or deposition of colloidal nanoparticles [20–23] onto the surface. Direct formation of gold nanoparticles on the surface involves the growth of gold nanoscale features through ion reduction [24], thermal evaporation, ultrasound [25] or electrodeposition [26–28] of gold on substrates that have been patterned through micro- or nano- fabrication techniques such as electron beam lithography.

These techniques are known to create precise periodic arrays of nanoparticles, however they require specialized equipment and set-up, are restricted to small-area applications, and are expensive. Deposition [29,30] of preformed colloidal gold nanoparticles offers an inexpensive alternative for incorporation of gold nanoparticles onto surfaces requiring no specialized equipment. This method takes advantage of widely-studied colloidal gold nanoparticle synthesis techniques to obtain desired shapes and sizes of gold nanoparticles in solution [31–33] with the flexibility to modify large-area surfaces. In addition to selecting the particle size and shape, varying the immobilization state provides multiple degrees of freedom to create a wide variety of gold nanoparticle-enhanced surfaces.

The methods of transfer of nanoparticles from colloidal solution of them are widely used to immobilize gold nanoparticles onto the surface, for ex- ample self-assembly or Langmuir-Blodgett (LB) method . One should also take into account that many of indicated above additives such as thiols and others stabilizers are toxic. Another problem with AuNPs immobilization on the surface is the removal of organic molecules of surfactants from the layer of gold nanoparticles. Generally a heat treatment is used to remove indicated above additives, therefore an agglomeration of nanoparticles takes place at times. As a result, there are difficulties with controlling both the cluster size, and the adhesion of coatings formed [34].

In order to control the immobilization of gold nanoparticle, there are three main factors that must be considered: (1) the properties of the immobilization surface, (2) the properties of the gold nanoparticles in solution, and (3) the interaction of the gold nanoparticles with the surface.

The most common strategy for immobilization of gold nanoparticles is through modification of the surface with molecules containing a thiol or amino moiety to covalently bond gold nanoparticles to the surface through their high affinity to gold. Direct covalent binding of the surface to gold is advantageous as it allows the immobilization of both charged and uncharged particles, without the need for specific particle functionalization. Both the functionality of the linker molecule as well as the surface modification properties play an important role in determining the immobilization outcome.

Control of the spacing and aggregation of gold nanoparticles through covalent interactions with the surface is limited. Therefore, several approaches to pre-condition the particles into the desired aggregation state prior to deposition has been employed.

Similar to covalent immobilization techniques, deposition is usually carried out by submerging the substrate in the colloidal gold nanoparticle solution. For electrostatic immobilization, the ionic strength of the particle solution becomes a prominent factor to modulate the particle-surface interactions as it affects both the apparent charge of the particles and the surface. In a nanoparticle system containing charged capping agents, the overall ionic strength of the solution can be controlled by both the excess capping agent concentration and the addition of salt.

In addition to modulating the solution properties to control the particle-surface interactions, the ionic properties of the surface are very important and can be engineered to control the deposition of gold nanoparticles. However, this study is based on the deposition of AMIET-AuNPs to HF passivated silicon surface and 3-mercaptopropyl trimethoxysilane (MPTMS) functionalized silicon surface.

5.2 Experimental

5.2.1 Materials and methods

AMIET-AuNPs dispersed in $CHCl_3$ has be used as the starting materials. silicon wafer (Si) <100> as a solid substrate to deposit the AuNPs. 28% ammonia and 30% hydrogen peroxide from Kanto Chemical Co. Inc were used to prepare the RCA cleaning solution. Super dehydrated n-Hexane (C_6H_{12}) from FUJIFILM Wako Pure Chemical Corporation was used to prepare the AMIET-AuNPs spreading solution. Ultrapure water by Merck Direct-Q UV was used as washing and immersing solvent during sonication.

5.2.2 Si surface cleaning and HF passivation

Si wafer was cleaned softly with the soap foam followed by 3 times sonication while immersing in ultrapure water. 50 ml 30% hydrogen peroxide (H_2O_2) and 50 ml 28% ammonia (NH_4OH) added 200 ml ultrapure water in a beaker is called the RCA cleaning solution. The initial cleaned Si wafers were then dipped into the RCA cleaning solution and heated at 80ºC for about 30 mins. Afterwards, the heating was turned off and the beaker was taken out cautiously and allowed to cool for at least 10 mins. Then three subsequent sonication with fresh UPW was conducted and preserved while immersed in UPW. RCA cleaning turns the hydrophobic Si surface to hydrophilic. For HF treatment the RCA cleaned Si is shortly dipped in 2% HF aqueous solution in a teflon

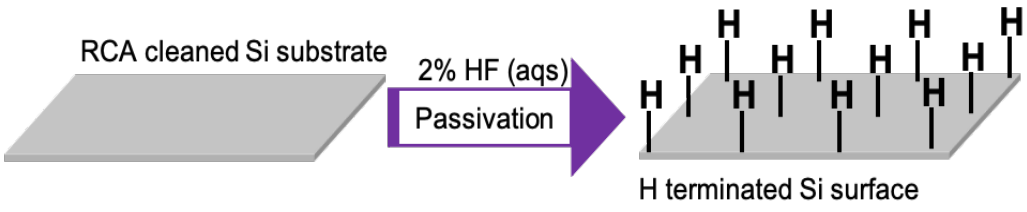

Fig-5.1 Schematic presentation of the deposition of AMIET-AuNPs onto Si wafer.

beaker (precaution: the corrosive and reactive nature of HF to glass). The HF passivation yield hydrogen terminated surface. The complete procedure can be summarized as shown by Fig-5.1.

5.2.3 Si surface cleaning and functionalization with MPTMS

The Si surface was cleaned by piranha solution which the combination of sulfuric acid (H_2SO_4) and hydrogen peroxide (H_2O_2) because piranha solution is a strong oxidizer and clean the organic residue. Moreover, it hydroxylate most surfaces and make extremely hydrophilic that is essential to bind more MPTMS on the Si surface during functionalization. However, in this experiment the H_2SO_4 and H_2O_2 were mixed with the ratio of 7:3. Same as before, the soap cleaned Si wafers were immersed in piranha solution and heated at 80ºC for about 30 mins. Afterwards, the heating was turned off and the beaker was taken out cautiously and allowed to cool for at least 10 mins. Then three subsequent sonication with fresh UPW was conducted and preserved while immersed in UPW. Before proceed for functionalization the wafer was lifted and dried with air blow then immersed in MPTMS solution (1 ml MPTMS +12 ml toluene) and heated at 70 ºC for 3 hours and left immersing for more 24 hours.

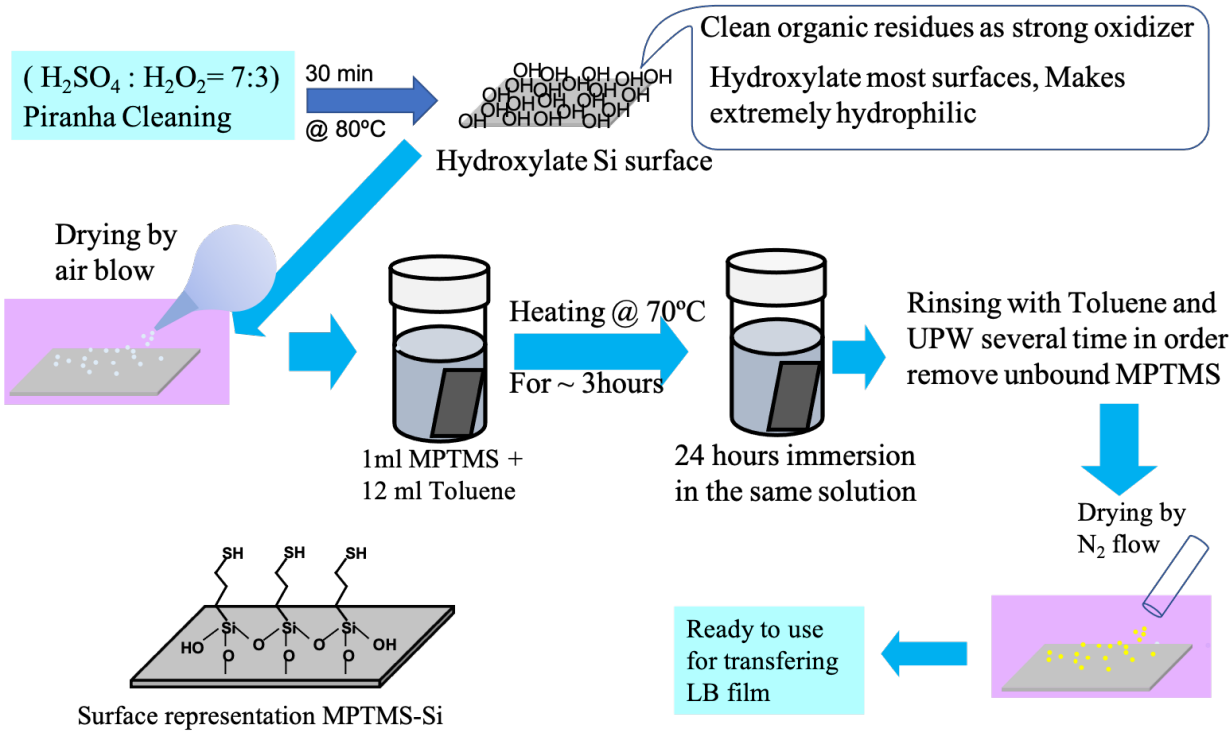

Fig-5.2 Schematic representation of piranha cleaning and MPTMS functionalization of Si wafer.

Then the MPTMS functionalized Si surface was rinsed with toluene and UPW several times in order to remove dangling or unbound MPTMS and dried with nitrogen flow. The complete procedure can be briefly represented in Fig-5.2.

5.2.4 Selecting proper solvent for spreading

Different solvent dispersed AMIET-AuNPs has been attempted to spread over water surface in order to confirm the spreading. Interestingly, it is noticed that chloroform dispersed AMIET-AuNPs is not able to spread all over the water surface; while trying with other solvents, only in case of super dehydrated n-hexane dispersed AMIET-AuNPs, the spreading was appreciable. Therefore, in order to prepare the nanoparticles film using Langmuir technique, super dehydrated n-Hexane has been extensively used to prepare the spreading solution all over the experiments. The spread-ability of n-Hexane has shown better over chloroform is because of its lower value of surface tension (18.43 mNm^{-1}) than that of water (27.50 mNm^{-1}). Therefore, n-hexane has low cohesive attraction and more adhesive attraction that facilitates the spreading of AMIET-AuNPs while dispersing in n-hexane. The representation of solvent spreading behavior is as in Fig-3

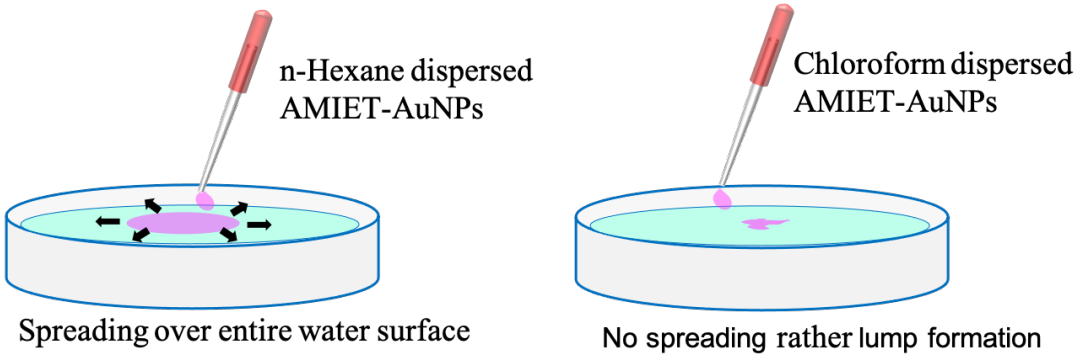

Fig-5.3 Schematic illustration of spreading of AMIET-AuNPs dispersed in two different solvents

5.2.5 Langmuir trough and surface pressure measurements

The schematic diagram of the experimental set up is shown in Fig-5.4. Our NIMA Langmuir trough had a fully opened area of ~98 cm^2 with 50 cm width, and the length of the trough was allowed to vary to control the area of the trough and total subphase volume 57 ml. Before each

experiment the Langmuir trough was cleaned 3 times with isopropanol. After cleaning, the barriers of the trough were compressed, and the initial surface pressure of pure water was found to be < 0.2 mN/m at maximal compression. 7.5 µl AMIET 302-AuNP (n-hexane) were spread over 57 ml water surface on the Langmuir trough. Before starting compression it is allowed 30 mins for solvent evaporate. Then the barrier as start to compress and the isotherm was recorded as shown in Fig-5.5.

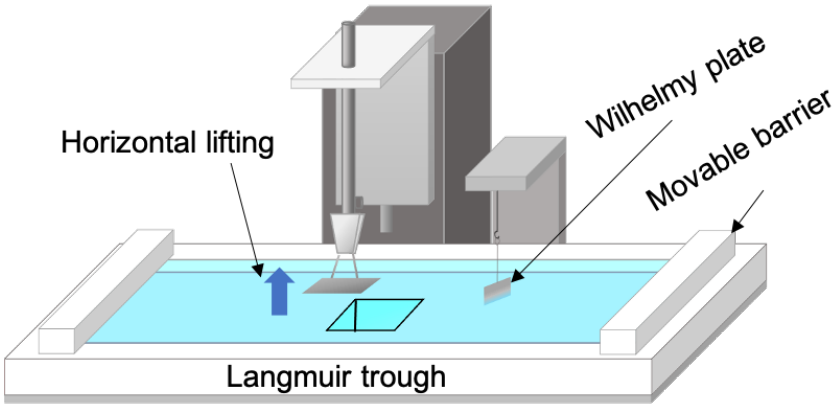

Fig-5.4 Eperimental setup of LB-Film deposition

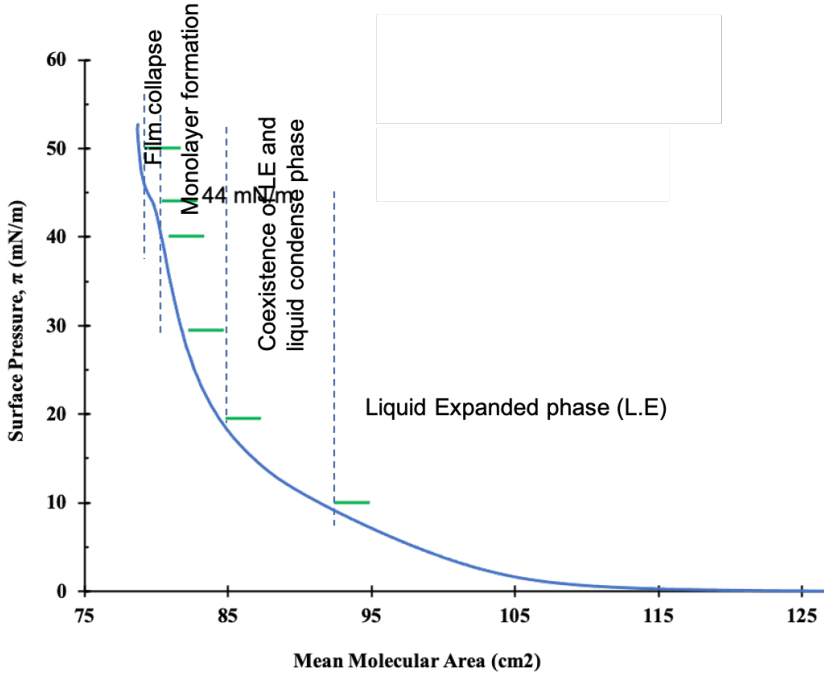

Fig-5.5 *π-A* isotherm of AMIET 302-AuNPs on air-water

According to the obtained *π-A* isotherm it was predicted that the monolayer was formed between the surface pressure 20 to 43 mNm^{-1}. Moreover, in order to investigate the AuNPs film on air-

water surface the film was transferred to HF passivated Si substrate and MPTMS functionalized Si substrate by scoop up or horizontal lifting technique.

5.2.6 Deposition on TEM grid

The AMIET-AuNPs were also attempted to transfer to TEM grid from the air-water interface. it was found the uplift stroke or vertical lifting as in Fig-5.6 (a)from TEM grid through the interface yields better deposition than horizontal lifting as demonstrated by Fig-5.6 (b). Moreover, it is noticed that upon vertical lifting the particles are accumulated at the edge of TEM grid. Therefore, TEM grid was attached vertically to a support and emerged under the interface before spreading the nanoparticles solution and lifted accordingly at the corresponding surface pressure.

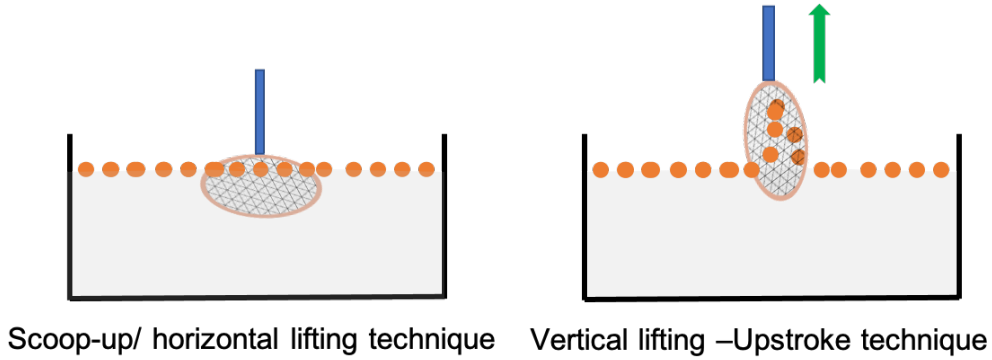

Fig-5.6 Transfer technique of the film of AMIET-AuNPs to TEM grid from air-water interface

5.3 Results and discussion

Nanoparticles can be observed through AFM measurements to assess their surface topography [35,36] and ensure their deposition onto silicon substrates. It is observed that relatively few particles adhere to the HF passivated Si surface upon transfer of AMIET 302-AuNPs up to 20 mNm^{-1} surface pressure, predicting that the weak van der Waals interaction between the particles may results in low adhesion to the Si surface. Nevertheless, as the particles are closer with continued compression, sufficient AuNPs are attached to the substrate when scooping up the particles.

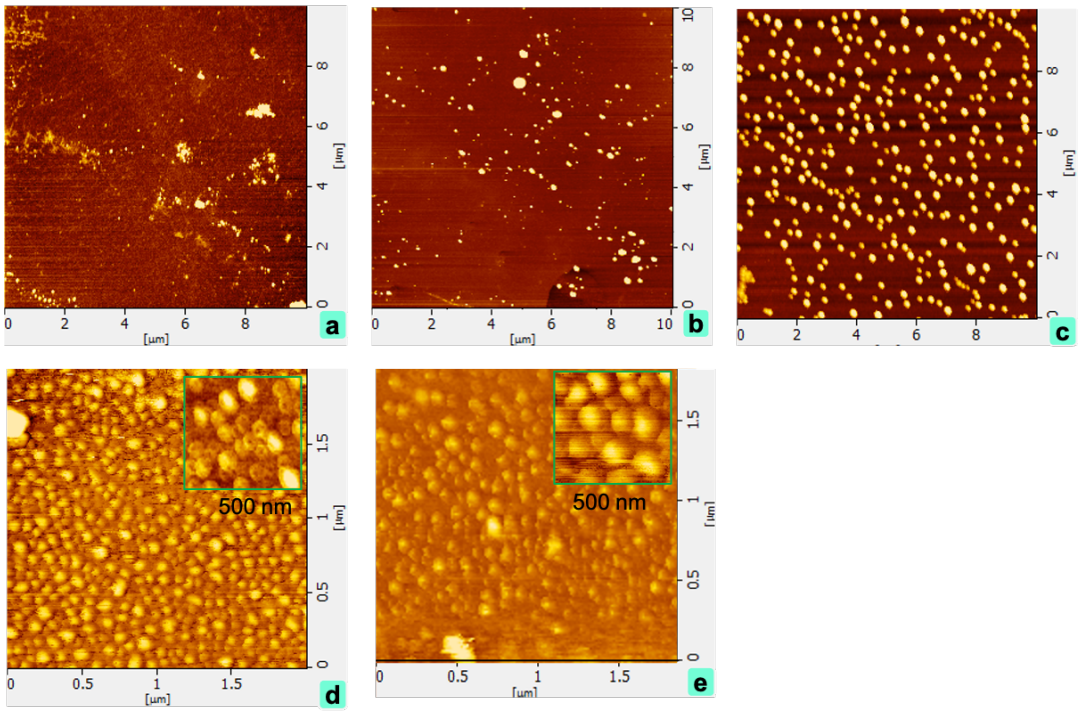

Fig-5.7 AFM images of AMIET 302-AuNPs deposited onto the HF passivated Si surface at different surface pressure a) 10 mN/m, b) 20 mN/m, c) 30 mN/m, d) 40 mN/m, and e) 44

The AFM topography of AMIET 302-AuNPs as seen in Fig-5.7e suggests that a particular type of compact monolayer is formed just before the collapsing pressure ~44 mNm^{-1}.

At various surface pressures, the AuNPs transferred to the MPTMS functionalized Si wafer are also similar to those transferred to an HF passivated surface.

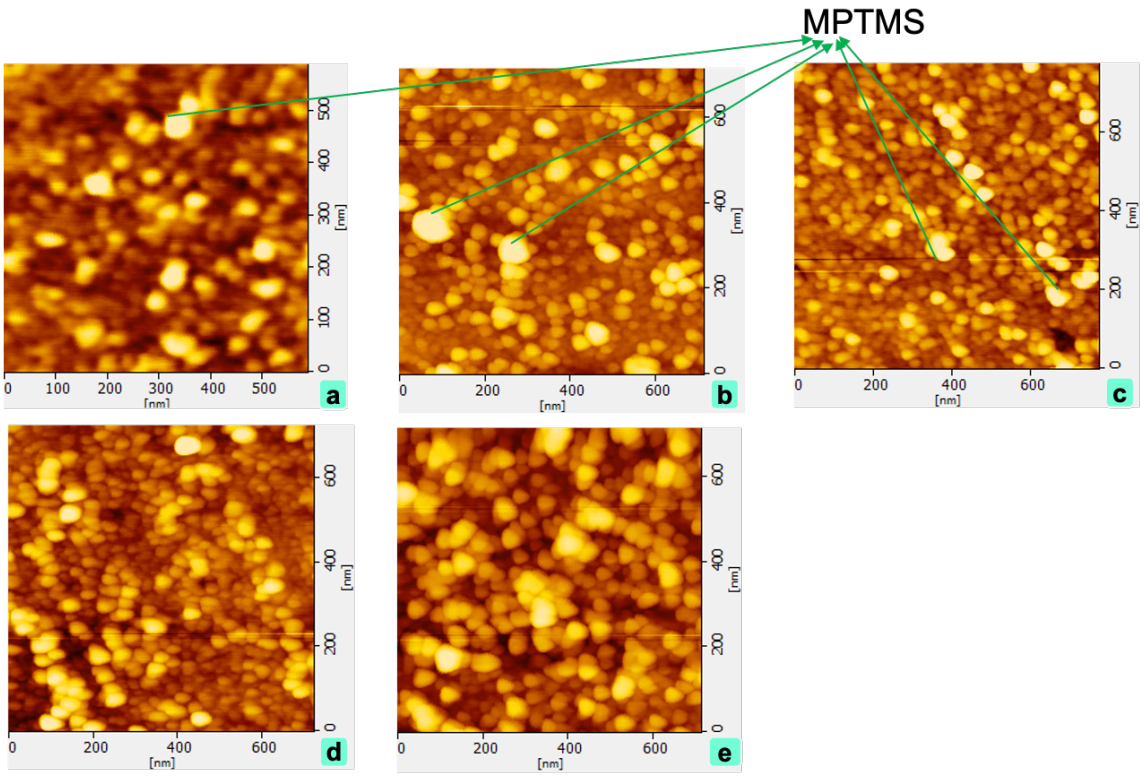

Fig-5.8 AFM images of AMIET 302-AuNPs deposited onto the MPTMS- Si surface at different surface pressure a) 10 mN/m, b) 20 mN/m, c) 30 mN/m, d) 40 mN/m, and e) 44 mN/m

Nevertheless, the presence of steep MPTMS in combination with AuNPs cannot be ignored, as shown in Fig-5.8. MPTMS domains built on steep slopes are inseparable from the surface of Si due to their self-polymerization tendency. As shown in Fig-5.9 the TEM image of the AMIET-AuNPs film also shows similar deposition of particles to the grid with respect to surface pressure, i.e. more particles are adherent to the TEM grid as they get closer during compression. It is also noted that almost no particles are transferred to the substrate or grid from all three depositions at low surface pressure. Despite this, both AFM topography and TEM micrography displays a spherical shape of the prepared AMIET-AuNPs as deposited at high surface compression.

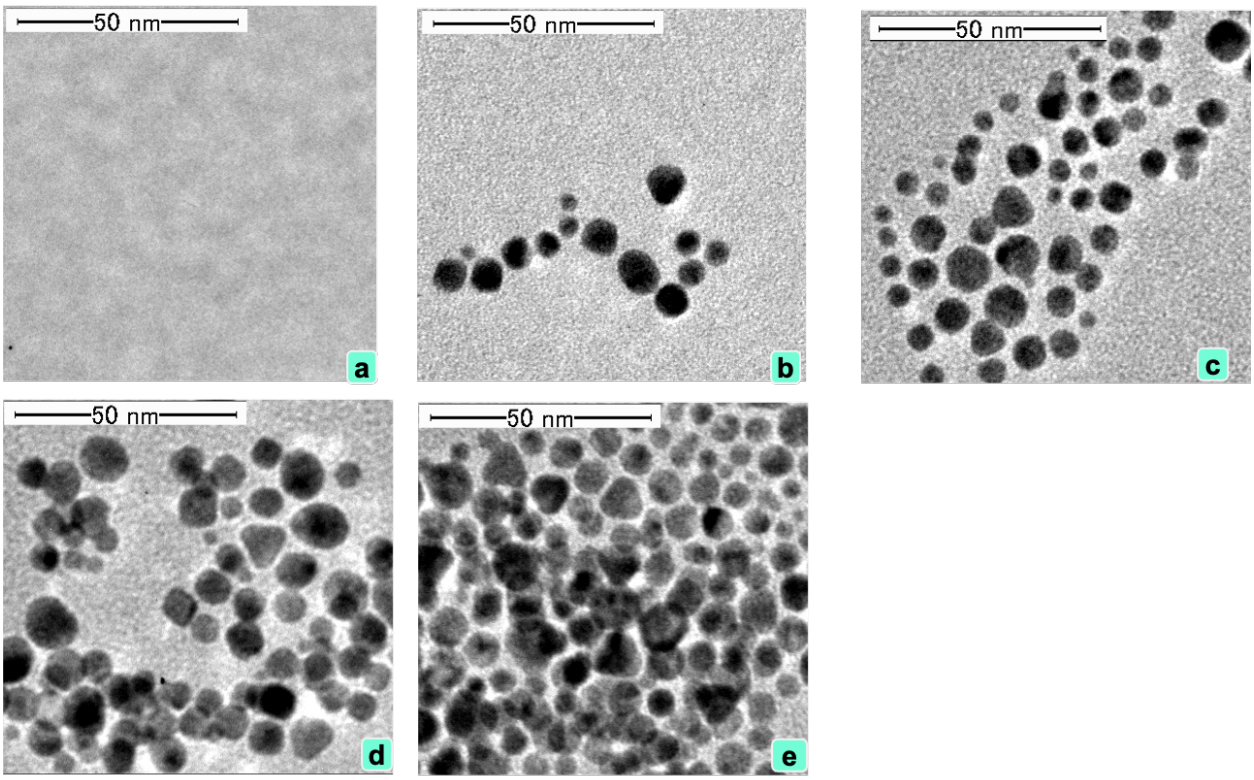

Fig-5.9 TEM images of AMIET 302-AuNPs at different surface pressure a) 10 mN/m, b) 20 mN/m, c) 30 mN/m, d) 40 mN/m, and e) 44 mN/m

5.4 Conclusion

Deposition of AMIET-AuNPs onto modified Si surfaces has been investigated since it was observed that no particle can be transferred to bare Si, probably due to insufficient interaction between the small gold nanoparticles and the Si surface. However, the use of HF passivated and MPTMS-Si surfaces suggests that if adequate adhesion is created by the surface modification of the substrate, then AMIET-AuNPs can be transferred effectively.

5.5 References

[1] M.-C. Daniel and D. Astruc, *Chem. Rev.*, **104**, 293–346 (2004).

[2] M.Y. Icimoto, A.M.M. Brito, M.P.C. Ramos, V. Oliveira, and I.L. Nantes-Cardoso, *Catalysts*, **10**, 78 (2020).

[3] M.H. Jazayeri, H. Amani, A.A. Pourfatollah, H. Pazoki-Toroudi, and B. Sedighimoghaddam, *Sens. Bio-Sensing Res.*, **9**, 17–22 (2016).

[4] C. Oliver, *Methods Mol. Biol.*, **588**, 369–373 (2010).

[5] R. Kozlowski, A. Ragupathi, and R.B. Dyer, *Bioconjug. Chem.*, **29**, 2691–2700 (2018).

[6] R.T. Busch, F. Karim, J. Weis, Y. Sun, C. Zhao, and E.S. Vasquez, *ACS Omega*, **4**, 15269–15279 (2019).

[7] P. Khashayar, G. Amoabediny, B. Larijani, M. Hosseini, and J. Vanfleteren, *Sci. Rep.*, **7**, 1–8 (2017).

[8] K.K. Paul and P.K. Giri, *Elsevier, Oxford*, **1**, 786–794 (2018).

[9] H. Bin Jeon, P.V. Tsalu, and J.W. Ha, *Sci. Rep.*, **9**, 1–8 (2019).

[10] M. Donoval, A. Kuzma, A. Satka, M. Daricek, and P. Telek, *Optik (Stuttg).*, **127**, 6322–6328 (2016).

[11] J.H. Lee, H.Y. Cho, H.K. Choi, J.Y. Lee, and J.W. Choi, *Int. J. Mol. Sci.*, **19**, 1–14 (2018).

[12] J.D. Driskell, R.J. Lipert, and M.D. Porter, *J. Phys. Chem. B*, **110**, 17444–17451 (2006).

[13] K. Kobayashi, J. Wei, R. Iida, K. Ijiro, and K. Niikura, *Polym. J.*, **46**, 460–468 (2014).

[14] F.L. Heredia, P.J. Resto, and E.I. Parés-Matos, *Biosensors*, **10**, 1–14 (2020).

[15] H. Han, J. Park, S.Y. Nam, K.J. Kim, G.M. Choi, S.S.P. Parkin, H.M. Jang, and J.T.S. Irvine, *Nat. Commun.*, **10**, 1–8 (2019).

[16] S. Phokha, S. Pinitsoontorn, P. Chirawatkul, Y. Poo-arporn, and S. Maensiri, *Nanoscale Res. Lett.*, **7**, 1–13 (2012).

[17] F.O. Silva, M.S. Carvalho, R. Mendonça, W.A.A. Macedo, K. Balzuweit, P. Reiss, and M.A. Schiavon, *Nanoscale Res. Lett.*, **7**, 1–10 (2012).

[18] C. Simitzi, P. Harimech, S. Spanou, C. Lanara, A. Heuer-Jungemann, A. Manousaki, C. Fotakis, A. Ranella, A.G. Kanaras, and E. Stratakis, *Biomater. Sci.*, **6**, 1469–1479 (2018).

[19] Y.-J. Chen, W.-H. Chang, C.-Y. Li, Y.-C. Chiu, C.-C. Huang, and C.-H. Lin, *Mater. Des.*, **197**, 1–11 (2021).

[20] V. Rehacek and I. Hotovy, *J. Electr. Eng.*, **68**, 487–491 (2017).

[21] H. Yin, C. Wang, H. Zhu, S.H. Overbury, S. Sun, and S. Dai, *Chem. Commun.*, 4357–4359 (2008).

[22] D. Buttard, F. Oelher, and T. David, *Nanoscale Res. Lett.*, **6**, 1–8 (2011).

[23] D. Aureau, Y. Varin, K. Roodenko, O. Seitz, O. Pluchery, and Y.J. Chabal, *J. Phys. Chem. C*, **114**, 14180–14186 (2010).

[24] S. Hadano, H. Handa, K. Nagai, T. Iyoda, J.Z. Li, and S. Watanabe, *Chem. Lett.*, **42**, 71–73 (2013).

[25] C. De Rosa, F. Auriemma, C. Diletto, R. Di Girolamo, A. Malafronte, P. Morvillo, G. Zito, G. Rusciano, G. Pesce, and A. Sasso, *Phys. Chem. Chem. Phys.*, **17**, 8061–8069 (2015).

[26] Y.D. Park BW, Kim DS, *Korean J. Chem. Eng.*, **28**, 64–70 (2011).

[27] X. DAI and R.G. COMPTON, *Anal. Sci.*, **22**, 567–570 (2006).

[28] S. Wyantuti, Y.W. Hartati, M.L. Firdaus, C. Panatarani, and R. Tjokronegoro, *Int. J. Sci. Technol. Res.*, **4**, 135–139 (2015).

[29] T. Feng, L. Ding, L. Chen, and J. Di, *J. Exp. Nanosci.*, **14**, 13–22 (2019).

[30] K. Fujiwara, H. Kasaya, and N. Ogawa, *Anal. Sci.*, **25**, 241–248 (2009).

[31] J. Kimling, M. Maier, B. Okenve, V. Kotaidis, H. Ballot, and A. Plech, *J. Phys. Chem. B*, **110**, 15700–15707 (2006).

[32] M.S. Verma, P.Z. Chen, L. Jones, and F.X. Gu, *RSC Adv.*, **4**, 10660–10668 (2014).

[33] M. Grzelczak, J. Pérez-Juste, P. Mulvaney, and L.M. Liz-Marzán, *Chem. Soc. Rev.*, **37**, 1783–1791 (2008).

[34] L.B. Gulina, A.A. Pchelkina, K.G. Nikolaev, D. V. Navolotskaya, S.S. Ermakov, and V.P. Tolstoy, *Rev. Adv. Mater. Sci.*, **44**, 46–53 (2016).

[35] P.C. Lansåker, A. Hallén, G.A. Niklasson, and C.G. Granqvist, *AIP Adv.*, **4**, 107101 (2014).

[36] G. Jiang and S. Xie, *Polymers (Basel).*, **11**, 1–11 (2019).

Chapter VI Summary

6. Summary of the thesis

In this work, polyoxyethylene alkyl amine surfactants that are widely used in industry were used as a reducing agent to synthesis gold nanoparticles. The synthetic route and the ratio of reactants and were carefully optimized to achieved the in-situ functionalized gold nanoparticles. It was observed that only specific ranges of concentrations of AMIET can produce gold nanoparticle with less residual organic and clear ruby red appearance. Though out prepared AMIET-AuNPs has a wide range of particles, it is responsive due to its strong surface plasmon resonance that predicts its potential in application area.

The most important fact of this work is the phase transfer of the aqueous gold nanoparticles which was challenging in terms of the repeatability. However, the complete transfer of AMIET-AuNPs was ensured using pH induced phase transfer method. This methods also assures the complete transfer can be achieved without any significant aggregation while preserving it original morphology. Even, this method is functionable independently on the particle size and organic solvent density in comparison to water.

Furthermore, surfactant removal were conducted through a particular approach without using laborious instrument and chemical. It is shown that the approach potentially the clean and remove the surfactant from colloidal solution while dispersed in chloroform after phase transfer. The most striking fact that after cleaning the AMIET-AuNPs can be readily dispersed in various organic solvent with no significant aggregation or coagulation.

Finally, the thin film formation of AMIET-AuNPs on air-water interfaces was studied to better understand fabrication capability. It is almost unheard of to deposition such small AuNPs that are polydisperse from the literature perspective. Nevertheless, our experiment indicates that deposition can be successful if adequate adhesion between AMIET-AuNPs and the solid surface can be achieved. It is necessary to conduct further research to improve film transfer onto solid surfaces.

As AMIET-AuNPs have not previously been reported in the literature, based on the outcome of this investigation, the following contributions can be imparted to the original knowledge.

i.) The polyoxyethylene alkyl amine has been demonstrated to be an efficient ligand for gold nanoparticles. It was shown that the dual nature of ethoxy plays and important role in phase transfer reaction.

ii.) The binding mode of AMIET on a gold surface was established and the origin of nanoparticles charges was clarified. The negative charge of AMIET-AuNPs results from electron delocalization of in gold associated ligands and is pH dependent.

iii.) The effect of pH and excess AMIET on the AuNPs were carefully investigated. It was found that the nanoparticle aggregation at pH-6.5~9.0 was attributed to desorption of the ligand caused by the ligand binding sites. Moreover, it was shown excess AMIET can interrupt the stability of AuNPs colloid.

iv.) Outside the stipulated pH range (pH-6.5~9.0) AMIET coated AuNPs exhibited enhanced stability that proved that the long alkyl chain could wrap around small (2-18 nm) gold nanoparticles.

v.) The unique feature of AMIET-AuNPs established in this thesis is the reliable and repeatable phase transfer was achieved based on coagulation and flocculation of the dispersed particles through a liquid-liquid interface. The factors involves is nature of AMIET and it configurational change depends on pH and surrounding environment.

6.1 Ideas for continued research

The deposition of gold nanoparticle onto solid surface from the air-water interface is often challenging. Our research on this subject still under thriving condition. The limitations associated with the investigation is basically the interaction between gold nanoparticles and solid surface. Moreover, the problem associated with MPTMS functionalization is formining uniform layer onto Si surface. As MPTMs is highly moisture sensitive, self polymerization it may forms sticky glue layer during post washing in order remove unbound Silane.The domains are rougher and composed of less well-ordered monolayers and more disordered polymers with randomly distributed thiol headgroups on the uppermost surface. In this case, 3-mercaptopropylsilatrane (MPS) can overcome the present shortcomings. The MPS films also have higher mercaptan surface density than that of the MPTMS films, resulting in higher saturation coverage of the gold colloid monolayers on the MPS-coated substrates. MPS results in more uniform and reproducible films due to its insensitivity to moisture. Moreover, smooth adhesion layer (like chromium, MPS) on Si surface will be attempted for maximum immobilization of AuNPs.